Identification of Influential Parameters Affecting Power System Voltage and Angular Stability Analysis

A thesis submitted to the University of Manchester for the degree of

Doctor of Philosophy

in the Faculty of Science and Engineering

2019

Mr Buyang Qi

School of Electrical and Electronic Engineering

List of Contents

Word Count: 47,902

List of Figures

List of Tables

Nomenclature

List of Symbols

A	Set of available components (probabilistic reliability analysis)
$B(\alpha,\beta)$	Beta function with shape parameters
$C(\blacksquare)$	Copula function
d	Duration of demand
e	Base of the natural logarithms
$f(\blacksquare)$	A function
$F(\blacksquare)$	Multivariate cumulative distribution function
G	Generator
H	Generator inertia constant
$H(\blacksquare)$	Right-continuous Heaviside step function
L	Load
n	Number of trials/parameter value
N	Number of parameters
O	Impact of parameter calculated through One-at-A-Time method
p	Parameter number of uncertain network
P	Real power
$P\{\blacksquare\}$	Probabilistic power system stability analysis
Q	Reactive power
Q^2	Percentage of output variability
r	Level parameter of Morris Screening method
S	Sensitivity index of Sobol total indices method/apparent power
U	Set of unavailable components (probabilistic reliability analysis)/voltage

V	Voltage
Var	Variance of dataset
x	Input parameter
X	Sample value of random variable/input matrix (sensitivity analysis)
$\overline{X}$	Mean value of samples
y	Output parameter
Y	Output matrix (sensitivity analysis)
Z	Impedance
α	Shape parameter for probabilistic distributions
β	Shape or scale parameter for probabilistic distributions
$\Gamma(\blacksquare)$	Gamma function
δ	Generator rotor angle
Δ	Operator representing the variation/step parameter(Morris Screening method)
ε	Error
λ	Complex eigenvalue of the system critical mode (small-disturbance stability)/rate parameter (probabilistic distributions)
μ	Mean value
ξ	Damping ratio of the system critical mode (small-disturbance stability)
$\prod \blacksquare$	Complete set of system components for probabilistic reliability analysis
ρ	Correlation coefficient measurement
σ	Standard deviation/modal damping (small-disturbance stability)/scale parameter (Rayleigh distribution)
$\sum \blacksquare$	Correlation matrix

τ	Rank correlation coefficient measurement
ω	Modal frequency (small-disturbance stability)
$\blacksquare!$	The factorial of $\blacksquare$

Subscriptions and Superscriptions

d	Index value, where $d = 1, 2, 3$ ...
g	Generator
i	Index value, where $i = 1, 2, 3$ ...
j	Index value, where $j = 1, 2, 3$ ...
n	Index value, where $n = 1, 2, 3$ ...
$base$	Base case
con	Conventional
$diff$	Difference
L	Load
max	Maximum
min	Minimum
$nose$	Nose point
RES	Renewable Energy Source
SG	Synchronize Generator
‘	Referred value

Acronyms

APRI	Amperage (Overload) Probabilistic Reliability Index
CCT	Critical Clearing Time (Transient Stability)
CDF/*cdf*	Cumulative Distribution Function
CIGRE	International Council on Large Electric Systems
CPU	Central Processing Unit

CS	Case Study
DER	Distributed Energy Resources
DFIG	Doubly Fed Induction Generator
DLF	Deterministic Load Flow
DNO	Distribution Network Operator
EE	Elementary effect
EENS	Expected Energy Not Supplied
EPRI	Electric Power Research Institute
EUE	Expected Un-served Energy
FCC	Full Converter Connected
GB	Giga Byte
GSA	Global Sensitivity Analysis
FACTS	Flexible AC transmission System
HVDC	High Voltage Direct Current
IEEE	Institute of Electrical and Electronics Engineers
ISO	Independent System Operator
LF	Load Factor
LLPRI	Load Loss Probabilistic Reliability Index
LoEE	Loss of Energy Expectation
LoLE	Loss of Load Expectation
LoLP	Loss of Load Probability
LSA	Local Sensitivity Analysis
MC	Monte Carlo
MSSA	Morris Screening Sensitivity Analysis
mvG	Multivariate Gaussian
NETS-NYPS	New England Test System-New York Power System

OPF	Optimal Power Flow
PC	Personal Computer
PCC	Partial Correlation Coefficient
PCM	Probabilistic Collocation Method
PD	Probability Distribution
PDF/*pd*f	Probability Distribution Function
PDSA	Probabilistic Dynamic Security Assessment
PL	Penetration Level
PLF	Probabilistic Load Flow
PMU	Phasor Measurement Unit
PRA	Probabilistic Reliability Assessment
PRI	Probabilistic Reliability Index
PSS	Power System Stabilizer
PV	Photo Voltaic
RAM	Random-Access Memory
RES	Renewable Energy Sources
RMS	Root Mean Square
ROCOF	Rate of Change of Frequency
SA	Sensitivity Analysis
ST	Sobol Total effect
SVC	Static VAr Compensator
TNSP	Transmission Network System Operator
TSA	Transient Stability Assessment
TSI	Transient Stability Index
VoLL	Value of Lost Load
VPRI	Voltage Violation Probabilistic Reliability Index

VSF	Voltage Sensitivity Factor
VSPRI	Voltage Stability Probabilistic Reliability Index

Abstract

Identification of influential parameters affecting power system voltage and angular stability analysis

Mr Buyang Qi, The University of Manchester, April 2019

This thesis investigates the effects of system uncertain parameters on power system voltage and angular stability analysis in network with Renewable Energy Sources. The main outcome of this research is the fast and accurate ranking of the system parameters based on their influence on power system voltage and angular stability.

The planning and operation of modern power systems have changed significantly compared to conventional power systems due to the addition of new types of load devices and renewable energy sources. These new technologies exhibit significant temporal and spatial uncertainties in generating and loading profiles within power systems and introduce additional level of uncertainty in network operation. This research proposes a probabilistic analysis approach for the evaluation of the effect of uncertain parameters on power system voltage and angular stability. The Morris Screening sensitivity analysis method coupled with a multivariate Gaussian copula to account for parameter correlations is used for the assessment of the importance of correlation modelling between uncertain parameters.

This research for the first time combines and validates the identification of critical parameters affecting system stability in general by using sensitivity analysis method. It also for the first time establishes the importance of modelling parameter correlation by using Copula theory. The approach proposed in this study facilitates efficient identification of important system parameters that needs to be accurately

modelled for reliable system stability studies and such ensures cost effective use of human and financial resources by system operators.

Declaration

No portion of the work referred to in the thesis has been submitted in support of an application for another degree or qualification of this or any other university or any other institute of learning.

Copyright Statement

Acknowledgements

I would like to express my sincere gratitude to my supervisor Prof Jovica V. Milanović for the guidance and advice I received from him during this research. His commitment to excellence and details inspired me for the production of the high-quality research, the results of which are presented in this thesis. His endless support greatly enhanced my progress in professional development.

My gratitude also goes to the members of Power Quality and Power Systems Dynamics group at The University of Manchester, especially to Dr Kazi Hasan, Dr Atia Adrees, Dr Panagiotis N. Papadopoulos, Dr Yue Zhu, Mr Wentao Zhu and Dr Jelena Ponoćko for their patience and supports provided to my work and the constructive opinions offered through discussions.

My special gratitude goes to my friends who have been by my side during this research. On our adventures toward higher degrees we share happiness and achievements. The precious and enjoyable times we experienced, and the unforgettable memories will always be cherished by me. May we all have a bright future.

Most importantly, I would like to express my thankfulness to my parents and my big happy family for their spiritual and financial support during this research. It is their understanding and endless love that encourages me on my pursuit of this degree and my conquering of the difficulties along the way.

To my family

Chapter 1 : Introduction

Modern power systems have been developed into highly interconnected and complex dynamic systems which have been deeply embedded into our society. The malfunction of a power system can cause great losses as production and living of modern society relies highly on the stable operation of the power system. Many research efforts in the past have been devoted to improving the reliability, efficiency and power quality of power systems. With the adoption of technologies such as renewable energy sources (RES) related generations, new types of loads, and flexible hierarchical control structures, future power systems can be operated in a more environmentally friendly, highly flexible, and more sustainable manner compared to ‘traditional’ power systems with conventional controlled power sources and structures. The planning and operation of modern power systems have changed significantly compared to conventional power systems due to the addition of these new technologies. The key characteristic of RES generation and new types of load is that their operation is highly temporal and spatial dependent. Hence, additional uncertainties are introduced from both sides, the network generation and loading [1]. However, to what extent can these network uncertainties affect power system stability related analysis remains unclear. This research aims to propose an approach in order to identify the influential system uncertain parameters and evaluate their corresponding effects on power system dynamic behaviour under various system operation conditions, and to establish the level of required accuracy of critical parameters modelling for the purpose of minimising the risk of power system voltage and angular instability.

1.1 Background

The UK power system is on the track to the development of a low-carbon, cleaner system by replacing fossil energy source with renewable energy source. According to the report regarding the electricity energy trends published by the Department of Business, Energy & Industrial Strategy, from 2011 to 2017, the percentage of coal decreased from nearly 30% to less than 10% while the percentage of wind increased from 4% to 14%, the same increase trend can be observed on other renewable energy sources like bioenergy and solar [2]. In 2018, the penetration level of low-carbon generation continuous to increase and accounts for 53% of

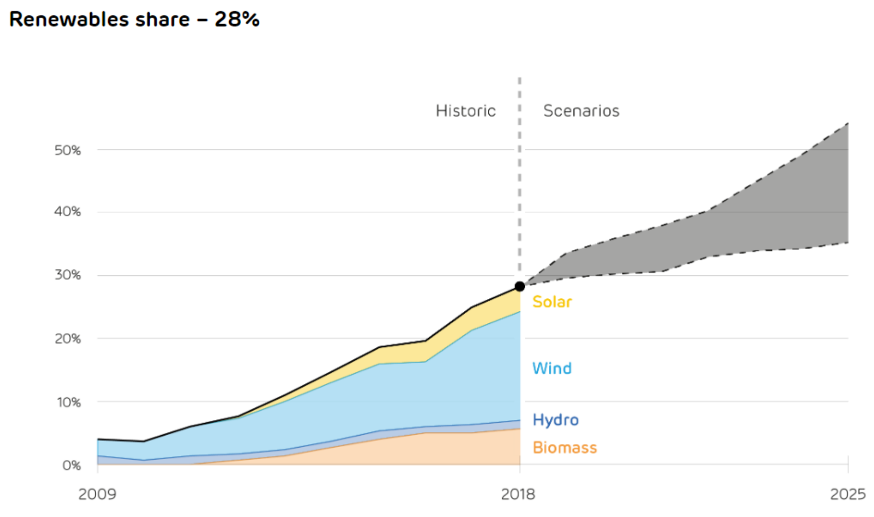

Fig. 1.1 The renewable generation share of Britain's power system in 2018 [3]

Britain's electricity, while coal has become a cold-weather backup fuel after years of precipitous decline [3]. Fig. 1.1 shows the penetration level of renewable generation share between 2009 and 2018, it can be observed that more than 28% of electricity came from renewables in 2018 and it is forecasted that half of Britain's electricity will be provided by renewables by 2025 [3]. The Distributed Energy Resources (DERs) and Renewable Energy Sources (RESs) with stochastic and intermittent nature which are replacing conventional operated power sources can lead to highly uncertain generation scenarios [1]. The stability analysis for power systems with high-penetration level of RES generation can be affected by the above-mentioned uncertain network parameters [4]. Due to the fact that power systems nowadays are forced to be operating closer to their stability margins in order to fulfil the increasing loading demands as well as to increase the efficiency of their use, it is vital to fully unveil the effects and risks these uncertain parameters introduced to systems from the perspective of power system stability.

1.2 Motivation

The variability exhibited by these new technologies voids traditional deterministic stability analysis since the 'worst case scenario' analysis of the network may lead to an overly conservative system design [5-7]. Probabilistic assessment methods can be helpful when uncertain parameters are included into system stability assessment. The probabilistic approach to network stability assessment is getting steadily adopted by researchers to be applied to all types of stability studies [1, 8-13]. The Monte Carlo (MC) simulations are commonly used to perform these probabilistic studies [4, 8, 14-16].

Due to the size of the power systems and the increase in the number of uncertain parameters, high computation resources are required when MC simulation is applied to probabilistic power system stability analysis. Monitoring every uncertain component in the evaluation of system performance within a power system is impractical and uneconomical. A power system can be stable for a physical disturbance while unstable for another at a given equilibrium set [17]. Not all uncertain parameters can have the same impact on the system operation. In such cases, priority ranking of system uncertain parameters, based on their influence on different stability aspects, can help the system operators to ensure optimal dynamic performance of the system with minimal use of human and computational resources.

Previous study employed sensitivity analysis (SA) techniques for the identification of influential parameters affecting small-disturbance stability within a network with RES generation [18]. The influence of load models, uncertainty in loading demand and RES generations on power system small-disturbance stability is analyzed in this study. The advanced Morris screening sensitivity analysis method (MSSA) is compared with the commonly used local sensitivity analysis method (LSA) and the global sensitivity analysis method (GSA) and its efficiency and accuracy have been demonstrated. This research expands the application of MSSA to the priority ranking of critical system parameters affecting the voltage and angular stability of the network with RES generation.

The research discussed above employs independent probability distributions for the modelling of uncertain parameters. The random sampled data set obtained in this way however, does not represent the correlations among uncertainties within the real system, hence the results of the analysis may not be accurate enough [19-25]. This research hence employs copula method for the accurate modelling of the correlation structures between system uncertain parameters.

This research uses the load margin, damping of the critical eigenvalues, and transient stability index (TSI) as stability indices for voltage, small-disturbance and transient stability analysis, respectively. The uncertainties of RES generation and loading (following the daily loading curve) are modelled probabilistically. The sensitivity analysis methods are applied for the priority ranking of critical uncertain parameters based on their influence on power system stability analysis, while the copula approach is used to model the correlation between input parameters.

1.3 Definition of Power System Stability

Power system stability has been considered as a critical problem for secure system operation since the 1920s [26]. The first laboratory test of power system stability was conducted in 1924 on miniature systems [27]; and the first field test of stability was reported in 1925 on a practical power system [28]. Traditionally, the salient stability problem on most power systems has been transient instability. As the industry evolved with the absorption of new technologies and controls, different types of system instability have been encountered [17]. There have been several early-year reports by CIGRE and IEEE Task Forces which define and classify power system stability [29-31]. These early works are believed out-of-date since they failed to reflect current industry needs completely. The new version of definition of power system stability was proposed in 2004 and states as follows [17]:

"Power system stability is the ability of an electric power system, for a given initial operating condition, to regain a state of operating equilibrium after being subjected to a physical disturbance, with most system variables bounded so that practically the entire system remains intact."

Power system stability depends mainly on the original operating conditions and the nature of the contingencies. It can be seen from the definition that the stability of an electric power system is the adjusted motion around an equilibrium set. Instability can happen when the balance between two opposing forces is affected after a disturbance. The system is required to either return to the initial operating condition or regain a new operating condition in a reasonable time after the system is subjected to disturbances. One thing that should be recognised from this definition is that the equilibrium should be stable in the sense of Lyapunov [17].

During the operation of power systems, small disturbances occur as loads are connected or disconnected continually, while the system must be able to react to these changes without failure. There is also a non-negligible likelihood for the network to be subjected to large disturbances of a severe nature due to faults or the sudden loss of major components. A large disturbance may lead to structural changes of the network since protection devices can operate to remove the faulty components. In these circumstances the rest of the power system must regain a state of operating equilibrium quickly and restore power supply to affected loads [32].

Power systems are large in size and contain numerous components which have potential hazards of generating disturbances. It can be extremely costly to design a power system that is stable for every possible contingency. A more practical and economical way is to select contingencies based on their probability of occurrence. Hence at a stable operation point the network can have a finite region within which it maintains feasible operational parameters which changes with the operating condition. Power system having larger range of operational parameters is considered to be a more robust system [17]. Since modern power systems are highly interconnected, the response of a power system after a contingency may involve many components and the instability in one tiny part of the system has the potential of generating cascading failure to a major portion of the system.

Although power systems experience variations in small magnitudes during operation continually, it is generally a valid assumption to consider that the system is originally in a steady-state condition. In this case the assessment of system stability when subjected to a specific disturbance can be conducted in a more straightforward way.

1.4 Classification of Power System Stability

When accessing problems related to power system stability, it should be noted that instability issues can take different forms and be affected by many factors. Different forms of instability issues can be contributed to by different factors, and may require different methods for improvement of stable operation. When solving instability problems it is convenient to divide stability issues into appropriate categories. A set of three commonly-used considerations were proposed as a guidance for stability classification [33]:

i. Consideration of the physical nature of the disturbance which caused instability. This can indicate where the instability can be observed.
ii. Consideration of the size of the disturbance which caused instability. This can reveal the appropriate calculation method.
iii. Consideration of the time span and devices involved during the system reaction of disturbance.

Fig. 1.2 presents an overview of the classification of power system stability with different categories and subcategories following the provided guidance.

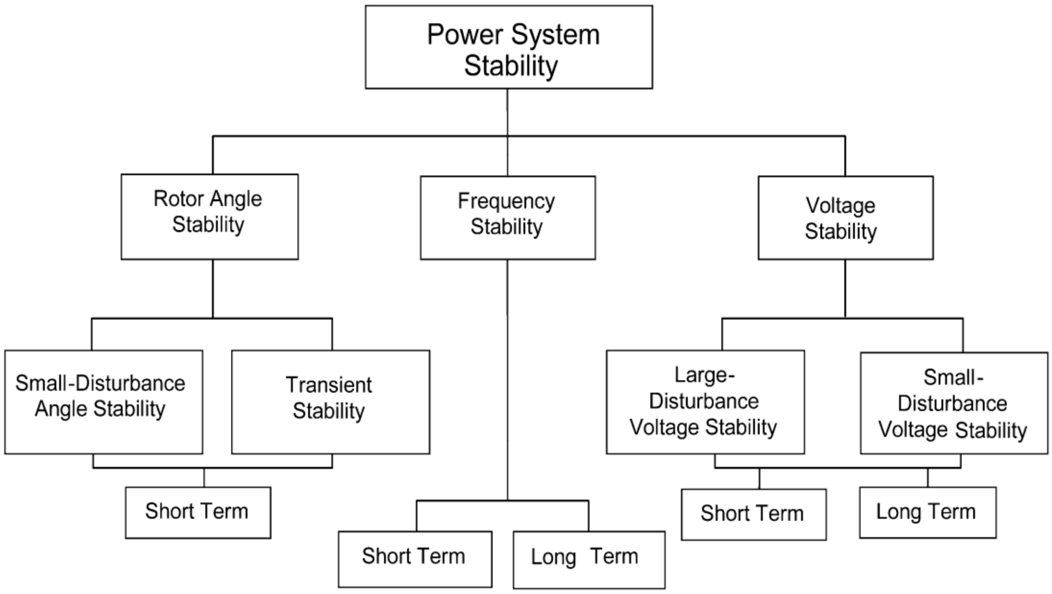

Fig. 1.2 Classification of Power System Stability [33]

1.4.1 Rotor Angle Stability

Rotor angle stability states the ability of the synchronous machines in an interconnected power system to maintain their synchronous after the system is subjected to a disturbance. Instability may occur if the disturbance causes angular swing variance in some generators and result in their loss of synchronism with other generators [17]. The opposing forces which should be balanced for rotor angle stability are the output electromagnetic torque and input mechanical torque of the rotating machines within the system (electromechanical oscillations) [32]. After the system being subjected to a contingence, the equilibrium between balanced torques can be upset and result in acceleration or deceleration of the influenced rotors. Hence the angular position of the temporarily faster generator is in advance compared to the relatively slow generator. Depending on the highly nonlinear power-angle relationship, the angular separation between generators can either be reduced by transferring part of the load from the slow generator to the faster one, or increased beyond a certain limit where further increment of angular separation is accompanied by decreasing power transfer. The angular stability of a power system relies on whether or not the system can absorb the kinetic energy generated by these rotor speed differences [17]. Numerous controllers are involved in the regulation of generator's output and can significantly contribute to rotor angle stability.

Two restoring torques play vital roles in the rotor angle stability regulation procedure: *synchronizing torque* and *damping torque*, in phase with rotor angle deviation and speed deviation, respectively. If one goes further down to the sub-categories of instability, the lack of *synchronizing torque* or *damping torque* will result in *aperiodic instability* or *oscillatory instability*, respectively [33].

By inspecting Fig. 1.2 one can observe that two sub-categories were derived from rotor angle stability based on the size of stability problems, *small-disturbance rotor angle stability* and *large-disturbance rotor angle stability*. These sub-categories facilitate more detailed analysis of instability issues since they unveil the size of disturbances [33].

Small-disturbances refer to sufficiently small contingencies introduced to power system that allow system equations to be linearized for the purpose of analysis [17]. Contingencies like continually occurring changes in load and power flow fall in this sub-category. *Small-disturbance stability* analysis involves study of local area mode oscillations and inter-area oscillations. The time-frame of interest for this kind of stability issues are typically 10 to 20 seconds [34] while can be extended to 1 or 2 minutes in very large systems [32]. The lack of *synchronizing torque* and the lack of sufficient *damping torque* are believed to be the two critical triggers of small-signal instability. Modern power systems use continuously acting generator voltage regulators to eliminate aperiodic instability caused by the lack of *synchronizing torque*. High response exciters that are typically used in modern power systems however, may contribute to reduction of damping torque or even result in negative damping torque which contributes to small-disturbance rotor angle instability [17].

Small-disturbance rotor angle stability problems can be local or global in nature [17]:

i. *Local problems* affect a small portion of the power system. These kinds of instability involve rotor angle oscillations of an individual power plant against the rest of the system. Damping of these oscillations depends on the generator excitation control, the strength of the power system and the plant output.

ii. *Global problems* involve the swinging oscillation between multiple groups of generators and can have widespread effects. The nature of global problems is very different to local problems. A major trigger for inter-area oscillations is proved to be load characteristics.

Large-disturbance, or *transient disturbance*, refers to severe disturbances like short circuit or loss of power plant which can change the topology of a power system. The original operating state of the system and the severity of the disturbance are the two key factors that can influence system transient stability. In power systems, the typical severe transient disturbances can be in the form of a fault on transmission facilities and loss of generation or large loads. The severe transient disturbance can result in large change of rotor angles, power flows, bus voltages and other system variables. The time frame of interest for large-disturbance stability study is usually 3-5 seconds after the system is subjected to a disturbance. However, with extremely large systems with salient inter-area swings, the time frame can be extended to 10-20 seconds [33].

Since the time frame for the study of rotor angle stability is relatively short (with maximum time frame around 2 mins), this type of stability issues is categorized as *short term phenomena*, according to Fig. 1.2.

1.4.2 Frequency Stability

Frequency stability refers to the ability of the power system to maintain steady operation frequency after the system is subjected to a severe disturbance leading to a significant imbalance between generation and load. Instability of system frequency usually has the form of sustained frequency swings and can result in tripping of generating units and loads [17]. The time frame of interest can be short from fraction of seconds (responding time for component like generator controls and protections) to several minutes (responding time for component like prime mover energy supply systems and load voltage regulators). Hence in Fig 1.2 the sub-categories for frequency stability are divided into *short-term* phenomenon and *long-term* phenomenon.

For frequency stability problems the general trigger-factors are insufficient equipment responses, poor coordination of control and protection component, or insufficient generation reserve [17]. Severe disturbances can cause a large interconnected system to break into separate small islands. The stability in this case depends on the overall response of the islands from the perspective of their mean frequency. Many studies have been done for the analysis of frequency stability issues, e.g., [35-37]. It should be noted that for systems with low inertia in particular, the dynamic performance of the system can be highly sensitive to frequency variation, hence frequency stability problems are always a matter of careful consideration. For example, replacing synchronous machines with converter-embedded wind or PV generators can result in reduced system inertia and make the system more vulnerable to frequency instability [34].

1.4.3 Voltage Stability

Voltage stability refers to the ability of a power system to maintain steady voltages on all system buses after the system was subjected to disturbances. Power system voltage stability depends on whether or not the equilibrium set between load demand and load supply can be regained or maintained after the system is subjected to a disturbance [17]. Power system voltage instabilities occur in the form of voltage variances on some system buses. These variances in bus voltages may lead to voltage collapse, loss of load in an area or tripping of power plants by their protection mechanism, ending up in cascading system outages. Generators within the power system may lose their synchronism with the rest of the network as a result of these outages [38]. The timeframe of interest for power system voltage stability varies from few seconds (short-term phenomenon) to tens of minutes (long-term phenomenon), according to Fig. 1.2.

Voltage collapse refers to the process of the events accompanied by voltage instability which lead to a blackout or surprisingly low voltages in parts of the power system [33, 39]. Intentional or un-intentional tripping of some loads can happen after voltage collapse while system tries to maintain steady state operation at low voltage.

The trigger factor for power system voltage instability is usually related to the loads. When subjected to disturbances, power consumed by the loads tends to be restored by system movements provided by components like distribution voltage regulators, tap-changing transformers and motor slip adjustment. Depending on their power-voltage characteristics the restored loads can increase the reactive power consumption and lead to further voltage reduction [33, 39-41]. The voltage drops caused by active and reactive power flow through inductive reactance of the system is proved to be a major factor contributes to power system voltage instability. This sets limits to the capacity of power transfer and voltage support for a given network. Voltage instability can happen when a disturbance increases the reactive power demand to the amount that available reactive power sources cannot fulfil [17].

As seen in Fig. 1.2, to reveal the appropriate analysis method for power system voltage stability problems, it is useful to separate the study into two sub-categories based on the size of disturbances, *small-disturbance voltage stability* and *large-disturbance voltage stability*.

i. *Small-disturbance voltage stability* states the ability of the system to maintain stable voltages on buses when subjected to small contingences like incremental changes in system load [17]. System equations can be linearized with proper assumptions for analysis and factors that influence stability can be identified. However for nonlinear effects like tap changer controls the nonlinear analysis should be used in a complementary manner [42, 43].

ii. *Large-disturbance voltage stability* states the ability of the system to maintain stable voltages on buses when subjected to large contingences like loss of generation or system fault [17]. Analyses of this kind of stability issues require the examination of the nonlinear response of the system over a period of time which captures all possible performance of devices involved during the disturbance.

It should be noticed that the distinction between voltage and rotor angle stability is based on the imbalance-influenced opposing forces and the principal system variable in which the consequent instability is apparent [17].

With the classification of power system stability problems, the analysis of instability issues can be produced effectively and conveniently. This research mainly focuses on the analysis related to power system small-disturbance voltage stability and small/large-disturbance angular stability in order to evaluate the impact of uncertain system parameters on network dynamic behaviour.

1.5 Applications of Power System Stability Studies

A power system must keep it integrity after disturbances and have the ability to withstand a wild variety of faults for reliable service. However, limited by economic and technical restrictions power systems in practice can only be designed to be stable for selected disturbance based on their probability of occurrence and severity. Power system stability related studies can ensure secure operation of transmission networks by:

i. Ensuing proper selection and deployment of protective and emergency control facilities.

ii. Obtaining power system stability limits and ensuring operation stays within these limits.

Power system stability studies provide good references for the system operators when monitoring system components from potential instability hazards. One of the tasks for a power system operator is to make sure that the system plants are operating under acceptable conditions and output reliable electric power after subjected to credible events under heavily stressed scenarios. There are several roles of system operators according to [44]. For example, the ISO (Independent System Operator) is responsible for planning and operation of the network, and TNSP and DNO (Transmission Network System Operator, Distribution Network Operator) should be responsible for their own portion of the network [34]. The stable and economical operation of a power system within security limit is of great interests to these operators. Two types of studies, operational studies which focus on short-term secure and reliable operation of the network, and planning studies which are looking at long-term market-profiting operation of the network, are considered by operators. Table 1.1 below presents the applications of stability studies in different areas and time frames of system analysis. Power system transient, small-disturbance and voltage stability problems are equally important for all areas of the

Table 1.1 Power system stability aspects and their implications in system-wide regime [34]

Power System Phenomenon	Interest of ISO (whole system)	Interest of TNSP, DNO (part of the network)	Operational Studies (short-term)	Planning Studies (long-term)
Transient Stability	✓	✓	✓	✓
Small-signal Stability	✓	✓	✓	✓
Voltage Stability	✓	✓	✓	✓
Frequency Stability	✓	×	✓	×

network and are of interest of both short-term operational studies and long-term planning studies. The frequency stability is usually of concerned for operators responsible for the whole system, and when the operational studies are considered.

1.6 Historical Timeline of Power System Stability Studies

The industry had discovered the importance of power system stability in the early 1920s [26]. The traditional salient power system stability issues were considered to be transient stability [14]. With the development of components like high-speed fault clearing tools, high response exciters and special stability controllers and protection mechanisms the transient stability performance of power systems have been improved significantly.

In the early 1930s, system dynamics still needed to be analysed by hand-calculating swing equations using step-by-step numerical iteration. The modelling of generators and loads were simplified as fixed voltage behind transient reactance and constant impedances, respectively. The assessment of power system stability was significantly enhanced from 1950s with the use of computers. Simulations of system dynamics could be used for the analysis of the dynamic characteristics of generators and power plants [45]. The development of electric energy transmission networks and interconnection of different small power systems for economic reasons lead to inter-area oscillations and voltage stability issues [15]. The challenges in 1960s were the rising system complexity and increased consequences of instability since most power systems in the U.S. and Canada, and other parts of the world were becoming part of one or two large interconnected systems. The related problem of stability and the importance of power system reliability were unveiled by the Northeast Blackout in the USA on November 9, 1965. Researchers have successfully developed components like SVC (static VAr compensator), FACTS [46] (flexible AC transmission system) and HVDC (high voltage direct current) converters to solve small-disturbance stability and oscillation problems within large interconnected power systems.

Power system frequency stability problems have become a concerning issue during 1970s and 1980s as they were experienced following major system upsets. Several investigations were performed for the analysis of underlying causes for frequency stability issues and dynamic long-term simulation programs were developed to assist in their analysis [47-51]. Many of these investigations focused on the performance of thermal power plants during system upsets [36, 52-54]. A report by IEEE Working Group in 1983 provided guidelines for enhancing power plant response to major frequency disturbances [55]. In 1999, a CIGRE Task Force Report was presented unveiling analysis and modelling needs of power systems during major frequency disturbances [56].

Power system voltage stability problems also started to be deeply analysed since 1970s as this type of instability was the cause of several severe system collapses [33, 39, 57]. Large interconnected power networks did not face voltage instability until early 1980s. Voltage stability problems were associated with weak radial distribution systems, and were a result of heavy loading and long-distance power transfer in stronger networks. Consecutively Powerful analytical tools were developed [42, 58, 59] and well-established criteria and study procedures evolved [43, 60].

For the planning and stable and secure operation of a modern power system all the above-mentioned stability problems are of concern. With the development of transmission technologies, the possible types and combinations of power transfer transactions may grow enormously. The traditional structured and conservative system operation manner has been replaced by competitive utility environment. The modern trend for power system planning and operating is to make use of the online dynamic security assessment with the help of computer hardware and stability analysis software [45].

Fig. 1.3 presents a timeline view for historical appearances of different power system stability problems.

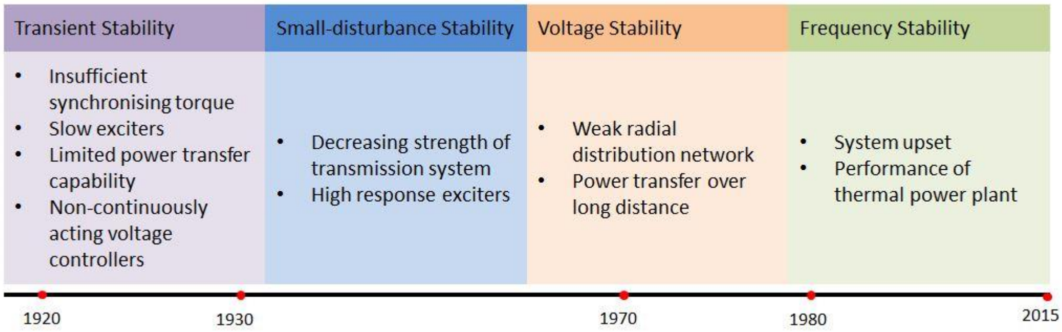

Fig. 1.3 Historical appearances of power system stability problems [34]

1.7 System Simulations for Stability Studies

In power system *transient stability* simulations, the consecutive steps of load flow, defined initial conditions and defined disturbance events are usually considered. The influence of transient disturbance on system behaviour can be observed through power flows, bus voltages, machine rotor angles and speeds [34]. Due to the non-linear power-angle relationship, a common practice for transient stability analysis is through time-domain simulation.

For power system *small-disturbance stability analysis*, the consecutive steps of load flow, defined initial conditions and model analysis are often involved. Eigenvalues and eigenvectors can be obtained through modal analysis, which determine the stability and controllability/observability of a power system, respectively [34].

Voltage stability simulation involves real solutions of system power flow equations, with the consecutive steps of load flow, defined initial conditions, and real power-voltage (P-V) and reactive power-voltage (Q-V) curves analysis.

For *frequency stability* simulations, the constructive steps of load flow, derived disturbance events and calculations of frequency deviation/rate of change of frequency (ROCOF) relays are always involved.

The analyses of different types of power system stability issues require calculation of different stability indices to quantify the system dynamic behaviour.

1.8 Summary of Past Work on Probabilistic Stability Analysis

This section of the thesis provides brief summary of the past researches in the area of stability analysis of power systems with RES generation.

Research results presented in [61] focused on probabilistic approach for the evaluation of the transient stability of a wind farm. The probabilistic modelling of wind farm, fault parameters (type, location, impedance, FCC, duration) and uncertain load had been considered. The procedure and resulting index provide the measurement of the likelihood of power system with RES generation to encounter transient instability due to a transmission line fault. The critical transmission lines can be identified through this approach. However, the application of this approach was only illustrated on a simple 4-bus system with limited number of uncertain parameters. In [62] the influence of wind speed and wind penetration on transient stability of a two-area four-machine system are studied. The wind speed was modelled probabilistically, and the wind turbine model and wind generation penetration level were considered. This paper clearly addressed the risk of transient instability a power system may face due to the added uncertain wind turbines. However, the application is still limited to a simple power system model.

In [9] the probabilistic small-disturbance stability analysis for power systems with Plug-in Electric Vehicle and wind generation was presented. This paper addressed the requirement of the detailed modelling of Plug-in Electric Vehicle for modern power systems. It also highlighted the benefit of the application of quasi-Monte Carlo method on stability studies. However, this research did not focus on the quantitative measurement of the influence of the uncertain parameters' on power system small-disturbance stability. An analytical probabilistic analysis of small-disturbance stability of power system with wind generation had been presented in [8, 63]. The proposed method directly calculated the PDF of the critical eigenvalues of a large-scale network from the PDF of a grid-connected wind power generation in order to access the impact of RES generation penetration. These papers illustrated that RES generation can cause the system to lose stability when a range of operating conditions and uncertainties in general were considered even though the system was deemed to be stable based on deterministically studies. This highlighted the problems associated with high penetration of RES generation on power system small-disturbance stability. The spatial correlation of wind generation was also studied. However these studies did not evaluate to what extend can the small-disturbance stability be influenced by penetration of RES generation.

The study reported in [63] focused on the assessment of voltage stability of a large-scale power system with wind generation. The multi-point linearization technique was used in probabilistic analysis to achieve better computational accuracy.

The impact of large wind power generation on frequency stability was studied in [64]. This research concluded that a range of options can be considered to provide wind turbine support to system frequency in an emergency situation. These options include voltage or alternatively frequency dependent active power control. Paper [65] presented a risk assessment approach to analyse power system security for operational planning under high penetration of wind power generation. The steady-state voltage and overload evaluations and frequency response adequacy assessment can be run simultaneously through the proposed approach. The paper also addressed the need to reconsider potential impacts of frequency events in modern RES penetrated networks which are experiencing more frequent frequency violations.

It can be concluded that the probabilistic analysis of the stability of RES penetrated power system is attracting more and more attention in recent years due to the increased penetration of grid-integration of RES generation. The variability of RES generation could bring operational risks in maintaining small-disturbance and voltage stability, and the lack/reduction of inertia may reduce the frequency response capability of a network. Previous work mainly focused on the small-disturbance stability problems, and the uncertain RES generation considered was mainly wind turbines. None of the past publicly available research has combined the general analysis of voltage and angular stability of large network with significant RES penetration, nor the influence of different operational or parametric uncertainties on the results of this assessment.

1.9 Research Aims and Objectives

The current industry approach for power system stability analysis is to develop mathematical models for every single power plant within the system and perform simulations to evaluate system dynamic behaviour following a disturbance. However, since modern power systems are large in size and complex in structure, using the above-mentioned approach can consume huge amount of resources. The fact is that power plants within a network can have different sensitivity to contingencies and different types of contingencies can have different occurrence possibility. The key questions that this research is trying to answer is: Which of the multitude of diverse parameters of the system, for example mathematical models of different components and power system operation conditions, are important to be modelled and monitored? What is the level of uncertainties of different model parameters that can be tolerated to ensure reliable assessment of power system dynamic behaviour? The purpose of this research is therefore to develop an efficient and budget-saving approach for power system planners and operators to monitor and access power system stability with minimal resources.

This research aims to develop a probabilistic approach for the identification and priority ranking of the influential parameters for accurate assessment of power system stability, and to establish the level of required level of uncertainties of critical parameters in order to minimise the risk of different forms of power system instability. The outcomes of this research should be a generalised approach which can be used for reliable and efficient power system voltage and angular stability related analysis.

The following objectives have been specified for the purpose of achieving the above-mentioned aims.

i. Literature review to summarise the state-of-the-art of research in the area of modelling of uncertain system parameters, and the priority ranking of critical system parameters based on their influence on different aspects of power system stability analysis.

ii. To perform probabilistic load flow calculations with appropriate modelling of a range of uncertainties in a network with renewable generation to establish a range of possible operating conditions for subsequent stability analysis.

iii. To model suitably large test network in DIgSILENT PowerFactory for power system voltage and angular stability analysis.

iv. To access the applicability of established sensitivity analysis methods for power system related studies. And to illustrate the effect of modelling the correlations between system uncertain input and output parameters through sensitivity analysis methods.

v. To compare the employed sensitivity analysis methods based on their performance when applied to power system analysis studies. Find the appropriate approach for fast implementation in modern power system.

vi. To establish representative case studies for the assessment of power system stability margins under different operation conditions, for example, various system load levels, proportion of renewable generations, uncertainty levels, fault locations, etc.

vii. To access the applicability of copula methods for the correlation modelling between uncertain power system parameters to illustrate the importance of correlation modelling of uncertain parameters for power system stability related studies.

viii. To illustrate the developed methodology on appropriate models of power system transmission network.

1.10 Main Contributions of the Research

The work within this thesis contributes to the area of power system stability analysis and is exclusively focused on the analysis of system dynamic behaviour when network is operating under the conditions where uncertain parameters are connected. The main outcome of this research is the proposed sensitivity analysis approach for the identification of critical parameters affecting power system voltage and angular stability as a whole. The results proved that by accurately modelling the most important influential uncertain parameters, the system dynamic behaviour and stability margin can be estimated with sufficient accuracy. This can help to achieve better system management with less monitoring and provide efficient and fast evaluation of system operating conditions in the presence of operational uncertainties.

The contributions of this thesis can be summarised as follows. (Paper numbers, given in parenthesis, after each paragraph indicate that the relevant contribution has been published in the international journal or in the proceedings of the international conference. A full list of the author's thesis-based publications is provided in Appendix D.)

i. The probabilistic assessment of power system voltage stability in a network with renewable generation. This analysis identifies the critical buses within the test network, and evaluates the influence of uncertain parameters on power system load margins under different loading levels.

The results extend the probabilistic voltage stability assessment of power system with uncertain parameters [D2, D3].

ii. The implementation of sensitivity analysis methods in power system voltage stability related studies. The thesis compares the performance of six commonly used sensitivity analysis methods when applied to complex power systems. The relationships between uncertain system input parameters and output dynamic behaviour have been illustrated and evaluated. The Morris Screening Method has been selected as the best option among the evaluated six sensitivity analysis methods as it is both the most efficient and sufficiently accurate [D4]

iii. The identification of critical parameters affecting power system voltage and angular stability in networks with renewable generations. This research for the first time combines and validates the identification of critical parameters affecting system stability globally, i.e., considering more than one stability criterions by using efficient sensitivity analysis method, the Morris Screening Method [D1, D5].

iv. The use of copula method for the correlation modelling between uncertain system input parameters. This research for the first time establishes the importance of modelling parameter correlations for the identification of critical parameters affecting global system stability [D1, D5].

v. Global power system stability analysis for various system operating conditions considering the power system behaviour when the network faces complex conditions, including various loading levels, various renewable generation penetration levels, various fault locations, various fault durations, etc. These results help the assessments of power system dynamic behaviour of modern uncertainty-rich networks and facilitate the planning and operation of modern power systems [D1, D5].

1.11 Thesis Overview

This thesis contains 7 chapters in total. The contents within the chapters are outlined below:

Chapter 2: Modelling and Analysis of Uncertain Power Systems

This Chapter provides a review of the state-of-the-art of modelling and analysis techniques of uncertain power systems. The stability indices and the deterministic and probabilistic approaches for power system stability analysis are also reviewed. A comparison between deterministic and probabilistic assessment has been performed. The probabilistic approaches are proved to be a more suitable method for stability analysis of modern networks. The probabilistic simulation techniques for power system stability analysis and the probabilistic modelling of system uncertain parameters have been reviewed. This chapter also introduces sensitivity analysis methods for stability analysis of uncertain power systems.

Chapter 3: Network and Simulation Techniques

This Chapter introduces the test network and simulation techniques used in this research. A detailed layout of the test network with uncertain RES has been introduced. The probabilistic modelling of system uncertain loads and RES generation are demonstrated. This chapter also introduces the load models used for this research, together with the simulation requirement and procedure for probabilistic power system analysis. Optimal power flow calculation which has been used in this research for conventional generation re-dispatch has also been discussed.

Chapter 4: Probabilistic Ranking of Critical Parameters Affecting Voltage Stability

This Chapter of the thesis demonstrates the implementation of probabilistic analysis on power system voltage stability analysis. The approach has been applied for the simulation of the complex operation conditions a modern power system may face when uncertainties are introduced. The load buses have been analysed and ranked based on their robustness against voltage collapse. The weak areas within the test network have been identified. The effects of uncertain load, wind generation, or PV generation on power system voltage stability margins have been illustrated.

Chapter 5: Voltage and Angular Stability Analysis of Uncertain Power Systems using Sensitivity Analysis Methods

In this Chapter six sensitivity analysis methods have been used to perform power system voltage stability analysis. This Chapter also establishes case studies with different load levels to validate the robustness of the sensitivity analysis approaches for power system stability studies. The performances of the six sensitivity analysis methods are compared and the Morris Screening Method has been recommended as the best method to use, among the six considered approaches since it combines both the accuracy and the computational efficiency in one package. The application of Morris Screening method on voltage and angular stability analysis has been discussed in this chapter and the influential parameters within uncertain power systems have been identified.

Chapter 6: Stability Analysis Considering Parameter Correlations

This Chapter employs copula method for the modelling of the correlations between system uncertain loads and RES generation. The results presented in this Chapter and those presented in Chapter 5 are compared to demonstrate the importance of accurate correlation modelling between input uncertainties when performing power system stability analysis.

Chapter 7: Conclusions and Future Work

In this chapter the conclusions of this research are summarized. The potential directions for future implementation and research in this area are also identified.

Chapter 2 : Modelling and Analysis of Uncertain Power Systems

A range of well documented tools are available to researchers for power system analysis and modelling of uncertainties. In this section, deterministic and probabilistic approaches for power system stability studies are presented and compared including review of most frequently used power system stability indices. Probabilistic modelling of different uncertain parameters has been also discussed and appropriate conclusions drawn. Finally, the chapter reviews the most frequently used sensitivity analysis methods in power system stability studies.

2.1 Power System Stability Indices

The dynamic behaviour of different categories of power systems are affected by different parameters. For *transient stability* related analysis, the commonly used approach is usually focused on the evaluation of the maximum relative rotor angles between generators after a fault [66].

The *small-signal stability* of a system is determined by the roots of the characteristic equation of the system first order approximations [67]. Calculation of the eigenvalues of the system critical mode is required, as shown in (2.1). Equation (2.2) calculates the damping ratio of the eigenvalues of the system critical mode.

$$\lambda = \sigma \pm j\omega \tag{2.1}$$

$$\xi = \frac{-\sigma}{\sqrt{\sigma^2 + \omega^2}} \tag{2.2}$$

In (2.1), λ is the eigenvalue of the system critical mode, σ is the real part of the eigenvalue and represents the damping of the critical mode, while $j\omega$ is the imaginary part of the eigenvalue where ω represents the frequency of the critical mode. ξ in (2.2) is the damping ratio of the critical mode. According to the damping ratio ξ of the eigenvalues of the system critical mode, if a complex eigenvalue has negative real part, the oscillations will decay and lead to the stable operation of the system. It is desirable to have a larger damping ratio ξ since it can result in faster system stability operation restoration after a disturbance [68]. A typical threshold of ξ > 5% is often implemented for control design purposes [69].

The critical index for *voltage stability* analysing is the voltage sensitivity factor (VSF as shown in (2.3)) and the stability criterion is $VSF_i > 0$ [34]. In equation (2.3), ΔV_i measures the variation of load bus voltage between operating point and voltage collapse point while ΔQ_i measures the variation of system reactive power. This index measures the sensitivity of load bus voltage to variations in load reactive power. Recent studies also employ loadability, or system load margin, which measures the maximum load the system can support before voltage collapse, as voltage stability index [70, 71]. Fig. 2.1 and Fig. 2.2 show the Q-V and P-V curves commonly used in voltage stability analysis as a demonstration of the stability indices.

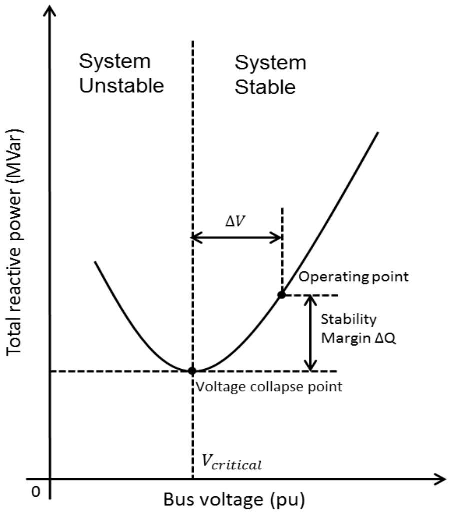

Fig. 2.1 The Q-V curve

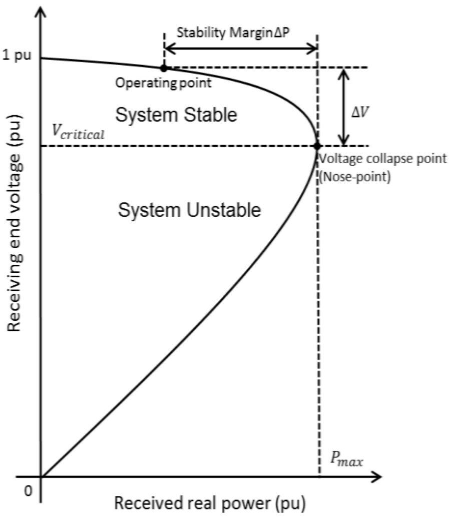

Fig. 2.2 The P-V curve

$$VSF_i = \frac{\Delta V_i}{\Delta Q_i} \tag{2.3}$$

For *frequency stability* analysis the important indices are frequency deviation [64] and rate of change of frequency (ROCOF) [72]. Frequency deviation is the absolute value of the difference between the system rated frequency and frequency nadir (frequency nadir measures the lowest frequency value after a disturbance). The frequency deviation should normally not exceed 2 Hz for 50 Hz system [73, 74]. ROCOF is the time derivative of the power system frequency. It identifies the significant load-generation imbalance conditions in which system inertia is low due to disposal of synchronous generation [75].

Researchers usually establish several operation conditions to access power system dynamic behaviour for traditional networks. Modern power systems face complex operation conditions as they have parameters which exhibit stochastic behaviour. Different contingencies can have different occurrence probabilities [17] and considering all possible disturbances can be quite impractical. Hence a probabilistic approach for system stability assessment is more efficient and accurate compared to a deterministic approach, especially when applied to networks with uncertain parameters connected.

2.2 Power System Stability and Reliability Assessment: Probabilistic vs Deterministic Approaches

Power system analysis methods are used for network stability and reliability assessment during operation and planning stages. The *stability assessment* focuses on the ability of a network to maintain stability under normal operation conditions, and to regain stability after a disturbance. [33]. The *reliability assessment* measures the ability of a bulk system to deliver electricity to all points of utilization within accepted restraints and in the desirable amount [76]. The objective of *system planning* is to achieve a minimum cost strategy for expansion of generation, transmission and distribution system while supplying the forecasted load within a set of technical, economic, and political constraints [77-79].

Probabilistic and *deterministic* approaches are the two most commonly used methods for power system stability and reliability assessment. Traditionally, deterministic frameworks were used as the implementation is straightforward. For example, when point-estimation method is used, only a limited number of contingencies are selected to be applied to certain operating condition based on the experience of the researchers. The state matrix of the test network can be constructed with fewer parameters and the output matrix can be solved using small amount of calculation resources. They are suitable for the applications within networks with simple structures. However, the power industry has been through a significant restructuring all over the world since the 1990s, which has changed the traditional vertically monopolistic structure into competitive and deregulated markets structure to chase increased efficiency in the electricity production and utilization [80]. Modern power systems are also increasingly relying on utilization of RES generation instead of conventional fossil fuel powered generators. Deterministic approaches can be inadequate due to the fact that they fail to capture the complex operating conditions of the system when transmission networks include new types of power electronics-interfaced generation and load technologies, which introduce additional uncertainties. The deterministic assessment approach might lead to an overly conservative estimate of the stability issue since it always considers the 'worst-case' scenario [34], or underestimate the severity of a scenario by using average values. The probabilistic approaches, on the other hand, can increase utilization capacity of existing assets, hence they can be more suitable for future power systems. This section will give a review of the existing deterministic and probabilistic approaches for the assessment of power system stability and reliability during operation and planning. A comparison between deterministic and probabilistic approaches will be provided, and the needs for the probabilistic approach will be identified.

2.2.1 Deterministic Assessment of Power System Stability, Reliability and Planning

2.2.1.1 Power System Stability analysis

Transient stability analysis has been widely utilized in power system dynamic security analysis for decades. The early approaches for transient stability analysis use deterministic stability criteria. These criteria consider several extreme operation conditions and critical disturbances which were hand-picked by ‘expert experience’ [80]. The considered critical disturbances were mainly load levels, fault types and fault locations and ‘extreme’ values like minimal/maximum/average values were used in calculation.

Small-disturbance stability analysis is important since it can be used to ensure the secure and healthy operation of power system with growing uncertainties [80]. The investigation of small-disturbance stability of a power system requires detailed modelling of system dynamic components and relevant control systems [81]. The early approaches for small-disturbance stability assessment were based on deterministic framework, and only the hand-picked operation conditions were considered like transient stability analysis.

The deterministic assessment of power system stability can provide a straightforward understanding of the system contingencies and typical operation conditions which represent system general behaviour. They can be fast applied to networks with simple structures and give the estimation of system stability margin. However it ignores the stochastic nature of a real power system and cannot accurately represents a modern deregulated power system with high penetration level of new types of loads, generators, network topologies and component faults with probabilistic characteristics [82].

2.2.1.2 Power System Reliability analysis

The N-1 criterion is usually used for the assessment of *power system reliability.* The reliability of a power system is evaluated based on the ability of a power system to withstand any prescribed outage situations within acceptable constraints [83]. It should be noted that deterministic approach of power system reliability analysis only considers a state condition for a specific combination of bus loads and generating unit outages, it fails to recognize the unequal probability of the occurrence of the evens that can lead to potential operating security limit violations [80]. Deterministic approach for power system reliability analysis is theoretically not suitable for use in modern deregulated electricity market.

2.2.1.3 Power System Planning

The deterministic approaches for power system planning consider only the extreme situations which are chosen based on subjective judgements. A system designed based on deterministic planning methods can withstand severe situations that have a low probability of occurrence. However, it cannot address all the transmission challenges and uncertainties when designing a modern power system which faces complex uncertain operating conditions [80]. The Deterministic Load Flow (DLF) was traditionally employed in the area of power system planning within a vertically integrated power system. The main outcomes through the DLF method are the magnitude and phase angle of the bus voltage as well as the active and reactive power flowing in each line. This method only considers the system condition of a set of determined values selected by system planner and ignores some power system uncertainties (loss of generator, variation in load demands, etc.). A huge amount of computing resources are required if a planner wants to carry out DLF analysis for every possible modern system outages [80].

2.2.2 The Needs for the Probabilistic Approach

Section 2.2.1 gives an overview of the deterministic approaches utilised in power system stability, reliability and planning assessments. Deterministic methods evaluate a system based on 'point estimate' and always tend to make an overly conservative estimation of the scenario [34]. The major drawback of deterministic methods is that they are not able to meet modern industry requirements. A more effective and reliable method is needed. Researchers make use of the probabilistic approaches which can provide realistic and accurate modelling of power system behaviours. The probabilistic assessment of power system dynamic is able to capture single and multiple component failures and recognize not only the severity of the disturbances but also their likelihood of occurrences [84]. Probabilistic approaches have certain advantages over the deterministic methods. For example, only a limited number of contingences can be considered in deterministic assessment whereas a wide variety of contingencies can be selected with probabilistic assessment. The generation and load profiles are usually presented as high-medium-low level in deterministic studies while these parameters can be presented in more accurate hourly/daily/seasonal/annual patterns in a probabilistic study [6, 85].

2.2.3 Probabilistic Assessment of Power System Stability, Reliability and Planning

2.2.3.1 Probabilistic Power System Stability Analysis

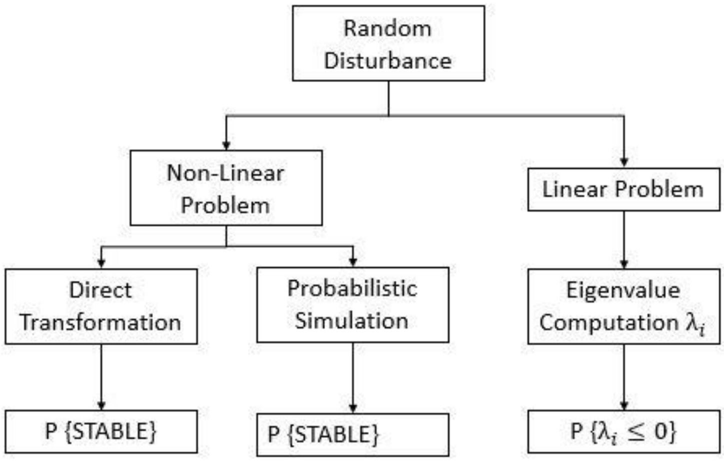

Fig. 2.3 The flow chart of probabilistic power system stability analysis [89]

For Power system *transient stability* assessments, there are two general probabilistic methods: conditional probability theorem-based methods and Monte-Carlo simulation-based methods. The first attempt of using probabilistic methods in transient stability studies was produced in the 1980s [86-88]. These early researches were focused on the probabilistic aspects of fault type, fault location, fault clearing time and system operating conditions. A complex analytical transformation was considered by Anderson & Bose in 1983. The proposed block diagram was presented in Fig. 2.3 [89].

Following on, in 1988 a transient stability analysis was proposed that derived the joint probability distribution function (PDFs) for the critical clearing time (CCT) [90]. In 1995, a bisection algorithm with the ability to reduce the computation time required for power system transient stability analysis was introduced [91]. A risk-based security index which determines the operating limits in electric power systems was reported in 1997 [92]. More recently, a grid-computing technology which significantly improves the computing efficiency of power system stability analysis was conducted [82, 93]. A typical procedure for probabilistic transient stability analysis is shown in Fig. 2.4 [94].

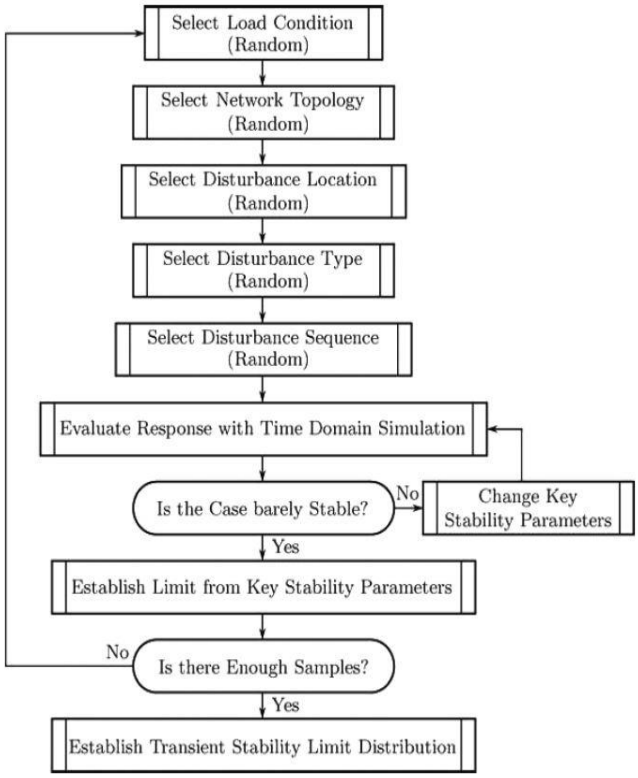

Fig. 2.4 The block diagram for probabilistic transient stability analysis [94]

The utilization of probabilistic assessment for power system *small-disturbance stability* started in the late 1970s. Researchers employed linear, time variant state-space models to study perturbations of the system state variable from the nominal values at a specific operating point [95, 96]. In recent researches, sensitivity analysis methods are employed to provide an approach to identify the most influential uncertain parameters in networks with renewable generations [34]. The Morris screening method was employed by Hasan et al providing an accurate yet efficient approach for the ranking of the most influential input parameters which affect power system small-disturbance stability [97]. For the analysis of the dynamic behaviour of large-scale power systems with higher accuracy requirement, many research efforts make use of the Monte-Carlo technique [98, 99]. A typical procedure for Monte-Carlo based small-disturbance stability analysis is shown in Fig. 2.5 [94].

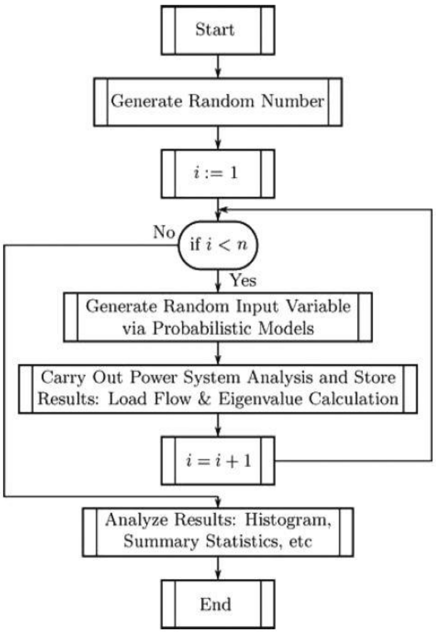

Fig. 2.5 The block diagram for Monte-Carlo based probabilistic small-disturbance stability analysis [94]

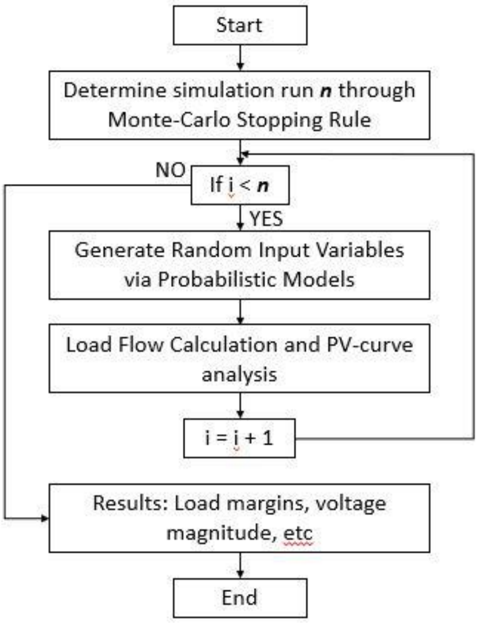

Fig. 2.6 The block diagram for Monte-Carlo based power system voltage stability analysis

For probabilistic power system voltage stability analysis, a Monte-Carlo based approach with probabilistic distributed generation scenarios and active/reactive load margin uncertainty have been applied in [100]. Maximum entropy method with Gaussian/Normal distributed system loads were implemented in [101]. Contingency enumeration based approaches with normal distributed load uncertainty have been introduced in [102]. Probabilistic eigenvalue analysis (through normal parametric distribution has been used in [4]. Probabilistic collocation method has been proposed in [1]. Fig. 2.6 is a flow chart for the Monte-Carlo based power system voltage stability analysis.

2.2.3.2 Probabilistic Power System Reliability Analysis

The researches on probabilistic approach for power system reliability assessment started relatively late compared to stability assessments. Probabilistic power system reliability assessment are experiencing slow development due to the difficulties encountered in the categories of concept-difficulties, modelling-difficulties, computation-difficulties and data collecting-difficulties [83]. A Probabilistic Dynamic Security Assessment (PDSA) was carried out in a project sponsored by Electric Power Research Institute (EPRI) in 2007. The method presented in the EPRI technical report is based on Cumulants and Gram-Chailier Expansion method and Probabilistic Load Flow analysis (PLF) [103]. PDSA provides a measure of the dynamic security region boundary, it can be used to identify critical potential generator or grid failures and help operators locate the corresponding effective prevention and mitigation actions [104]. PDSA also provides useful references to questions like ‘what are the weak spots within the power system’ or ‘what is the most critical component for system dynamic stability’. This method combines deterministic and probabilistic approaches and provides a practical hybrid

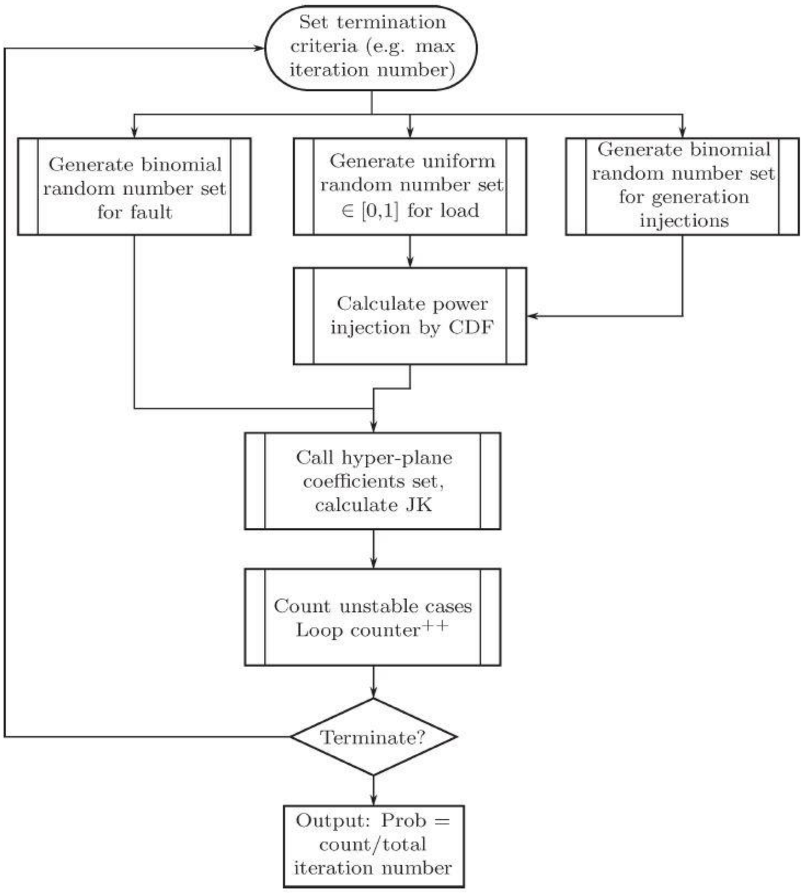

Fig. 2.7 Monte-Carlo approach for dynamic system security assessment and system planning [104]

methodology for power system reliability assessment. A block diagram is presented in Fig. 2.7 [104] showing the PDSA method.

Since power system is large in size and complex in structure, the reliability assessment can be tricky. Researchers had divided the network into different hierarchical levels based on functionalities of different subsystems in 1984 [105]:

- Hierarchical Level I (HLI) consists of generation plants of a power system.
- Hierarchical Level II (HLII) consists of transmission and generation plants of a power system.
- Hierarchical Level III (HLIII) consists of distribution, transmission and generation plants of a power system.

Some key reliability criteria were also summarized in [106]:

- Loss of load probability (LoLP)

  The LoLP states the probability that there are no enough generation for load throughout the year.

- Loss of load expectation (LoLE)

  The LoLE states the annual average time when the daily peak load is expected to exceed the available generation capacity. Loading curves can be obtained by accessing system operation log-data. LoLE is mainly used in generation capacity planning.

- Loss of energy expectation (LoEE)

  The LoEE represents the expected energy that will not be supplied when available generation cannot meet the load requirement. It has the same characteristic with the expected energy not supplied (EENS) and expected un-served energy (EUE). It is considered to be a more realistic measure of the power system with growing energy regulations today.

- Value of lost load (VoLL)

  VoLL and EUE are mainly used in the power system expansion planning for the purpose of economic optimization.

The above-mentioned power system reliability assessment approaches and criteria were used for power system risk assessment. A good summary of the power system risk assessment methods is provided in [107]. Detailed outage models, probabilistic reliability assessment approaches and their applications have been covered in this book.

The Probabilistic Reliability Assessment Methodology (PRA) provides an effective approach to assess the occurrence possibility of a distribution and its relevant impacts by introducing the probabilistic reliability index (PRI). PRA successfully combines the advantages of deterministic and probabilistic methods and offers a practical hybrid approach to reliability assessment. PRI can be defined as equation (2.4) [83]:

$$PRI = \sum Dis\_probability_i * \ sys\_impact_i \tag{2.4}$$

where $Dis\_probability_i$ is the occurrence possibility of a selected disturbance and sys_impact_i is the severity of the disturbance. Hence PRI is defined as the product of an impact by a probability. i represents the disturbance event and is expressed as $i \in (Simulated\ disturbances)$.

There are 4 typical types of PRI indices [83]:

i. Amperage (Overload) Probabilistic Reliability Index (APRI):

$$APRI = \sum Dis\_probability_i * \ A\_impact_i \tag{2.5}$$

where A_impact_i represents the severity of the overload disturbance, measured in MVA.

ii. Voltage Violation Probabilistic Reliability Index (VPRI):

$$VPRI = \sum Dis\_probability_i * \ V\_impact_i \tag{2.6}$$

where V_impact_i represents the severity of the voltage violation disturbance, measured in kV.

iii. Voltage Stability Probabilistic Reliability Index (VSPRI):

$$VSPRI = \sum Dis\_probability_i * \ VS\_impact_i \tag{2.7}$$

with VS_impact_i expressed in state "1" or "0", which indicates that the disturbance causes the system to voltage instable or stable, respectively.

iv. Load Loss Probabilistic Reliability Index (LLPRI):

$$LLPRI = \sum Dis\_probability_i * LL\_impact_i \tag{2.8}$$

where LL_impact_i represents the severity of the load loss disturbance, measured in MW.

The parameter $Dis\_probability_i$ in these indices represents the likelihood of power system experiencing the specific disturbance at any time during the operation. It is a function of the availability of every piece of equipment in the power system [83]:

$$Dis\_probability_i = \prod_{i \in U} u(c_i) \prod_{j \in A} a(c_j) \tag{2.9}$$

where U is the set of unavailable components and A is the set of available components. $\prod components$ is the complete set of all system components and is defined as $\prod components = A \cup U$.

In Probabilistic Reliability Assessment, a set of parameters that simultaneously experience malfunctions caused by the same disturbance can be defined as a common mode failure. These failures can be modelled as a single availability rate hence reduces the computational burden compared to analysis at every situation individually. The PRA introduces 5 types of analysis criteria, stating as Interaction Analysis; Situation Analysis; Root Cause Analysis; Weak Point Analysis and Probabilistic Margin Analysis [83]. In this thesis, the interaction analysis has been performed for the correlation modelling between uncertain parameters. The test network is subjected to various operation conditions for the analysis of their corresponding dynamic behaviour under the frame of situation analysis. The weak point analysis has been employed to identify the critical parameters for power system stability analysis (critical bus/load/RES generation/line, etc.). The probabilistic margin analysis has also been employed for the stability margins of power system voltage and angular stability analysis.

The power system probabilistic reliability assessment provides an approach to answer questions like ‘where the system malfunction is located’, ‘how likely the disturbance is going to happen’ and ‘how much operating margin the system has for adjustment’. Using of PRA study can help in the following [108]:

- Assessment of system reliability.
- Ranking of the disturbances based on their contribution to reliability indices.
- Identification of the most critical system components contribute to outage situations.
- Identification of the weak branches and buses during instability issues.

Based on much more established PRA and its principles a similar approach has been applied in this thesis in probabilistic power system stability analysis.

2.2.3.3 Power System Planning

In power system planning assessments, the following aspects are required: generating available operation scenarios, performing stability, reliability and economical assessments and calculating of optimal system parameter options. The restructuring and deregulation of the power industry is accompanied with a growing trend in the inclusion of system uncertainties during system planning and operation. Considering every possible system disturbance when planning modern power system can create massive computational burden. Therefore, more effective management techniques are required in the ever-expanding large-scale interconnected network. Probabilistic Load Flow (PLF) was first proposed in 1996 [105] and has been widely used in the area of power system operation and planning. The PLF evaluates probability density functions of all state variables. The outputs are network quantities indicating the possible ranges of the load flow result [109]. PLF can provide an accurate and effective approach for the system planners to analyse future system conditions. The selected optimal system planning blueprint is a compromise between overall cost and system functionality. A general block diagram for probabilistic power system planning is presented in Fig. 2.8 [80].

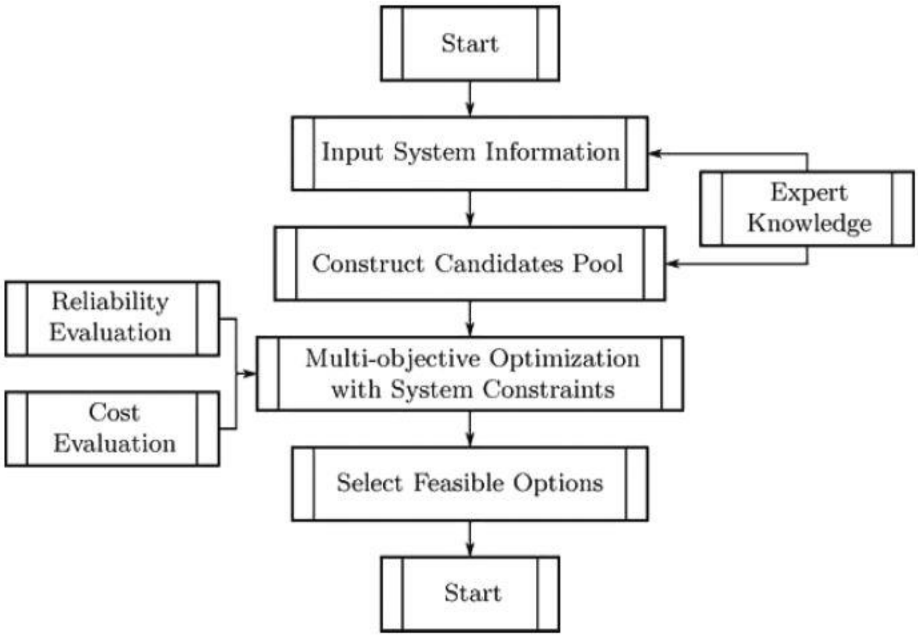

Fig. 2.8 Block diagram presenting general probabilistic system planning analysis [80]

2.2.4 Summary on Power System Analysis Methods

The development of power systems in recent years is experiencing significant structural changes due to the addition of new types of load and generation technologies and deregulated market environment. The number of disturbances is also increasing due to application of new technologies and higher dependence on weather conditions. Under such circumstance the traditional deterministic approaches for power system stability, reliability and planning assessment are rapidly becoming unsuitable since they can only evaluate system behaviour using limited-selected number of scenarios. The simulation results of a deterministic approach are overly conservative and inaccurate compared to the real conditions the modern power system faces. It is also impractical to consider every possible situation with deterministic methods simply because of the large amount of calculations requested which is economically unacceptable. The probabilistic based methods are much more preferred when assessing modern power system dynamics. With the aid of computers and relevant software packages, complex interconnected power systems with a variety of new generating, transmitting and loading components can be accurately simulated prior of building them. Probabilistic power system assessment can provide a practical way for system planner and operators to evaluate power system dynamic performance effectively and accurately.

2.3 Modelling of Uncertainties

Modern interconnected power systems are large in size and complex in structure. The development of power system leads to system restructure in order to meet the demands of today’s deregulated highly flexible market. Numerous components and restraints which comply with market requirement have been added to power networks. The key characteristics of modern power systems are considered to be an unprecedented mix of a wide range of electricity generating technologies, hierarchical control structure and new types of loads. This proliferation of system parameters with intermittent nature brings uncertainty problems to system stability, and the effort to push exiting assets to their operating limits in order to be competitive in nowadays electricity markets threatens the system security even more [110]. For the accurate simulation of system response in different situations and system-states, researchers always make use of probabilistic methods since they consider 'probability distribution' of the parameters. The probabilistic methods can answer questions related to system operation conditions like 'what can happen', 'how likely is it to happen' and 'how severe it can be' [34]. This section will summarize past approaches considering the suitable probability distributions (PD) for various system components for accurate system dynamic analysis.

A typical probabilistic assessment for system dynamic analysis contains three steps: input parameter modelling, power system stability analysis and representation of system outputs. The three steps can be presented in block diagrams as shown in Fig. 2.9 [34].

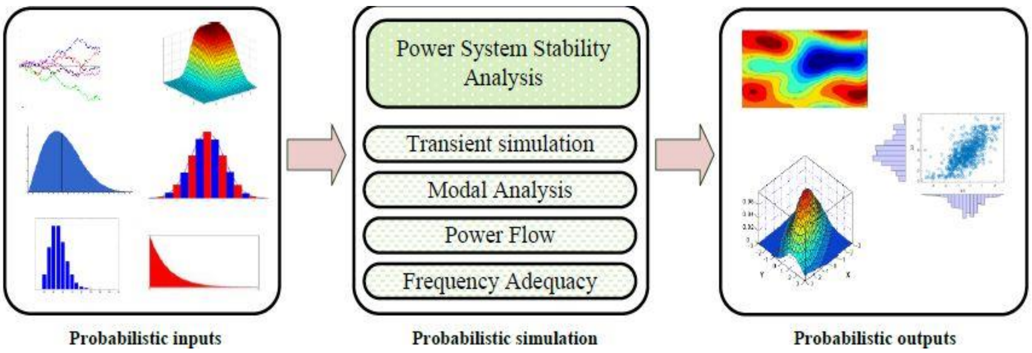

Fig. 2.9 The framework of a probabilistic power system stability analysis [34]

Power system uncertainty parameters can be classified in two types based on their potential influence: *structural uncertainty* and *parametric uncertainty*. The structural uncertainty involves system elements like components and branch availability, i.e., loss of transmission line. The parametric uncertainty involves system parameters like load demand [111]. To perform uncertainty modelling and generate the corresponding probability distributions of system inputs, the characteristic of the parameters should be considered, for example,

- Linearly growing parameters can be modelled as normal (Gaussian) probability distribution.
- Exponentially growing parameters can be modelled as lognormal probability distribution.
- Events with k outcomes can be modelled as multinomial distribution.
- Independently event can be modelled through Poisson, exponential or Gamma probability distribution.

There are many probability distribution functions (*pdf*s) that can be used in modelling of system uncertainty parameters. These *pdfs* are defined by critical factors which can decide the shape, location and scale of a distribution. The general *pdfs* for selected probability distributions and their relevant critical factors are listed below:

- Beta Distribution, with the Beta function $B(\alpha,\beta)$, as shown in (2.10):

$$f(x;\alpha,\beta) = \frac{1}{B(\alpha,\beta)}\, x^{\alpha-1}(1-x)^{\beta-1} \tag{2.10}$$

  where α is the first shape parameter and β is the second shape parameter of the Beta function B which is a normalization constant to ensure that the total probability is 1. x is the realization of a random process X.

- Binomial Distribution (discrete), the probability mass function is shown in (2.11):

$$f(x) = \frac{n!}{x!(n-x)!}p^x(1-p)^{(n-x)} \tag{2.11}$$

where n represents the number of trials and $p \in (0,1)$ represents the probability of success for each trail. This equation gives the probability of getting exactly x successes in n trails. $x!$ is the factorial of x.

- Exponential Distribution, as shown in (2.12):

$$f(x;\lambda) = \lambda e^{-\lambda x}H(x) \tag{2.12}$$

where $\lambda > 0$ is the rate parameter of the distribution. $H(x)$ is the right-continuous Heaviside step function where $H(0) = 1$. e is the base of the natural logarithm.

- Gamma Distribution, as shown in (2.13):

$$f(x;\alpha,\beta) = \frac{x^{\alpha-1}e^{-(\frac{x}{\beta})}}{\beta^\alpha \Gamma(\alpha)} \tag{2.13}$$

where α is the shape parameter and β is the scale parameter. This function gives a random variable X that is gamma-distributed with shape α and scale β, $\Gamma(\alpha)$is the gamma function. e is the base of the natural logarithms.

- Lognormal Distribution, as shown is (2.14):

$$f(x) = \frac{1}{x\sigma\sqrt{2\pi}}\exp(-\frac{(lnx-\mu)^2}{2\sigma^2}) \tag{2.14}$$

where $\mu \in (-\infty, +\infty)$ represents mean value of the variable's natural logarithm, and $\sigma > 0$ represents the standard deviation of the variable's natural logarithm. Parameter μ and σ are the location and scale parameters for the normally distributed logarithm $ln(x)$.

- Normal Distribution, as shown in (2.15):

$$f(x) = \frac{1}{\sigma\sqrt{2\pi}} e^{\frac{(x-\mu)^2}{2\sigma^2}} \tag{2.15}$$

where μ and σ represents the mean and standard deviation of the variable. e is the base of the natural logarithm.

- Poisson Distribution (discrete), as shown in (2.16):

$$f(x\ events\ in\ interval) = \frac{e^{-\lambda}\lambda^x}{x!} \tag{2.16}$$

where $\lambda > 0$ represents average number of events per interval, also called the rate parameter. e is the base of the natural logarithm, $x!$ is the factorial of x.

- Rayleigh Distribution, as shown as (2.17):

$$f(x;\sigma) = \frac{x}{\sigma^2} e^{\frac{-x^2}{2\sigma^2}} \tag{2.17}$$

where σ is the scale parameter of the distribution with the value of $\sigma > 0$. e is the base of the natural logarithm.

- Weibull Distribution, as shown in (2.18):

$$f(x;\alpha,\beta) = \frac{\beta}{\alpha} \left(\frac{x}{\alpha}\right)^{\beta-1} e^{-(x/\alpha)^\beta} \qquad x \geq 0 \tag{2.18}$$

where α represents the scale parameter and β represents the shape parameter of the distribution. e is the base of the natural logarithm.

Probability distributions can be categorised into continuous and discrete distributions. In a continuous distribution, data can be obtained at any point within a specific range. In discrete distributions only certain values are valid to be sampled. System dynamics like the amount of generation or load in a network, the transmission capacity of a line, network losses or generation cost can be modelled with continuous distributions, while parameters like No. of generators in the network, fault occurrence, fault types or fault locations can be modelled using discrete distributions. Continuous dynamic analysis requires solving algebraic equations of modelled system components numerically. On the other hands, discrete dynamic events like tap changing transformers and protective devices are represented through logic rules [34].

Power system variables which can lead to stability issues can either be system parameters or system contingencies. Different power system variables can be represented with different probabilistic distribution functions. Normal distributions are used for probabilistic modelling of power generation, wind power, and power system loads [9, 61, 112-115]. Weibull distribution was used for the probabilistic modelling of wind power and solar power [9, 61, 114-119]. Beta distribution has been used for solar power modelling [119]. Probabilistic modelling of fault occurrence had been performed through Poisson and binomial distributions [120-

Table 2.1 Probability distributions of system input parameters [34]

System Variables	**Fitted Probabilistic Distributions**
Power Generation	Normal [9, 61]
Wind Power	Weibull [9, 114-119], normal [112]
Solar Power	Weibull [114], beta [119]
Power System Load	Normal [9, 113-115]
System Contingencies	**Fitted Probabilistic Distributions**
Fault Occurrence	Poisson [120-122], binomial [122]
Fault Location	Uniform [61, 120]
Fault Duration	Rayleigh [61, 112]

122]. Uniform distribution was used for the probabilistic modelling of fault location [61, 120]. Rayleigh distribution had been used for probabilistic modelling of fault location in [61, 112]. The Table 2.1 gives a review of existing literature based on probability distributions of system input parameters [34].

It can be observed from Table 2.1 that Weibull distribution is a commonly used probabilistic distribution for the modelling of wind power. For the modelling of power system load, normal distribution is frequently used by researchers. Both Weibull and Beta distributions have been found to be used for the modelling of Solar power generation in power systems. Normal, Weibull and Beta distributions, all categorized as continuous distribution, are appropriate for probabilistic modelling of system loads, wind speed and solar irradiation, respectively, as all of them (loads, wind speed and solar irradiation) have continuous variables [34].

In probabilistic power system voltage stability analysis, different approaches for uncertainty modelling have been used in the past. In [100] the uncertainties in generation scenarios and active load margin have been modelled with normal distribution while reactive load margin has been presented with gamma distribution. The output parameters are modelled as discrete random variable. In [101] the random changing system loads have been modelled as Gausian/normal distributions. Jacobian method has been employed to determine the stability margin. In [123] the uncertainties in load have been modelled as normal distribution. The observed output parameters are the probability of voltage instability, the frequency of voltage instability and the required voltage stability margin. In [4] the load demand uncertainty has been modelled with normal distributions. The probability of stability has been given by the distribution of probabilistic critical eigenvalue.

In this research, load demand, wind power and solar irradiation are the three considered uncertainties for power system stability analysis. Based on the information provided in Table 2.1, Normal distribution, Weibull distribution and Beta distribution are chosen for modelling of the relevant uncertainties, respectively.

2.4 Probabilistic Simulation Techniques for Power System Stability Analysis

The probabilistic simulation techniques have been widely used in power system stability studies. These methods can be used to analysis the dynamic response of a power system when uncertain parameters are introduced. The probabilistic simulation techniques can accurately model the system uncertain operation conditions within a specified uncertainty level. In this section several commonly used probabilistic simulation techniques have been reviewed and discussed based on their capabilities.

2.4.1 Monte Carlo (Numerical) Method

Monte-Carlo method involves the repeated sampling of system uncertainties. A large data set can be retrieved from these samplings, and the distribution of an unknown probabilistic entity can be determined. There are two fundamental theorems of statistics underpinning the application of Monte Carlo method in uncertainty-related analysis: the Weak Law of Large Numbers [124], and the Central Limit Theorem [125]. The Weak Law of Large Numbers states that the sample average converges in probability towards the expected value, and the Central Limit Theorem states that the properly normalised sum of independent random variables tends toward a normal distribution. The simulation procedure involves inputs domain definition, probability distribution generation, performing deterministic computations on the inputs and aggregation of the results. The advantage of Monte-Carlo simulation is that the method is very flexible and virtually limitless for analysis. It is easily expandable and deployable. However, the simulation time can be quite long with large sampling database as random samples of size N are generated following the *pdfs* of the input variables, and the accuracy of the samplings is highly related to the Monte-Carlo run-time. The Monte Carlo stopping rule is needed to ensure that sufficient number of simulations are run to ensure required accuracy of the results. The outputs of this approach are an estimate values rather than the exact values and the stopping rule can help to determine the minimum number of simulations required to achieve a specified confidence level. The numerical steps for obtaining the minimum number of simulations are shown by equation (2.19) to (2.24) [125].

i. Take N samples and record $X_1, \ldots, X_N$.

ii. Continue sampling until $\frac{(T_{N+1})}{N} \leq \frac{\varepsilon_N^2}{\beta_N^2}$, with N+1 → N, and record X_N for N^{th} sample. Calculate:

$$\bar{X}_N = \frac{1}{N}\sum_{i=1}^{N} X_i \tag{2.19}$$

$$T_N = \sum_{i=1}^{N} (X_i - \bar{X}_N)^2 \tag{2.20}$$

iii. Stop sampling, then:

$$\lim_{\varepsilon_r \to 0} \frac{N}{n_0(|\mu|\varepsilon_r, \delta)} = 1 \tag{2.21}$$

$$\lim_{\varepsilon_r \to 0} pr(|\bar{X}_N - \mu| \leq |\mu|\varepsilon_r) = 1 - \delta \tag{2.22}$$

$$\lim_{\varepsilon_r \to 0} \left(\frac{E(N)}{n_0(|\mu|\varepsilon_r, \delta)}\right) = 1 \tag{2.23}$$

$$\beta = \emptyset^{-1}\left(1 - {}^{\delta}/_{2}\right) \tag{2.24}$$

In the above equations, n_0 is the initial iteration value, ε_r is the relative error for the samplings, β is the maximum uncertainty level that should be achieved, N is the actual sample size needed for the required accuracy ε_r with the coverage probability $1-\delta$ as ε_r tends towards 0. $\bar{X}$ is the mean value of the obtained result, μ is the real mean value of the studied variables, $\emptyset^{-1}$ is the inverse function of the normal distribution with $\delta = 1$ and $\mu = 0$.

Equation (2.25) is an expression for the relative error:

$$\varepsilon_r = \frac{\emptyset^{-1}\left(1 - {}^{\delta}/_{2}\right) * \sqrt{\frac{\sigma_N'}{N}}}{E(N)} \tag{2.25}$$

where σ_N' is the variance of the obtained result, and $E(N)$ is the mean value of the samples. The relative error ε_r is calculated in each simulation and is compared with a target relative error in Monte Carlo simulation. In this case the simulation can be terminated when the required level of confidence is achieved. The typical number of simulations required for power system stability related analysis is between 1000 and 5000. A detailed discussion of how these numbers are calculated is presented in Section 3.4 of the thesis.

A Monte-Carlo based approach with probabilistic distributed generation scenarios and active/reactive load margin uncertainty have been applied in [100]. Maximum entropy method with Gaussian /Normal distributed system loads were implemented in [101]. Contingency enumeration based approaches with normal distributed load uncertainty have been introduced in [123]. Probabilistic eigenvalue analysis (through normal parametric distribution has been used in [4]. Probabilistic collocation method has been proposed in [1].

The application of this method on voltage stability analysis has been found in [4, 63, 126, 127]. This approach has also been found to be used for angular stability analysis [10, 14, 128]

2.4.2 Markov Chain Monte-Carlo Method

The Markov Chain MC method requires the construction of a Markov Chain [129] with the target distribution. The developed Markov Chain can be utilized as a sample of the desired distribution. The coverage quality of the variability of the uncertain parameters can be improved with the increased number of sample size [34]. The general procedure for a Markov Chain Monte-Carlo simulation is,

- Choosing staring sample.
- Generating candidate points according to the proposed distribution.
- Repeating the previous step until the convergence criteria is met.

The Markov Chain Monte-Carlo method is more efficient than the Monte-Carlo simulation since it does not require prior information before simulation and the probabilistic distribution can be proposedly designed. This characteristic is useful when assessing rare failure events [130]. Application of this method on power system stability analysis has been found in [131, 132].

2.4.3 Point/Two-Point Estimate Method

This probabilistic simulation technique uses sample data to obtain the approximate value for some parameters. The steps involved in this approach are [34],

- Calculating key factors for each uncertainty,
- Performing deterministic studies at each key factor,
- Generating the *pdfs* of the key factors.

This method requires $2n$ calculations for n uncertain parameters. However, since this is a deterministic assessment, it has the limitation in the accurate modelling of system uncertain parameters, and the system dynamic behaviour can be affected. The application of this method in power system stability analysis has been found in [66, 133, 134].

2.4.4 Cumulant-Based Method

The cumulant of a probability distribution provides an analytical way for obtaining output variation based on input uncertainty. The steps for Cumulant-Based Methods are [34],

- Calculation of uncertain input cumulants,
- Performing $m + 1$ deterministic simulation calculations and numerically evaluate the sensitivity of the output for each uncertainty,
- Calculation of the system output cumulants,

- Generating *pdfs* based on system output central moments and standard moments.

This method can provide a less computational burden for system dynamic analysis [135] and avoid the convolution calculations in probabilistic power flow [136]. The application of this method in system stability analysis has been found in [134, 137, 138].

2.4.5 Probabilistic Collocation Method

The probabilistic collocation method uses a polynomial function of the system uncertain parameters to describe the system modal output. The following steps are included in this method [34],

- Rank the uncertainties based on a ranking algorithm and reduce the number of considered uncertainties based on the ranking.
- Establish orthogonal polynomials based on desired model to represent selected uncertainties.
- Determine the collocation points for each selected system uncertainties. Rank these points based on the joint probability density associated with the operating point.
- Calculate all coefficients for PCM model.
- Employing the PCM model functions in a standard MC simulation to generate a large data set for system output
- Producing *pdfs* based on the obtained data set.

This method is computationally efficient and time saving when applied to complex networks like the power system [139-141]. The application of this method for power system stability analysis has been found in [1, 62, 134].

2.5 Sensitivity Analysis Methods for Power System Stability Analysis

Sensitivity analysis techniques can provide a framework in the identification and ranking of the critical uncertain parameters in power systems when performing stability-related studies. Sensitivity analysis methods can numerically describe how the variability of the input parameter propagates through a modelled system and affects the output result [142]. Through the ranking of system parameters within a network, components with high impact on system stable operation can be modelled in greater detail and more closely monitored, while others can be treated less intensely to significantly reduce the computational resources required. Hence such a ranking of system critical parameters is favourable to system operators and stake-holders as the investment can be reduced and the profit will increase. Less data involved in power system status analysis can also reduce the computational time. In this case fast decision-making and corresponding system tuning can be achieved for better power quality provided to end consumers.

Previous works have employed ‘local’ linear algorithms for the ranking of important system parameters such as generators [143], load classification [144], PSS design [145], and PMU placement [146]. More recently an accurate yet computational intensive ‘global’ approach has been employed in the ranking of frequency support devices [147]. There also exist screening methods like the Morris Screening methods, which can provide features like reasonable computational cost and acceptable accuracy in one package. The ‘screening’ method has been proved to be effective in systems with a large number of uncertain inputs [142, 148, 149]. The computational cost and model complexity increase from local methods to screening methods and finally global methods.

2.5.1 Local SA Method

Local sensitivity analysis methods evaluate the local impact of one single input parameter on the model output and are performed by calculating the partial derivatives of the output with respect to the input. One commonly used local sensitivity analysis method is the One-at-A-Time method [148, 150]. This technique changes one input parameter at one time within a small step around its nominal value. This approach is easy to implement, and only $p + 1$ simulations are required for a system with p uncertain parameters. The results obtained through this approach are highly dependent on the choice of the input space. The sensitivity measure of this approach can be expressed as shown in (2.26):

$$O_i = \left(\frac{X_i}{Y_i}\right) \cdot \left(\left|\frac{Y_i - Y_{base}}{X_i - X_{base}}\right|\right) \tag{2.26}$$

Where $O_i$is the impact of parameter i on the model, X_i is the value of parameter i, Y_i is the model output for parameter X_i. X_{base} and Y_{base} are the input and output of base case scenario.

Local sensitivity analysis methods such as the OAT method have the advantage that only low computational efforts are required. It is a fast approach for deterministic analysis. However, they suffer from reduced accuracy due to the local, linear search. They can present unreliable results when the model is nonlinear [149].

There also exist other local sensitivity analysis methods, Adjoint modelling and Automated Differentiation [151, 152]. The local methods do not explore the full scale of the input space as they examine small variations and usually one variable at a time.

2.5.2 Screening SA Method

The screening sensitivity analysis methods run a multi-dimensional, semi-global search through the range of possible input values. They require fewer simulations compared to the global method. The screening methods are suitable for the application to systems with a large number of input parameters and the computational burden is high. The screening methods are considered to be 'moderate' approaches as they sacrifice a little accuracy for better efficiency. There also exist other screening methods namely supersaturated design [153], the screening by groups [154] and the sequential bifurcation method [155]. These methods can be used when the number of simulations has to be smaller than the number of inputs. The Morris screening method [148, 150, 156] is commonly-used for large system simulations since the implementation is relatively straightforward and generally performs better compared to similar ones [148-150, 156]. It generates a multidimensional semi-global trajectory within its search space when performing power system stability related studies.

For the implementation of the Morris screening method, there are three important measurements that need to be considered:

i. The elementary effect.

ii. The mean value of elementary effect.

iii. The standard deviation of the elementary effect.

The Morris Screening method changes one variable at a time with a magnitude of Δ. The elementary effect measures the output variance when an input is changed, as shown in equation (2.27)

$$EE_p^i(x) = \frac{[y(x_1, x_2, \ldots\ldots, x_{i-1}, x_i + \Delta, x_{i+1}, \ldots\ldots, x_p) - y(x)]}{\Delta} \tag{2.27}$$

In equation (2.27), $EE_p^i(x)$ is the elementary effect for inputs, p is the total number of input uncertainties, Δ is the step that relates to $1/(r-1)$, and r is the 'level' set for the Morris SA method (usually from 4 to 10).

The mean and standard deviations of the elementary effect are the sensitivity indices for the Morris screening method, and they are defined as equations (2.28) and (2.29)

$$\mu_p^* = \frac{1}{r}\sum_{i=1}^{r}\left|EE_p^i\right| \tag{2.27}$$

$$\sigma_p^* = \sqrt{\frac{1}{r}\sum_{i=1}^{r}(\left|EE_p^i\right| - \mu_p^*)^2} \tag{2.29}$$

The mean value of the elementary effect measures the sensitivity strength between inputs and outputs. An input parameter with a larger μ_p^* value indicates a higher impact on output, and hence the parameter is identified as 'critical'. The standard deviation of the elementary effect indicates the linearity between input and output. A high value of σ_p^* means the variable has a non-linear effect on the output and it has an interaction with other variables.

The Morris screening method requires $p * r + 1$ simulations for a system with *p* input variables.

2.5.3 Global SA Method

Global sensitivity analysis methods rank the input parameters by evaluating their effect on model output through the whole set of possible input values. The global methods can be performed on non-parametric uncertainties, for example correlation coefficients, or through the analysis of the output variation like the Sobol indices. The global sensitivity analysis methods produce the most accurate ranking results compared to local and screening methods, and hence are always used as benchmark when accessing accuracy. They, however, can be very computationally intensive and time consuming due to the massive global search that they are based on [148-150]. The number of simulations required for global sensitivity analysis methods are generally at the order of several thousands.

The global sensitivity analysis methods can be categorised into linear model-based methods and non-linear model-based methods based on their application environments.

For the correlation coefficient sensitivity analysis methods, this research employs the Pearson Correlation Coefficient method [157], the Spearman Correlation Coefficient method [158] and the Partial Correlation Coefficient method [156]. All 3 correlation coefficient methods are categorised as linear model-based methods. They are part of the 'sampling-based global' sensitivity analysis method. Assuming a sample of system inputs and outputs $(X^n, Y^n) = (X_1^i, \dots\dots, X_d^i, Y_i)_{i=1\dots.n}$ is valid. Then a linear model can be established to explain the behaviour of $\boldsymbol{Y}$ given the values of $\boldsymbol{X}$ [156].

The Pearson Correlation Coefficient is a quantitative measure which determines the linear dependency between the output $\boldsymbol{Y}$ and input $\boldsymbol{X}$. It is capable of ranking the input parameters based on their influence on the output parameters. The Pearson Correlation Coefficient method can be expressed as equation (2.30) [156],

$$\rho_{XY} = \frac{\sum_{i=1}^{N}[(X_i - \bar{X})(Y_i - \bar{Y})]}{\sqrt{\sum_{i=1}^{N}(X_i - \bar{X})^2} \cdot \sqrt{\sum_{i=1}^{N}(Y_i - \bar{Y})^2}} \tag{2.30}$$

Equation (2.30) is a linearity measure between the input $\boldsymbol{X}$ and output $\boldsymbol{Y}$. The numerator term expresses the covariance between variables. The denominator shows the standard deviation of the variables. Parameter $\bar{X}$ and $\bar{Y}$ are expressed by (2.31) and (2.32),

$$\bar{X} = \sum_{i=1}^{N}(X_i/N) \tag{2.31}$$

$$\bar{Y} = \sum_{i=1}^{N}(Y_i/N) \tag{2.32}$$

The Spearman Correlation Coefficient method is a Pearson Correlation Coefficient among the ranked variables when the correlation between $\boldsymbol{X}$ and $\boldsymbol{Y}$ is difficult or impossible to express in terms of ρ_{XY} [158]. The rank correlation coefficient is more appropriate to be applied to cases where non-linear transformations are applied to the random variables as linear correlations will not be preserved. These rank correlations measure the degree to which large or small values of one random variable associated with large or small values of another. They measure the association only in terms of ranks. It is used to access monotonic relationships between variables. If there are no repeated data values, a perfect Spearman correlation of +1 or −1 occurs when each of the variables is a perfect monotone function of the other. The Spearman's ρ is useful in describing the dependence between random variables since they are invariant to the choice of marginal distribution. The Spearman Correlation Coefficient sensitivity analysis method requires the calculation of the sum of the squares of the difference of the ranks using equation (2.33).

$$\rho = 1 - \left(\frac{6\sum d_i^2}{N(N^2-1)}\right) \tag{2.33}$$

In equation (2.33), N is the sample size of the variable dataset. $d_i = X_i - Y_i$, is the difference between the two ranks of each observation.

The Partial Correlation Coefficient can be used to measure the degree of association between output variable Y and input variable X_j. The effect of other inputs will be cancelled in this process. It can be expressed by (2.34),

$$PCC_j = \rho\left(X_j - \widehat{X_{-J}}, Y - \widehat{Y_{-J}}\right) \tag{2.34}$$

In (2.34), $\widehat{X_{-J}}$ represents the prediction of the linear model, $\widehat{Y_{-J}}$ is the prediction of the linear model where input X_j is absent. The application of Partial Correlation Coefficient method is based on the assumption of linear relations between input and output.

The above mentioned three correlation coefficient approaches are all based on a valid linear relationship between the outputs and inputs. Statistical techniques can be used to confirm the linear hypothesis by evaluating coefficient Q^2 [156], as can be shown in (2.35)

$$Q^2 = 1 - \frac{\sum_{i=1}^{m}\left[Y_i^p - \hat{Y}\left(X^{p(i)}\right)\right]^2}{\sum_{i=1}^{m}\left[Y_i^p - E(Y^p)\right]^2} \tag{2.35}$$

In (2.35), $(X^{p(i)}, Y_i^p)_{i=1\ldots m}$ is a m-size test sample of inputs and outputs. $\hat{Y}()$ is the predictor of the linear regression model. The value of Q^2 represents the percentage of output variability explained by the linear regression model, where $Q^2 = 1$ means a perfect fit. These linear measures are part of the 'sampling-based global' SA method.

The Sobol Total Indices method is a variance-based method. It is very suitable for implementations on non-linear and non-monotonic models [148, 156, 157]. This means the Sobol Total Indices method is the most generic method among all the six sensitivity analysis methods employed by this research. Monte-Carlo sampling-based methods have been used for estimating Sobol indices. The advantage of introducing Monte-Carlo sampling method is that it provides error made on indices estimates via random repetition. However, they are heavily time consuming due to the number of model calls to get accurate estimates of sensitivity indices. The Sobol total indices are the sum of all the sensitivity indices involving all uncertain factors as shown by (2.36) [147] [148]

$$S_T = S_i + \sum_{i<j} S_{ij} + \sum_{i\neq j, i\neq k, j<k} S_{ijk} + \cdots \tag{2.36}$$

In (2.36), S_i is the 1st-order sensitivity index for parameter i, S_{ij} is the 2nd-order sensitivity index describing the interactions between two uncertainties i and j $(i \neq j)$. The 1st-order sensitivity index can be expressed by (2.37). The variance of output of input i can be expressed by (2.38).

$$S_i = D_i(Y)/Var(Y) \tag{2.37}$$

$$D_i(Y) = Var[E(Y|X_i)] \tag{2.38}$$

The 2nd-order sensitivity index and variance can be presented by (2.39) and (2.40), respectively.

$$S_{ij} = D_{ij}(Y)/Var(Y) \tag{2.39}$$

$$D_{ij}(Y) = Var\left[E\left(Y\middle|X_i, X_j\right)\right] - D_i(Y) - D_j(Y) \tag{2.40}$$

For the 3rd-order sensitivity index S_{ijk}, the equations could be extended accordingly. These interactions will continue up to *p*th-order for p parameters.

The Sobol 1st-order index is determined by obtaining the correlation coefficient of the output vector from two model runs. During the model runs, all values of variables in X_i are common, while all other inputs use independent samples. In order to determine the Sobol total indices, the input data set X is partitioned into $X_{\sim i}$ and X_i, where $X_{\sim i}$ is the set of all input variables which include a variation in the *i*th index of X. The Sobol total effect is then calculated by (2.41):

$$ST_i = 1 - S_{\sim i} \tag{2.41}$$

In (2.41), $S_{\sim i}$ is the sum of all terms that include the variation in X_i.

2.5.4 Application Example of Sensitivity Analysis Methods

This section provides a simple example for the application of sensitivity analysis methods. The One-at-A-Time method, the Morris Screening method, and the Pearson Correlation Coefficient method have been selected for demonstration purpose as they are found to be commonly used among the three types of sensitivity analysis methods. A simple mathematical model with three input parameters, x_1, x_2, and x_3 is used. The model is expressed as (2.42):

$$y = x_1^2 + 8x_2 - 4x_3 \quad (0 \leq x_1, x_2, x_3 \leq 8) \tag{2.42}$$

2.5.4.1 Application of the One-at-A-Time method

For the application of the OAT method, a total number of *3+1=4* simulations is required to evaluate the influence of each parameter on output *y*. Since the results obtained through this approach are highly dependent on the choice of the input space, 2 groups of input dataset are selected, namely $case_1$ and $case_2$. In $case_1$, the base value is (6, 6, 6) with a step size $\Delta_1 = 2$. In $case_2$, the base value is (4, 4, 4) with the same step size $\Delta_1 = 2$. Table 2.2 records the input and output values for the above 2 case studies.

Equation (2.26) is used here to find the sensitivity of system output to input parameters. For example, the impact O_1 of parameter x_1 on output y under $case_1$ is calculated as:

$$O_{x1} = \frac{X_1}{Y_1} * \left|\frac{Y_1 - Y_{base}}{X_1 - X_{base}}\right| = \frac{8}{88} * \frac{|88 - 60|}{|8 - 6|} = 1.273 \tag{2.43}$$

Similarly, O_{x2} and O_{x3} under $case_1$ can be calculated as 0.842 and 0.615, respectively. The result ranks parameter x_1 as the most influential parameter. However, when $case_2$ is considered, the corresponding impact O_{x1}, O_{x2} and O_{x3} are 0.6, 1.0 and 0.2, respectively. This means for $case_2$, x_2 has now been calculated as the most influential input parameter. The limitation of local OAT method is unveiled by this simple case study.

Table 2.2 Input and output values

$case_1$			$case_2$		
Step	Input	Output	Step	Input	Output
1	(6, 6, 6)	60	1	(4, 4, 4)	32
2	(8, 6, 6)	88	2	(2, 4, 4)	20
3	(6, 8, 6)	76	3	(4, 2, 4)	16
4	(6, 6, 8)	52	4	(4, 4, 2)	40

2.5.4.2 Application of the Morris Screening method

For the application of the Morris Screening method, the base value has been set as (6, 6, 6) for input parameters (x_1, x_2, x_3), the level is r=5. The step size Δ_2 is calculated by multiplying the value of the range of the inputs and 1/(r-1), in this case, $\Delta_2 = 8 * \frac{1}{5-1} = 2$. A total of 3*5+1=16 simulations are required for this case study. Table 2.3 records the input and output values for this case study.

In Table 2.3, steps involving change in parameter x_1 are highlighted in green, while

Table 2.3 Input and output values

Step	Input	Output	Step	Input	Output
1	(6, 6, 6)	60	9	(0, 8, 2)	56
2	(6, 8, 6)	76	10	(0, 8, 4)	48
3	(4, 8, 6)	56	11	(0, 8, 6)	40
4	(2, 8, 6)	44	12	(0, 6, 6)	24
5	(2, 8, 4)	52	13	(0, 6, 4)	32
6	(2, 6, 4)	36	14	(0, 4, 4)	16
7	(2, 6, 2)	44	15	(2, 4, 4)	20
8	(0, 6, 2)	40	16	(4, 4, 4)	32

Change x_1 Change x_2 Change x_3

red and purple are used to highlight steps where x_2 and x_3 are changed, respectively. The elementary effects $EE_p^i(x)$ and the mean values of the elementary effects μ_p^* of the corresponding input parameters has to be calculated in order to evaluate the impacts on output. For example, the mean value of the elementary effect of x_1 is calculated as:

$$\mu_{x1} = \frac{|56 - 76| + |44 - 56| + |40 - 44| + |20 - 16| + |32 - 20|}{5 * 2} = 5.2 \qquad (2.44)$$

Similarly, the mean values of elementary effects of x_2 and x_3 are 8 and 4, respectively. In this case, the Morris Screening method successfully identified parameter x_2 as the most influential parameter for this simple model, with x_1, and x_3 to be the second and third influential parameters. This ranking result is as expected considering the form of the numerical model expressed as (2.42). The application of the Morris Screening method in power system stability related analysis has been demonstrated extensively in Section 5.3.2 of the thesis.

2.5.4.3 Application of the Pearson Correlation Coefficient method

For the application of Pearson Correlation Coefficient method, the input parameters are considered as uncertainties which follow a normal distribution with a mean value of 4 and standard deviation of 0.033 (3σ=10%). The input dataset is sampled for 100 times in order to obtain a sufficient representation of the uncertain parameters. Equation (2.30), (2.31) and (2.32) have been used when generating script in MATLAB for the analysis. The same simple numerical example given by (2.42) has been used. The Pearson Correlation Coefficient method gives the ranking of the input parameters as $x_2(0.6815) > x_1(0.5837) > x_3(0.3568)$ based on their influence of system output y. The result agrees with the Morris Screening method and is true to what is expected from the simple numerical model.

2.5.5 Summary on Sensitivity Analysis Methods

The previous study [18] provides a graphical representation of the work principle of the different categories of the sensitivity analysis methods discussed in two dimensions, as shown in Fig. 2.10 [18]. There are major differences between the sensitivity analysis methods from the perspective of the handling of the variables. The OAT method changes one parameter at a time within a small interval around its nominal value. The Morris screening method generates a multidimensional trajectory through the search space. The Correlation Coefficient method is designed to handle thousands of random generated samples within the search space. The Sobol indices method generates samples in a symmetrical geometric orientation. The demonstrations and results in section 2.5.4 present a numerical explanation of commonly used sensitivity analysis methods. The applications of these sensitivity analysis methods on power system stability analysis can be extended based on the principles and characteristics discussed in this research.

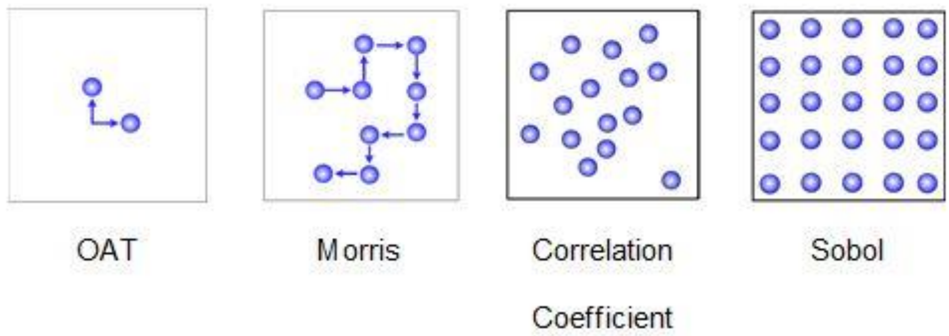

Fig. 2.10 Graphical representation of the sample generation technique of SA methods [18]

2.6 Summary

In this chapter, the power system analysis methods are discussed considering their key characteristics. The probabilistic modelling techniques of the uncertain parameters and their corresponding implementation scenarios are introduced. The performance of deterministic and probabilistic approaches is compared. Modern power system consists of large number of interconnected new technologies whose operation is highly temporal and spatial dependent. These new technologies increase both operational and parametric uncertainties in a network. The variability exhibited by these new technologies voids traditional deterministic stability analysis since the ‘worst-case scenario’ analysis of the network may lead to an overly conservative system design. A probabilistic approach to network stability assessment is getting steadily adopted by researchers to be applied to all types of stability studies. The most commonly used simulation methods are Monte-Carlo simulation, Cumulant-based method and probabilistic collocation method, as stated in Section 2.4. Finally, the sensitivity analysis methods which can be used for power system stability analysis are introduced and discussed, and the application of the most common methods has been illustrated on a simple numerical example.

Chapter 3 : Test Network and Simulation Techniques

In this study, all simulations are performed on a PC with Intel(R) Core™ i7-4770 CPU @3.40GHz and 16.0 GB of RAM. The simulations are performed with two major software platforms, Matlab R2015a and DIgSILENT PowerFactory 2017 SP1 (x64). The probabilistic modelling of input uncertainties and the calculation of the probabilistic load flow are performed through the OPF solver within MATPOWER, Matlab [159]. The P-V curve calculation, modal analysis, and RMS simulation for stability analysis are performed in DIgSILENT PowerFactory. The obtained outputs of different stability studies are processed within Matlab environment.

3.1 Test System Configuration

The test network used in this paper is a modified version of the IEEE 68-Bus test network. It represents the reduced model of NETS-NYPS (New England Test System-New York Power System). This model was introduced in [160] and used extensively in [161]. There are 16 generators and 68 buses in the network. The test network is divided into 5 sections with Generators G1-G9 located in NETS and Generators G10-G13 located in NYPS. G14, G15, and G16 separate as 3 equivalent areas connected to NYPS. G9 is equipped with a fast-acting static exciter (IEEE ST1A) and power system stabilizer (PSS). Other generators use slow exciters (IEEE DC1A). Speed governor systems are installed on all generators. G1 includes a GAST speed governor, G2-G8, G10-G16 contain IEEE G1 (steam turbine) and G3 and G9 contain IEEEG3 (hydro turbine). The test network is rated to provide an active power generation capacity of 17.26 GW (1 p.u.). Integration of renewable generation is simulated by using 7 equivalent wind generators and 7 equivalent PV generators, which are connected to 7 system buses (buses 60, 57, 68, 26 of NETS, and buses 53, 33, 17 of NYPS). The selection of the locations of the RES generation plants in the test system is made considering their potential effect on network dynamic behaviour. For example, RES plants are connected to bus 17 near the reference machine, bus 33 near critical generator G11, buses 26 and 68 near critical generator G9, and buses 60, 57 and 53 near the tie lines between NETS and NYPS area of the test network. All the synchronous generators are represented by the six-order dynamic models (listed in Table A.3, Appendix A.3).

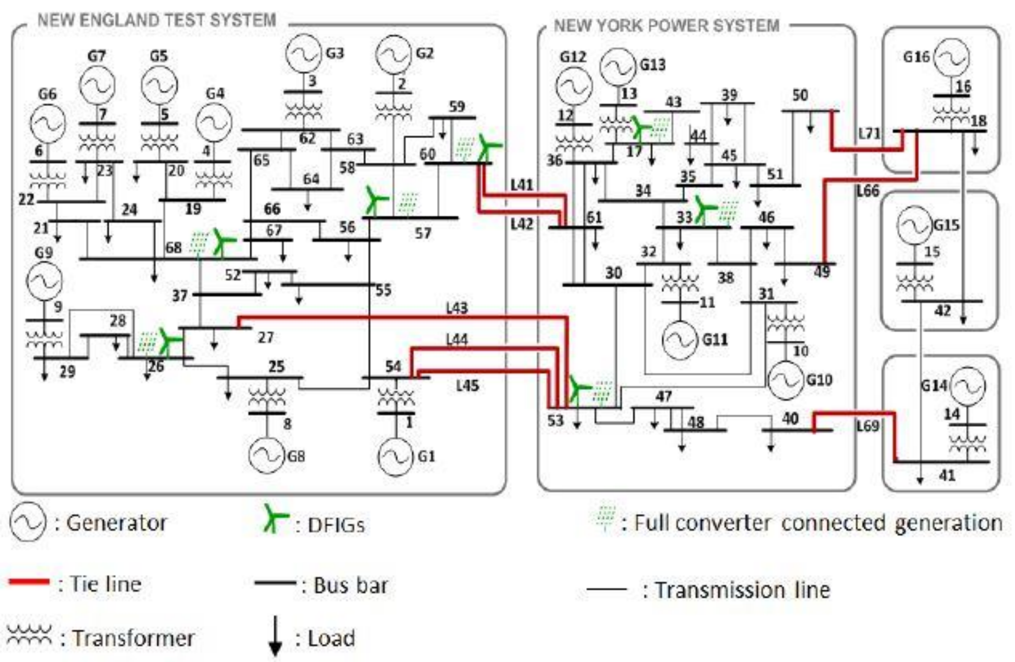

Fig. 3.1 Modified IEEE 68-Bus NETS-NYPS test system with RES generations

Transmission lines are modelled with the standard π circuit. Further data of the test network including parameter modelling are detailed in Appendix A.

Fig. 3.1 shows the layout of the test network. There are two types of Renewable Energy Sources (RES) used in the test network. The wind turbines are modelled as Doubly Fed Induction Generators (DFIGs) and the PV plants are modelled as Full Converter Connected Generators (FCCs) [162, 163]. The detailed control structures for the employed models can be found in Appendix B. The Grid Code of National Grid requires that generators should be able to operate between a 0.85 lagging power factor and a 0.95 leading power factor under rated active power generation conditions [164]. Hence the reactive power generation limit of the synchronous generators within the test network is set between -33% and 62% of the active power generation.

3.2 Probabilistic Modelling of Uncertain Input Parameters

In order to represent the operational conditions in a network with RES generation and uncertain loading demands, this research employs the probabilistic modelling of system loads, wind speed and solar irradiation as uncertain parameters. Table 3.1 illustrates the employed probabilistic distribution for selected system uncertainties and their corresponding model parameters. Past studies indicated that normal distribution is commonly used for modelling load uncertainty [4, 165, 166], hence adopted in this study. Similarly, uncertainties caused by variation in wind speed and solar irradiation for wind farm and PV plants were commonly modelled with Weibull [8, 9, 116] and Beta distribution [119, 167], respectively. The normal distribution is typically represented by mean (μ) and standard deviation (σ), Weibull distribution by scale parameter (α) and shape parameter (β), and beta distribution by shape parameters (a) and (b). The level of uncertainty of 10% adopted for modelling load uncertainty is the typical load forecast error. For Weibull and beta distribution the parameters follow a similar level of uncertainty as that for the load [4]. [18] includes 3 levels of uncertainties including low (1% variation), medium (5% variation) and high (10% variation). The model parameters for Weibull distribution under low and medium level of uncertainties are $\alpha = 3.1, \beta = 8.8$ and $\alpha = 2.5, \beta = 9.9$. The model parameters for Beta distribution under low and medium level of uncertainties are $a = 23.5, b = 1.3$ and $a = 17.5, b = 1.3$. The model parameters are calculated based on the selected level of uncertainties. It was found though, that the level of uncertainties does not affect the ranking of critical parameters for small-disturbance stability analysis.

A total of 49 uncertain input parameters including 35 loads, 7 wind farms and 7 solar farms have been modelled probabilistically in this study.

Table 3.1 Probabilistic distribution and model parameters of system uncertainties of the test network

Uncertain Parameter	Probability Distribution	Probabilistic Model Parameters	Level of Uncertainty
Load Demand (%)	Normal	$3\sigma = 10\%\ of\ \mu$	High (10%)
Wind Speed (ms^{-1})	Weibull	α=2.2, β=11.1	
Solar Irradiation (kWm^{-2})	Beta	a=13.7, b=1.3	

3.3 Classical Exponential Load Model

The static exponential load models are used in this research for the modelling of system loads. The international survey on load modelling among CIGRE Work

Group members between 2010 to 2012 suggested that the constant real and reactive power load model (constant P/Q) is the most widely used load model for steady state power system studies [168]. A simplified version of the exponential load model with neglected load dependence on frequency is used in this study, given by equation (3.1) and (3.2) [169].

$$P = P_n(\frac{U}{U_n})^{k_{pu}} \tag{3.1}$$

$$Q = Q_n(\frac{U}{U_n})^{k_{qu}} \tag{3.2}$$

where P and Q are the real and reactive power drawn by the load at voltage U and frequency f, P_n and Q_n are the real and reactive power drawn under rated voltage (U_n). The exponents k_{pu} and k_{qu} describe the change in load demand in response to variations in the supply voltage. If the voltage exponents in (3.1) and (3.2) are set at 0 and 2, the load exhibits constant power or constant impedance characteristics, respectively.

This study also includes the polynomial load model, as shown in equation (3.3) and (3.4).

$$P = P_n\left[p_1\left(\frac{U}{U_n}\right)^2 + p_2\left(\frac{U}{U_n}\right)^2 + p_3\right] \tag{3.3}$$

$$Q = Q_n\left[q_1\left(\frac{U}{U_n}\right)^2 + q_2\left(\frac{U}{U_n}\right)^2 + q_3\right] \tag{3.4}$$

This load model is often referred to as a ‘ZIP MODEL’, as it consists of constant impedance (Z), constant current (I), and constant power (P) load components. The parameters p_1 and q_1, p_2 and q_2, p_3 and q_3 represent the proportion of constant impedance load, constant current load, and constant power load, respectively. The sum of parameters p_1, p_2 and p_3 are 1 p.u. The sum of parameters q_1, q_2, and q_3 are 1 p.u as well.

3.4 Monte-Carlo Stopping Rule

In this thesis the Monte-Carlo simulation is used to generate the dataset of the uncertain input parameters. The MC simulation requires a certain number of repeated random sampling of uncertain data in order to represent the stochastic behaviour of system parameters. The (3.5) determines the number of required Monte Carlo runs [170].

$$\varepsilon > \left[\frac{\left\{ \phi^{-1}\left(1 - \frac{\delta}{2}\right) \cdot \sqrt{\frac{\sigma^2(X)}{N}} \right\}}{\bar{X}} \right] \tag{3.5}$$

In (3.5), ε is the sample mean error, $\phi^{-1}(\cdot)$ is the inverse Gaussian conditional probability distribution with a zero mean value and a one standard deviation value, $\sigma^2(\cdot)$ is the variance of a sample, δ is the required confidence level, and $\bar{X}$ is the mean of the samples.

Previous studies on the IEEE 68-Bus NETS-NYPS test system indicated that for transient stability studies the sampling number required for a 5% sample mean error with 99% confidence interval is 6000 simulations [163]. Also, it was found that 1000 simulations are required for small disturbance stability studies with a 0.3% sample mean error and 99% confidence interval [128]. For voltage stability, 1000 simulations are required for a less than 2% sample mean error and a 99% confidence interval. Therefore, 6000 simulations are run in this study to ensure the required accuracy.

Figs. 3.2, 3.3 and 3.4 show the error-vs-simulation-time curves for Monte Carlo simulations of small-disturbance, transient stability analysis, and voltage stability analysis, respectively, as a function of the numbers of simulations.

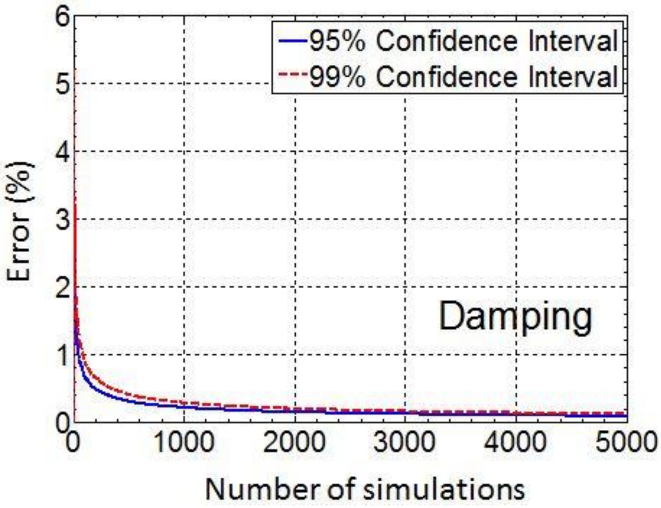

Fig. 3.2 Error-vs-Simulation-time curve for small-disturbance stability analysis

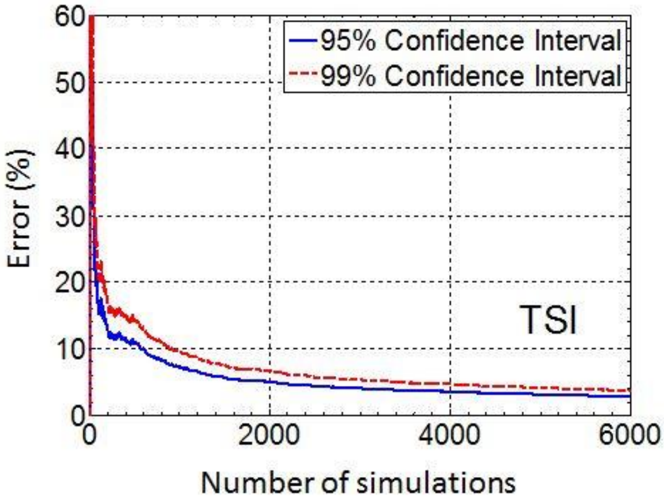

Fig. 3.3 Error-vs-Simulation-time curve for transient stability analysis

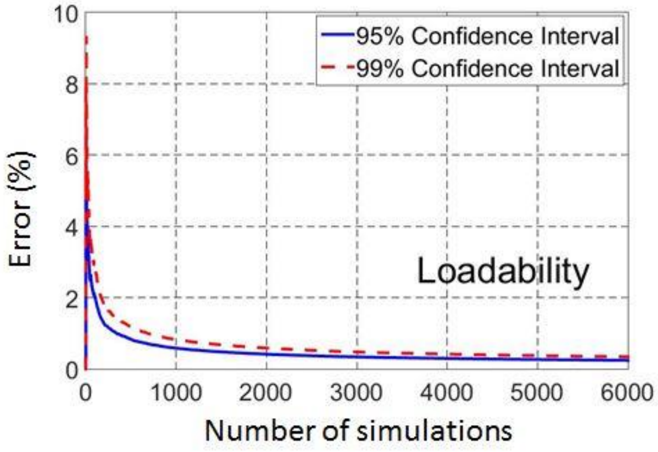

Fig. 3.4 Error-vs-Simulation-time curve for voltage stability analysis

3.5 The Optimal Power Flow Calculation

This study runs an OPF (Optimal Power Flow) calculation in order to achieve conventional generation re-dispatch. The renewables (RES) are not considered in the OPF formulation. The system loading and RES generation are produced randomly for each Monte Carlo simulation (with a given mean and standard deviation). The renewables are then treated as negative loads and in each iteration the conventional generation dispatched active power is calculated according to equation (3.6).

$$P_{con} = P_{load} - P_{RES} \tag{3.6}$$

In such a case, the OPF calculation is performed for the given loading scenario to minimise the total cost of conventional generation. The generators are subject to the standard cost function, as presented by (3.7) [159].

$$Cost = c_0 + c_1 P_g + c_2 P_g^2 \;\; \$/hour \tag{3.7}$$

The cost coefficient values for each generator are given in Table 3-2. For generators G1 to G9, these are adopted from [171], while for the remaining generators G10 to G16, these have been derived to achieve nominal generator outputs close to the standard power flow solution. The constraints on active and reactive power for each generating unit are also shown in Table 3.2. All bus voltages were constrained to between 0.9 and 1.1 pu.

The above mentioned OPF function and the parameters in Table 3.2 [159, 172] are integrated in the OPF calculation option in the Matpower 5.1 toolbox. The conventional generation dispatches are calculated by executing the Matlab codes.

Table 3.2 Data for optimal power flow solution with IEEE 68-bus test network

Generator	Bus	c_0	c_1	c_2	$P^{max}(MW)$	$P^{min}(MW)$	$Q^{min}(MVAr)$
G1	53	0	6.9	0.0193	375	100	-100
G2	54	0	3.7	0.0111	817.5	100	-100
G3	55	0	2.8	0.0104	975	100	-100
G4	56	0	4.7	0.0088	948	100	-100
G5	57	0	2.8	0.0128	757.5	100	-100
G6	58	0	3.7	0.0094	1050	100	-100
G7	59	0	4.8	0.0099	840	100	-100
G8	60	0	3.6	0.0113	810	100	-100
G9	61	0	3.7	0.0071	1200	100	-100
G10	62	0	3.9	0.0090	750	100	-100
G11	63	0	4.0	0.0050	1250	500	-100
G12	64	0	2.9	0.0040	1687.5	500	-100
G13	65	0	2.5	0.0019	4488.8	2000	-100
G14	66	0	3.3	0.0033	2231.3	500	-100
G15	67	0	3.8	0.0050	1250	500	-100
G16	68	0	3.5	0.0014	5000	3000	-100

3.6 Summary

This chapter introduced the test network configuration and the required parameters for simulations in order to give an overall introduction on the tools and platforms used for the research. The test network layout has been shown in Fig. 3.1. The modelling of network parameters (generators, lines, load flows, RES generation) are briefly discussed. Probabilistic modelling of system loads, wind speed and solar irradiation have been introduced and their corresponding model parameters are illustrated in Table 3.1. This research includes static exponential load models for stability related analysis. The dynamic load models are not included in this study as the focus of the thesis was the identification of critical parameters (including loads and RES generation) affecting power system stability. The simple static exponential load models are easy to implement and understand for the purpose of validating the proposed approach of this research. The static exponential load models are simple in structures and have few parameters. Compared to complex dynamic load models with more parameters, they benefit from a clear correlation pattern and greatly improve the efficiency when correlated loads are used for the analysis. This chapter also numerically specified the number of simulations required for different types of stability analysis when Monto-Carlo method is used. The conventional generators' cost functions and the corresponding optimal power flow calculation are required to set up initial conditions for probabilistic power system stability analysis are also discussed.

Chapter 4 : Probabilistic Ranking of Critical Parameters Affecting Voltage Stability

This section of the thesis presents a probabilistic method for the identification and ranking of critical uncertain parameters affecting power system voltage stability analysis. Renewable generation technologies with stochastic natures have been widely utilized in modern power systems. The uncertainties in generation together with highly flexible customer load demand bring challenges to system voltage stability. These threats require assessments of questions like ‘which part of the system is mostly likely to collapse’ and ‘which uncertainty will have the largest effect on system dynamic behaviour’. By answering these questions, one can provide references for the system planners and operators on system stability margin and monitoring requirements. The Monte-Carlo method is applied first to simulate/replicate system behaviours considering different input uncertain parameters. The influence of uncertainties in load demand, renewable generation and load models, are investigated separately. The load buses are ranked based on the sensitivity of bus voltage to increased system load. The critical and stiff buses are selected from the ranking. Finally, by comparing ‘nose-area’ covering, the effect of proposed uncertain parameters on system voltage stability can be evaluated.

The proposed methodology for this section includes the following steps:

i. Selecting case studies.
ii. Ranking of the load buses for each selected case study based on their loadability against a specified uncertain input parameter.
iii. Selecting three weak and three strong buses from the ranking above. Check if the rankings remain the same in all case studies.
iv. Investigating the distributions of nose points (voltage stability limits) to evaluate the effect of uncertain parameters on voltage stability analysis.
v. Change load models to see their influence on system voltage stability studies.

The parameter ‘loadability’ in this section refers to the average active power difference of a load bus between the nose point (voltage collapse point) and initial operating point.

4.1 Case Studies

The loading demand of a power system is not constant in the real-world operation. This can lead to a variation in system operating conditions. In order to ensure the employed study cases can cover most of the system operating conditions, the annual loading curve of NETS-NYPS is introduced as shown in Fig. 4.1. This curve contains the real data collected from real power system for the duration of one year. In Fig. 4.1, the y-axis is the system loading factor measured in per unit. The test system can withstand a maximum loading demand of 1.318 p.u (base case). This is calculated as the maximum active power the test network can provide before voltage collapses at any load bus within the network. Any operations beyond that limit would result in OPF calculation not converged (system rated operation point is treated as 1p.u, 17.26GW). The x-axis is the duration of demand measured in hours (from 1 to 8760 hrs in a year). For any loading factor L_i on the curve, the corresponding duration of demand t_{demand} means that the system load is no less than L_i for t_{demand} hrs. For example, when the system loading factor is at 0.568 pu, the corresponding duration of demand is at 2190 hrs, this means the system is operating at no less than 0.568 pu for 2190 hrs. When Monte Carlo method is used the annual loading curve can be simplified into sectors within which the load model parameters can be varied around a nominal value with specified uncertainty. In this research the annual loading curve is sampled at 12 different sections of demand as shown in Fig. 4.1 and Table 4.1. The samples are sectored every 10% of the duration of demand, except for sectors 1 (1%) and 2 (5%) where the curve is very steep and sector 12 (5%).

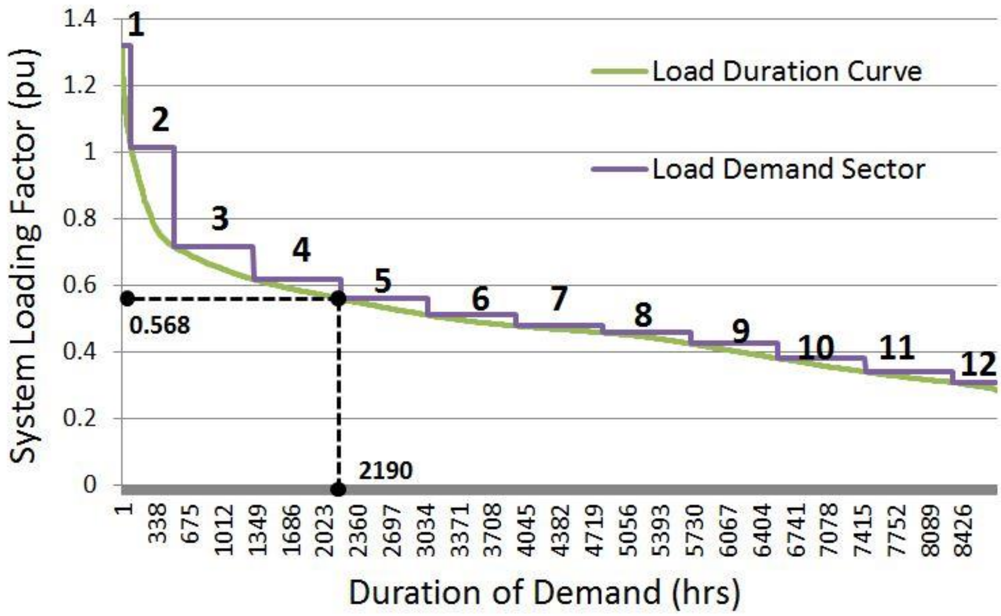

Fig. 4.1 The Annual loading curve for the test network

Two points on the curve, rated system operation point (second sector) and minimum system demand (fifth sector, without generator disconnection), are selected based on Table 4.1 with system loading factors to be 1p.u and 0.568p.u, respectively. In order to analysis the effect of RES generations on power system voltage stability studies, 30% of the generation is replaced by RES plants. Three loading scenarios are selected: Peak, High and Low load with 100% of system loading, 75% of system loading and 40% of system loading, respectively. Table 4.2 show cases of the system loading scenarios selected for this section. Peak loading has been considered as the base case scenario. In order to identify the weak buses in the system, the system loading is increased in steps until the weakest bus experienced voltage collapses. A peak load scenario cannot be analysed since it is not possible to increase system loading beyond the system maximum loading. Only high and low load scenarios have been analysed corresponding to a stressed system loading condition and a moderate system loading condition, respectively.

Table 4.1 Operation points obtained from annual loading curve based on duration of demand

Sectors	1	2	3	4	5	6	7	8	9	10	11	12
t_{demand} (%)	0	1	6	15	25	35	45	55	65	75	85	95
LF (p.u)	1.318	1.027	0.726	0.627	0.568	0.518	0.486	0.465	0.432	0.387	0.346	0.314

Table 4.2 Loading scenarios selected for the test network

Loading Scenarios	**System Loading**	**Proportion of Renewables**
Peak Load	100%	15%
High Load	75%	20%
Low Load	40%	33%

The detailed arrangement of the case studies in this section is shown in Table 4.3. The case studies are selected based on the principle that only one category of the uncertain parameters can be simulated as variable at one time. This allows a comparison between the effects of different uncertain parameters on the system voltage stability study. A total of 9 case studies are proposed. The case studies are separated into 3 groups: case studies 1-3, case studies 4-6 and case studies 7-9. The analyses of case studies 1-3 can rank the effects of uncertainties within wind farm generation, solar plant generation and load demand on the power system voltage stability study under a stressed operation condition. The analyses of case studies 4-6 provide the ranking of the effect of the employed uncertainties at a

Table 4.3 Case Studies

<table>
<tr><th>Case Study</th><th>1</th><th>2</th><th>3</th></tr>
<tr><td>Operating condition</td><td colspan="3">Loading level = 1 p.u.</td></tr>
<tr><td>Loading Factor</td><td>Variable</td><td colspan="2">Constant</td></tr>
<tr><td>Wind Speed</td><td>Constant</td><td>Variable</td><td>Constant</td></tr>
<tr><td>Solar Irradiation</td><td colspan="2">Constant</td><td>Variable</td></tr>
<tr><td>Load Model</td><td colspan="3">Constant Power</td></tr>
<tr><td>Case Study</td><td>4</td><td>5</td><td>6</td></tr>
<tr><td>Operating condition</td><td colspan="3">Loading level = 0.568 p.u.</td></tr>
<tr><td>Loading Factor</td><td>Variable</td><td colspan="2">Constant</td></tr>
<tr><td>Wind Speed</td><td>Constant</td><td>Variable</td><td>Constant</td></tr>
<tr><td>Solar Irradiation</td><td colspan="2">Constant</td><td>Variable</td></tr>
<tr><td>Load Model</td><td colspan="3">Constant Power</td></tr>
<tr><td>Case Study</td><td>7</td><td>8</td><td>9</td></tr>
<tr><td>Operating condition</td><td colspan="3">Loading level = 0.568 p.u.</td></tr>
<tr><td>Loading Factor</td><td>Variable</td><td colspan="2">Constant</td></tr>
<tr><td>Wind Speed</td><td>Constant</td><td>Variable</td><td>Constant</td></tr>
<tr><td>Solar Irradiation</td><td colspan="2">Constant</td><td>Variable</td></tr>
<tr><td>Load Model</td><td colspan="3">Constant Impedance</td></tr>
</table>

moderate operation condition. For case studies 7-9, the constant impedance load model is used instead of the constant power load model in case studies 1-6. This allows an investigation of the effect of different load models when performing voltage stability related studies.

4.2 Ranking of load buses

For each of the case studies stated above, the loading of all the system load buses is increased simultaneously until voltage of one of the bus collapses. The average values of the voltage difference between $V_{initial}$ and V_{nose} for each system load bus can then be obtained ($V_{diff} = V_{initial} - V_{nose}$). The load bus with the largest or smallest V_{diff} is considered as the weakest or strongest bus, respectively. The step size for system load increase is set to be adaptive. It will decrease before reaching the voltage stability limit. The initial step size is set at 0.5% pu, the maximum step size is set at 5% pu, while the minimum step size is 0.01% pu. The Monte-Carlo simulation is repeated 1000 times within each study case to ensure a 99% confidence that the difference between the true and sampled mean values is less than 1% of the true mean value, based on the Monte Carlo stopping rule discussed in Section 3.4 of the thesis.

4.3 Distribution of the nose-points

The analysis of the system behaviour to different uncertain parameters is performed by the investigation of the distribution of nose-points. For each category of the uncertainty selected, a group of 1000 P-V curves are plotted. With the identification of critical and stiff buses in different case studies, the data of total system load and voltage at collapse points is obtained and considered as nose-points. The nose points for 1000 Monte-Carlo simulations are then plotted into one scatter plot to see the effect of different uncertain parameters on system voltage stability. The size, shape and location of the nose-points distributions indicate the system's sensitivity to their corresponding uncertain input parameter. The probabilistic distribution functions of the voltage and active power of the scatter plot can also be obtained.

4.4 Change of load models

The effect of load models on system voltage stability behaviour can be investigated by employing different load models. This study uses constant power (P type loads) and constant impedance (Z type loads) load models. These two load models are among the most frequently used load models and can represent some household appliances and office equipment. Many loads with large ratios of resistive to inductive consumption are modelled as constant impedance load, for example heaters, ovens and dryers [173, 174]. Devices supplied through power electronic conversions are normally modelled as constant power loads, for example computers and monitors [174]. The constant power load models can be taken off-line by voltage protection devices when low-voltage threshold is reached, while constant impedance load models can withstand much lower low-voltage scenarios and result in late voltage collapse problems compared to P type loads. The comparisons are set between study cases 4, 5, and 6 and study cases 7, 8, and 9.

4.5 Identification of Critical and Stiff Buses

Table 4.4 below illustrates identified critical and stiff buses for the nine study cases. The results obtained in Table 4.4 should be analyzed on a group-of-bus basis instead of a single-bus basis. From Table 4.4 it can be observed that the group of the most-probable critical buses and the most-probable stiff buses remains almost the same under various conditions. The values of V_{diff} among the identified buses within their related groups are quite small. The identified critical buses are

Table 4.4 Identified critical and stiff buses

Case Study	**1**	**2**	**3**	**4**	**5**	**6**	**7**	**8**	**9**
Critical Bus	46	46	46	48	48	48	48	48	48
	47	47	47	47	40	40	40	40	47
	48	48	48	40	47	47	47	47	40
Stiff Bus	21	21	21	24	24	24	24	24	24
	28	28	28	21	21	21	21	21	21
	50	50	50	28	28	28	28	28	28

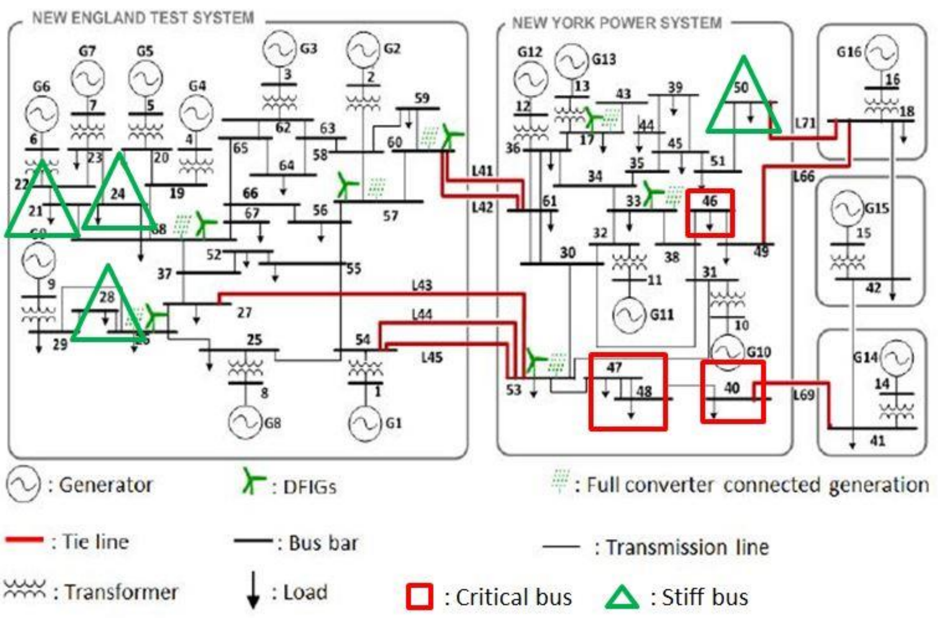

Fig. 4.2 The identified critical and stiff buses for the test network

highlighted in Fig. 4.2 (red square for critical buses, green triangle for stiff buses). This indicates that the buses in the NYPS area of the network are more susceptible to voltage collapse compared to buses in other parts of the system. The selection of critical and stiff buses of the test network is based on the probability of them experiencing voltage collapse for the chosen case study. For example, the buses whose voltage collapses first most of the time, i.e., buses that are most likely to experience voltage collapse, are identified as critical buses sensitive to the variations of loads connected to them.

4.6 Illustrative results

In this section, the scatter plots of nose-point area distributions are plotted as shown in Fig. 4.3, 4.4 and 4.5. From Fig. 4.3, 4.4 and 4.5, it can be observed that the clusters of nose points present different behaviour in terms of intensity, shape and location. Since the nose points are obtained when the system stability limit is reached, a wider spread nose-area will represent a larger variance in the voltage stability margin, hence a larger effect of parameter in question on system voltage stability analysis. In other words, the uncertain parameter causing a wider spread nose-area can have a greater effect on system voltage stability studies. In each of the case study groups, the nose-point distributions for a single uncertain parameter (orange circle for loading, yellow star for wind speed and purple diamond for solar power) are plotted against all uncertainties at one time (blue cross). By investigating the shapes for different distributions, we can find that the shapes for distribution of all uncertainties are almost identical with the most-effective uncertainty, only with some offset in position. This phenomenon, on the other hand, proves that the identification of the critical parameters following the proposed procedure is valid. It also proves that the identified parameters do have the dominant effect on power system voltage stability related studies.

Therefore, it can be said that among the three uncertain parameters considered in this study, when the system operation point is at a higher value (1p.u, 75% of system peak loading), the uncertainty in the variance of the loading factor is the most critical one, followed by uncertainty caused by wind speed and solar irradiation. However, the influence of wind speed on system voltage stability can increase rapidly and overtake the loading factor as the most important parameter when the system is operating at a lower demand (0.568p.u, 40% of system peak loading), as can be seen by comparing Figs. 4.3 and 4.4.

The effect of load models on system voltage stability analysis can be obtained by comparing Figs. 4.4 and 4.5. It is obvious that a system with a constant impedance load model i.e., more flexible loads can cause the system voltage collapse at a much higher total power and operate safely at lower voltage, compared to systems with constant power load models.

In the wider context of uncertainties considered, it has, however, been found that load models do not affect the ranking of critical buses.

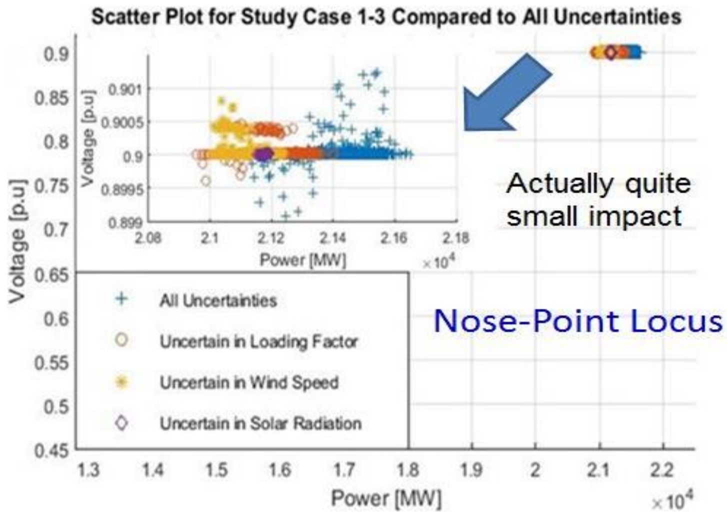

Fig. 4.3 Scatter Plot for Case Studies 1-3

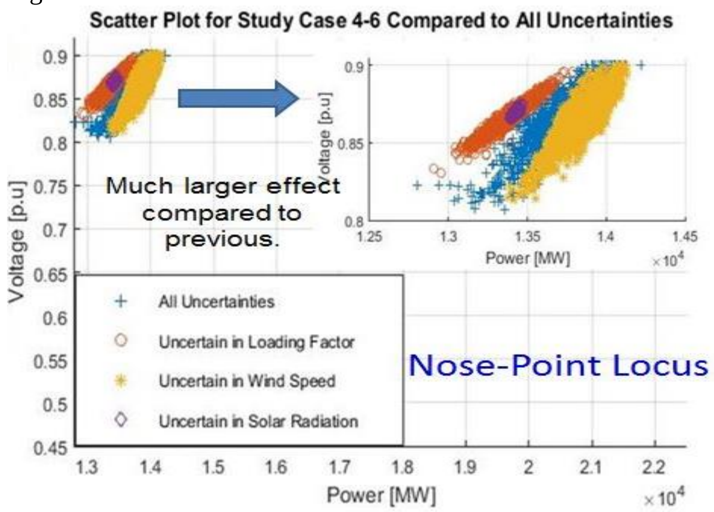

Fig. 4.4 Scatter Plot for Case Studies 4-6

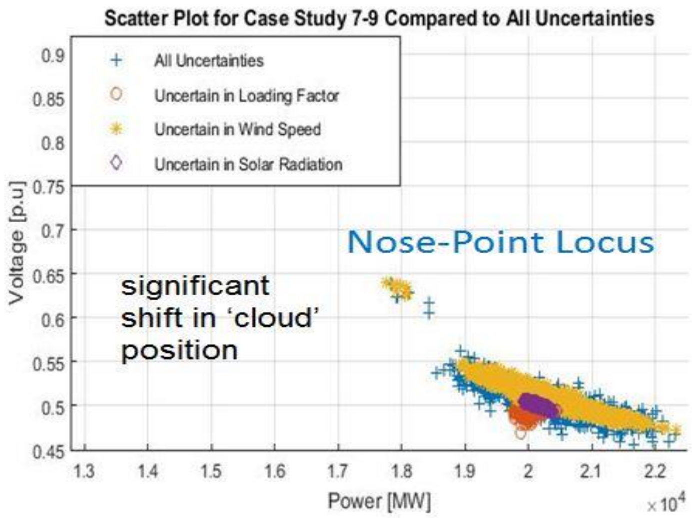

Fig. 4.5 Scatter Plot for Case Studies 7-9

4.7 A Quantitative Analysis of the Nose-Point Distributions

The quantitative analysis of results for the above case studies can be produced by generating probabilistic density functions (*pdf*s) based on nose-point distributions. Normal Distribution *pdf*s have been applied to the nine case studies in two dimensions, Voltage and Power. The obtained *pdf* parameters are listed in Table 4.5. Parameters $\mu_P[GW]$ and $\mu_V[p.u]$ represent the most-probable collapse of Power and Voltage, respectively. Parameters $\sigma_P[GW]$ and $\sigma_V[p.u]$ represent the standard deviation of the *pdf*s on the Power and Voltage axis, respectively. The ranking of critical uncertain parameters can be easily derived from Table 4.5 by comparing the values of $\sigma_P[MW]$ and$\sigma_V[p.u]$. The results are found to be the same as in previous two sections. Fig. 4.6 uses scatter plots of all 9 study cases to visually illustrate the results in Table 4.5. The clusters of points ('clouds') in Fig. 4.6 are plotted based on the parameters of the pdfs obtained from the 9 case studies. A total of 9 clusters of points are plotted. Each cluster contains 1000 nose-points obtained through the performed Monte-Carlo simulation for different case studies. For example, the clusters in the top-right corner are nose-points for study cases 1, 2 and 3 discussed in this section of the thesis.

Table 4.5 Quantitative analysis results

PDF parameters		$\mu_P[GW]$	$\sigma_P[GW]$	$\mu_V[p.u]$	$\sigma_V[p.u]$
Study Cases	1	21.20	0.07	0.90	0.00
	2	21.12	0.05	0.90	0.00
	3	21.17	0.01	0.90	0.00
	4	13.39	0.13	0.87	0.01
	5	13.85	0.14	0.87	0.02
	6	13.42	0.01	0.87	0.00
	7	20.04	0.11	0.50	0.01
	8	20.30	0.70	0.51	0.02
	9	20.08	0.09	0.50	0.00

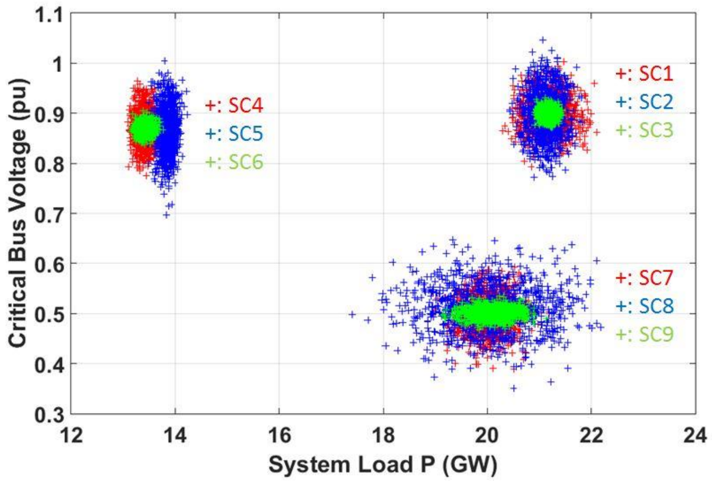

Fig. 4.6 Scatter plot for illustration propose of Table 4.5

4.8 Summary

In this chapter of the thesis, a probabilistic based ranking of the critical uncertain parameters based on their influence on power system voltage stability is presented. Two types of load model, constant power and constant impedance, are connected to the system for the investigation of the effect of load models on system voltage stability. The uncertain input parameters in the form of load demand, wind power generation and solar power generation, are introduced to the test network in order to simulate the stochastic operation conditions of a modern power system. The critical and stiff buses in the test network are first identified considering different study cases. The group of load buses 40, 46, 47 and 48, all in the NYPS area of the system, is identified as the most-probable critical buses in the test network irrespective of which uncertain input parameters and load models are used. System operators therefore, should invest more in monitoring equipment around the identified critical buses since they appear to collapse before the others under most of the conditions.

For the ranking of different uncertain parameters based on their influence on a system voltage stability analysis, it is found that at a higher level of system loading the variance in loads has the largest influence on system voltage stability, followed by variance in wind speed and solar radiation. However, at a lower level of system loading, the variance in wind generation overtakes system loading as the most influential uncertain parameter. These findings can provide a reference to the system managers and operators when they face different system operation conditions and help them to decide how to achieve better monitoring of the network with less resource. It is also noticed that at lower loading the system voltage stability becomes more affected in general by system uncertainties (of any type).

Finally, as expected, this study also indicates that the load models can have a significant effect on the locations of the system voltage collapse point. Constant impedance load models are proved to be a better choice compared to constant power load models since they can cause the system to be less prone to voltage collapse. The quantitative analysis of the results showed that a system voltage stability analysis is more sensitive to the uncertain parameters when constant impedance load models are used.

However, the results obtained in this chapter are only based on the evaluation of the effect of three types of uncertain parameters on power system voltage stability analysis (loads, wind generation and PV generation). In order to access the effect of an individual parameter on power system stability studies, one has to manually set case studies for that particular system parameter which would be very ineffective for applications in large complex network analysis. More elaborate methods which can be quickly and easily applied, and which have the ability to evaluate the effects of several uncertain parameters at a time and rank them based on the obtained results is required. This research employed the Sensitivity Analysis methods for that purpose and the application of these methods are discussed in the following chapters.

Chapter 5 : Voltage and Angular Stability Analysis of Uncertain Power Systems using Sensitivity Analysis Methods

Modern power systems are required to be operated in a flexible, environmentally friendly yet efficient manner; they should also have the ability to support fast-changing load demands as new types of loads can exhibit spatial and temporal uncertainties. These requirements can be fulfilled by more sophisticated construct of renewable generations, flexible hierarchical control structures, demand side management, use of energy storage, etc. The new technologies bring additional uncertainties in generation and loading profiles and challenge the stable operation of power systems. For the purpose of the safe operation of power systems, it is important for system operators to understand to what extend their systems can be influenced by the above-mentioned uncertainties. It is also important to establish the system stable operation margins from the perspective of power system security analysis. This makes the identification of the influential, uncertain input parameters within a network very important when we talk about a power system stability analysis, especially during the planning and operational stages of modern power systems. Sensitivity analysis methods can numerically describe how the system outputs are influenced by the inputs. In this chapter, six commonly used sensitivity analysis methods have been first applied to voltage stability analysis of uncertain power system and their performances are compared. The Morris Screening method has been selected as the best and its application is then extended to power system angular stability studies.

5.1 Stability Indices

Power system voltage and angular stability analysis discussed in this thesis comprises three categories of stability problems: voltage stability, small-disturbance stability and transient stability studies. Different stability indices are required when performing its corresponding category of stability analysis. In this research the load margin, damping of the critical eigenvalues, and transient stability index (TSI) are used as stability indices for voltage, small-disturbance and transient stability analysis, respectively.

5.1.1 Voltage Stability Index

Voltage stability problems are commonly found in heavily loaded networks as the reactive power provided by the system may not be sufficient to support the user-end voltages [33]. A commonly used approach for the assessment of power system voltage stability is the P-V curve analysis, where the stability index is the loadability (or load margin) of the system [175] as shown in Fig. 5.1. This index indicates the maximum active power the network can provide to meet the load demand before voltage collapse happens in the system. Fig. 5.2 shows the histogram of the critical loadability values obtained from 1000 MC simulations of a probabilistic assessment of power system voltage stability. Figure 5.1 is the same as Fig 2.2 shown in Chapter 2 and is reproduced here to help understanding contents of this chapter. The fitted probability density function (*pdf*), corresponding to normal distribution in this case, is also plotted in this figure to illustrate the variation in system loadability due to the stochastic behaviours exhibited by load and RES.

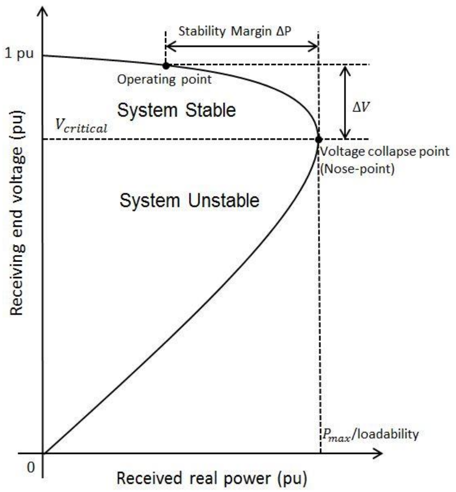

Fig. 5.1 The P-V curve

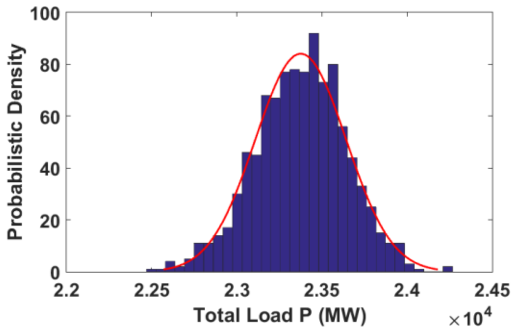

Fig. 5.2 Histogram-*pdf* of nose-point locus for voltage stability analysis based on 1000 Monte Carlo simulations

5.1.2 Small Disturbance Stability Index

For power system small-disturbance stability analysis, the modal analysis is employed in this study. The damping of the critical oscillatory mode is used as the stability index, as defined by (5.1) [15].

$$\xi_i = \frac{-\sigma_i}{\sqrt{\sigma_i^2 + \omega_i^2}} \tag{5.1}$$

In (5.1) ξ_i, σ_i and ω_i are the damping ratio, damping and frequency of the critical eigenvalue. Fig. 5.3 shows the histogram of the damping of the critical electromechanical mode obtained from 1000 MC simulations of a probabilistic assessment of power system stability. The histogram is again fitted with a *pdf* based on normal distribution to illustrate the effect of system uncertain parameters on a small disturbance stability related study.

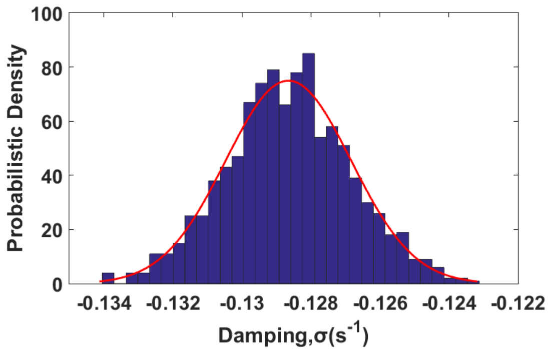

Fig. 5.3 Histogram-*pdf* of the damping of the critical mode for small-disturbance stability analysis based on 1000 Monte Carlo simulations

5.1.3 Transient Stability Index

Power system transient stability is most frequently analyzed using the time domain approach. The transient stability index (TSI) is commonly used as the stability index and is given by (5.2) [163, 176, 177].

$$TSI = 100 * \frac{360-\delta_{max}}{360+\delta_{max}} \tag{5.2}$$

In (5.2) δ_{max} is the maximum rotor angle separation between any two generators in the network after a fault. A negative TSI value indicates that the system is unstable. The larger the TSI the more stable the system is. Fig. 5.4 presents the histogram of the TSI obtained from 1000 MC simulations of a probabilistic power system transient stability assessment, and is fitted to a *pdf* to illustrate the effect of the considered uncertain parameters on system transient stability analysis. The TSI histogram is fitted with normal distribution as before for the ease of comparison, though normal distribution clearly is not the most appropriate fit in this case.

Another commonly used transient stability index is the settling time of the rotor angle of each generator. This index is used as the indication of oscillatory stability, given by (5.3)

$$Oscillatory\ Stability = \left|\frac{\delta_i final - \delta_i initial}{\delta_i initial}\right| * 100\% \tag{5.3}$$

Equation (5.3) measures the magnitude of oscillations of each generator's rotor angle for a period of time after the fault. The system is considered to settle to a new steady state if the index value is smaller than 5% [176].

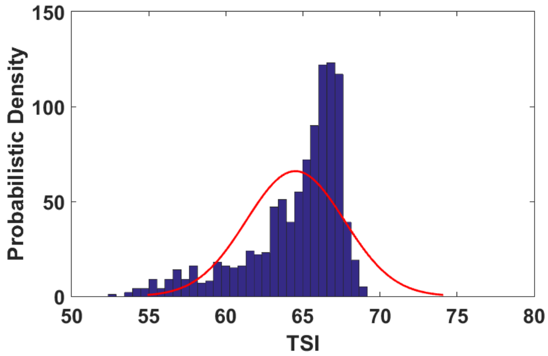

Fig. 5.4 Histogram-*pdf* of TSI for transient stability analysis based on 1000 Monte Carlo simulations

The Figs. 5.2, 5.3 and 5.4 are given for illustrative purposes only to show the results of probabilistic power system related stability studies. They are obtained by performing 1000 corresponding MC simulations for each of the three stability studies and for a specific operating condition using the IEEE 68-bus test network described in Chapter 3 of this thesis. Different operating conditions (loading level, uncertainty level, topology of the network, generation dispatch, etc.) would result in different shapes and spread of the obtained histograms and their corresponding fitted *pdf*s. Based on the fitted *pdf*s, the stability profiles of the test network can be

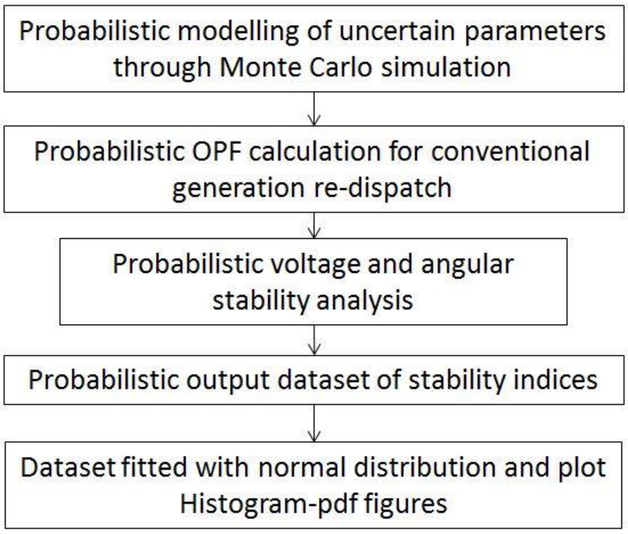

Fig. 5.5 Flow chart for combined voltage and angular probabilistic power system stability analysis

analyzed under varied operating conditions. When the stability limits are taken into consideration the risk of system instability can be assessed. Fig. 5.5 presents a flow chart of the generic procedures used for the probabilistic power system stability analysis in this chapter. This approach has been used to plot Figs. 5.2, 5.3, and 5.4 presented earlier. The procedure contains 5 major steps. At first, the dataset of the uncertain parameters is generated through Monte-Carlo simulation. Then the conventional generation re-dispatch is calculated with OPF solver. The third step involves the voltage and angular stability analysis of the test network. The calculated stability indices are then extracted from the raw data (step four) and finally fitted with a selected probabilistic distribution function (step five) for the demonstration of the network dynamic response to the introduced uncertainties.

5.2 Overview of Sensitivity Analysis Methods for Power System Stability Studies

In this section of the thesis, a total of six sensitivity analysis methods are discussed with respect to their suitability for identification and ranking of the critical uncertain system parameters based on their influence on power system stability analysis. Two evaluation dimensions, the accuracy and efficiency of the employed sensitivity analysis methods are compared, and their corresponding application scenarios are discussed.

The aim of the comparison is to find a sensitivity analysis approach which is suitable to be used for fast implementation in power system stability analysis. By doing this, the system stability margin can be established for network with penetration of new uncertain technologies. Ancillaries for the purposes of monitoring and fine-tuning of the system can be optimally planned and placed, hence reducing the resources and investment needed from operators.

This section presents a summary of some commonly used sensitivity analysis methods for the identification and ranking of critical parameters affecting power system stability. Voltage stability analysis has been selected and used in this section to access the performance of different sensitivity analysis methods when applied on power systems.

5.2.1 Selected Sensitivity Analysis Methods

This section employs six widely used sensitivity analysis methods for the identification and ranking of critical parameters affecting system stability of a power system with renewable generations:

i. The One-at-A-Time (OAT) method in the category of local sensitivity analysis methods. The One-at-A-Time (OAT) method is a linear regression-based approach. Its effectiveness is limited to linear 1st degree models which are considered to be with low-complexity. The simulation time and computational resources it requires are low since only *n+1* simulations are required for a system with *n* uncertainties.

ii. The Morris screening method (MSSA) belongs to the category of screening sensitivity methods. The Morris Screening method is suitable for implementation on non-monotonic, discontinuous models. These models are classified as high-complexity models due to their non-linear nature and inherent correlation between variables. However, by using a semi-global sampling approach this method only requires very little simulation time.

iii. The Pearson Correlation Coefficient method (PCCE) falls in the category of global sensitivity analysis methods. This is a linear regression-based approach, similar to the One-at-A-Time method. This method is usually found to be used on linear models. It is the most commonly used approach in science and engineering [147]. The model complexity this method can be applied to, and the number of simulations this method requires, are both considered moderate.

iv. The Spearman Correlation Coefficient method (SCCE) is also in the category of global sensitivity analysis methods. This method provides a nonparametric measure of rank correlations. It assesses how well the relationship between two variables can be described using a monotonic function. This method has been often applied to continuous and discrete ordinal models to access the monotonic relationship between variables.

v. The Partial Correlation Coefficient method (Partial) belongs also to the category of global sensitivity analysis methods. This method is a rank regression-based approach which is capable of measuring the degree of association between two random variables when the effect of a set of controlling random variables is removed.

vi. The Sobol Total Indices method (Sobol) is also one of global sensitivity analysis methods. This is a method which can be used on non-monotonic, non-linear, discontinuous models. Due to the detailed global search through the variables, the simulation time required for this method is very long.

Fig. 5.6 presents the relative computational effort and permissible model complexity of the discussed sensitivity analysis methods. It should be noticed that the more simulations performed, the more accurate the simulation results are considered to be due to a more detailed representation of the input matrix.

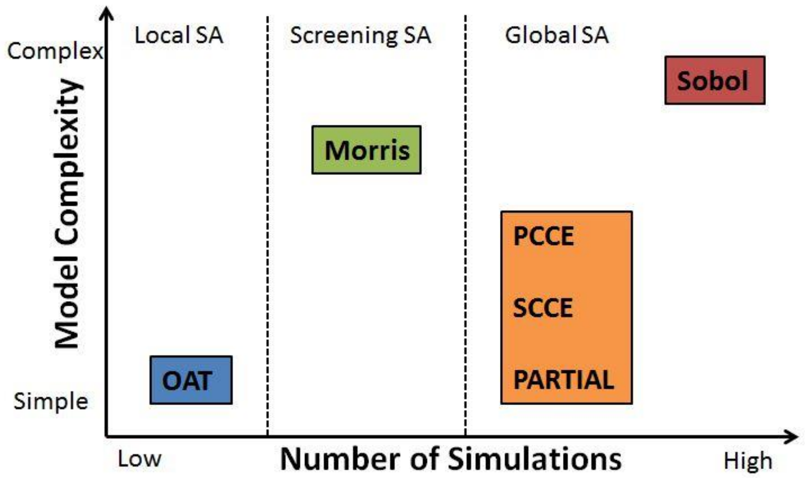

Fig. 5.6 Relative computational effort and complexity of the sensitivity analysis techniques

5.3 Application of Sensitivity Analysis methods on Voltage Stability Analysis

In general, the identification and ranking of the critical parameters affecting voltage stability requires 3 major software platforms for the modelling and analysis of the test network. The steps involved are:

i. The probabilistic modelling and sensitivity analysis sampling of input variables, which are calculated in MATLAB.
ii. The Optimal Power Flow calculation for conventional generation re-dispatch, which is performed in the MATPOWER toolbox included in Matlab.
iii. The P-V curve analysis, which is performed in DIgSILENT PowerFactory.

The first step of the analysis will generate stochastic datasets for the uncertain input parameters. It determines the system input parameter value matrix which can be used in the OPF calculation. This is done within MATLAB through Monte-Carlo simulations. In this section, the MATLAB code containing the sampling of uncertainties in load demand (with Normal Distribution), wind generation (with Weibull Distribution) and PV generation (with Beta Distribution), are established. The level of uncertainty is set to be $3\sigma = \pm 10\%$ *of* μ with Normal Distribution or equivalent when other distributions are used. This specific level of uncertainty was chosen since it represents a typical wind generation forecasting error over a 24-hour time horizon [178]. In this study the level of uncertainty for all 3 uncertain parameters is controlled to be the same in order to compare their influence on power system voltage stability.

The next step is to perform the Optimal Power Flow calculation within the test system through the MATPOWER toolbox for conventional generation re-dispatch purposes. In this step the generator operating condition with parameters like apparent power S, active power P and voltage V, are calculated. The bus loading on all system load buses is determined and the amount of renewable power generation is generated. The above data is then extracted in order to generate the input files for system stability analysis.

The above two steps are performed within the MATLAB platform. For a different sensitivity analysis approach the sampling number of uncertain parameters can be different, hence leading to different system operating conditions, number of simulations and corresponding sampling times. With each different operating condition the solution of Optimal Power Flow is different. The accuracy of the analysis is strongly related to the number of simulations performed. The more points sampled for input uncertain parameters within the uncertain domain, the more accurate the analysis results will be.

The third step of the analysis is the P-V curve calculation through power system dynamic simulation software, DIgSILENT PowerFactory. The P-V curve calculation is a commonly used method for finding the voltage collapse point of a power system. In this step the DIgSILENT PowerFactory takes in the previous generated system component parameters. The system is then stressed under a continuous increment in all bus loading until the system comes to its breaking point (where voltage collapse happens). The system load at that breaking point is considered as the loadability limit and the value is recorded for sensitivity analysis as an output matrix.

The last step of the analysis is the sensitivity analysis which unveils the influence of different uncertain parameters on system loadability margins. This step is performed again within the MATLAB platform by manipulating the employed sensitivity analysis methods. In this step the correlation coefficient between input parameters obtained through step 2 and system loadability obtained through step 3, are crosschecked. The system uncertain parameters with a higher correlation coefficient score are considered to be more influential when performing system voltage stability related studies.

Fig. 5.7 illustrates the steps required for the application of sensitivity analysis methods to power system stability-related studies in the available simulation environment.

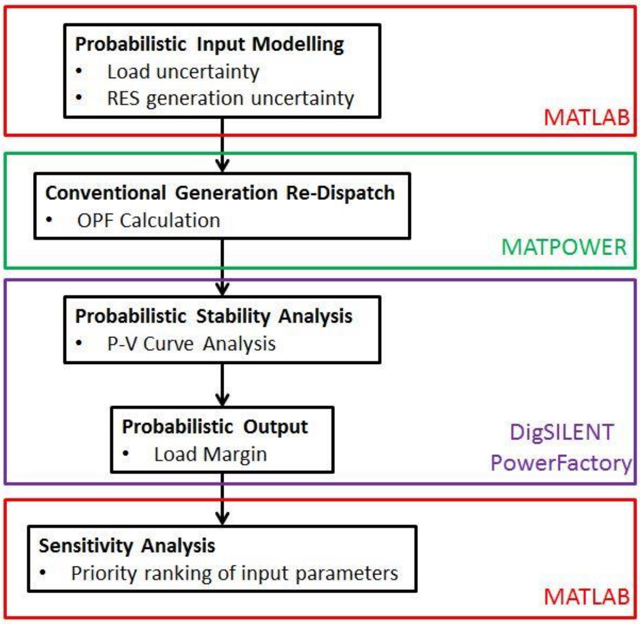

Fig. 5.7 Flow Chart for the Ranking Procedure

Fig. 5.7 above presents a flow chart for the applied sensitivity analysis procedure. Red boxes indicate the contained steps are performed in Matlab platform. Green box involves the use of MATPOWER solver. And steps within purple box are performed in DigSILENT PowerFactory. The interactions between different platforms involve data to be extracted from one platform and inserted to the following platform. Hence data management is important in this study.

5.3.1 Performance of the Sensitivity Analysis Methods

In this subsection of the report, the previously mentioned six sensitivity analysis methods are used for the ranking of critical system parameters affecting system voltage stability and the corresponding ranking results are demonstrated. The performance of the sensitivity analysis methods when applied to voltage stability assessment is discussed. Two case studies are designed and implemented in this section with different loading levels considered. The loading levels have been set to

Table 5.1 The RES Penetration Level for Different Case Studies

	Total System Load (MW)	Conventional Generation Capacity (MW)	RES Generation Capacity (MW)	RES Penetration Level
High Load Scenario (1pu)	21136	15634	5502	26%
Average Load Scenario (0.6pu)	14219	7837	6381	45%

1 pu for high loading scenario and 0.6 pu for average loading scenario. Table 5.1 contains the renewable generation penetration level for the two case studies. The RES penetration levels are calculated based on the proportion of them supporting total system load, e.g., 30% penetration level means that 30% of the load is supplied by RES. It should be noted that the RES penetration level in case of average load scenario is higher than that of high load scenario as the system load decreases while the number of connected RES remains the same.

5.3.1.1 Ranking of System Uncertain Parameters (High Loading Scenario)

Previous studies and the results obtained from Chapter 4 have already pointed out that with different system loading levels the system voltage stability limits can be different [39, 179]. In this case study, a relatively high loading level at 1 p.u is used. This can simulate system behaviour when a network is heavily loaded at its rated generation capacity and find the corresponding voltage stability margin of a stressed network.

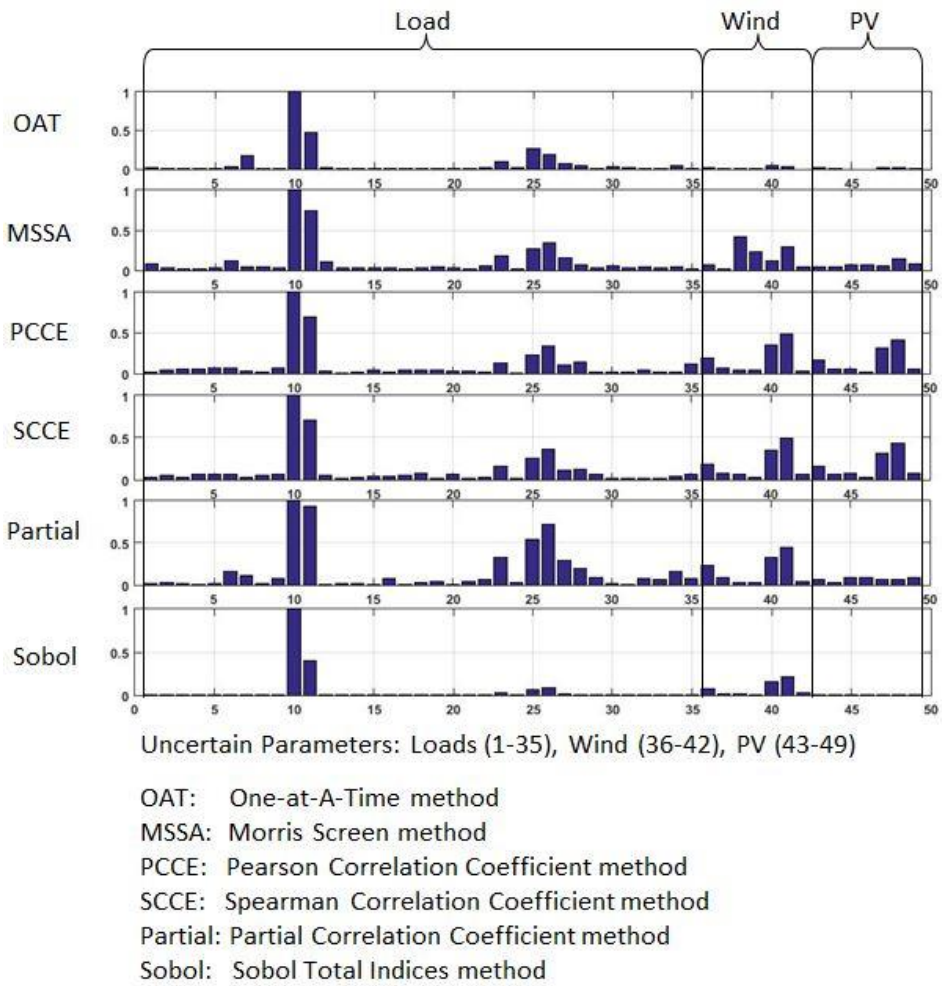

Fig. 5.8 Ranking of uncertain parameters through 6 sensitivity analysis methods under high loading scenario

Fig. 5.8 uses histograms to illustrate the ranking of critical parameters when different sensitivity analysis methods are used. The histograms can visually illustrate how sensitive the system voltage stability margins (as output variables) are to the uncertainties in different individual system uncertain parameters (as input variables). The effects of 35 bus loadings, 7 wind generation and 7 PV generation on system load margin have been recorded and illustrated by the height of the bars in the Fig. 5.8. The height of the bars in the histograms represents the weighted score given to individual input parameters by different sensitivity analysis methods. The range of the weighted ranking score varies between 0 to 1 for all the employed sensitivity analysis methods, where a score of 0 means the corresponding input variable has no influence on the output. A higher sensitivity analysis score means the output variance is more sensitive to the change of the corresponding input variable. In this case, the critical parameters for a power system voltage stability analysis can be identified and ranked based on the height of the bars. It can be observed that for this case study (1 pu loading level), all the employed sensitivity analysis methods pick No. 10 as the most influential parameter. The OAT method failed to identify the influence of RES generation on power system voltage stability, while all the other employed sensitivity analysis methods are able to illustrate the importance of RES generation. It is not surprising to observe a nearly identical trend in histograms for the Pearson and Spearman Correlation Coefficient methods as they share the same approach for variable sampling. The results obtained through the Morris Screening Method and the Partial Correlation Coefficient method share the same trend with the Pearson and Spearman methods which highlight the importance of parameters no. 10, 25, 35 and 40. The Sobol total indices method performs the most samplings and uses the longest simulation time. Its massive sampling through the research space makes it the most accurate in terms of importance measuring of input parameters. The results obtained through Sobol approach agree with the global and the screening method by identifying the same trend of important parameters. It also reflects that the other sensitivity analysis methods are over-weighting some of the parameters. This can result in the different ranking of the parameters between sensitivity analysis approaches. This is not to deny the accuracy of other sensitivity analysis methods, though. They can select almost the same top 10 influential parameters as Sobol method (No. 10, 11, 23, 25, 26, 36, 37, 40, 41, 42, 47, 48, etc.), though not in exactly the same ranking order. The identification of top 10 influential parameters out of 49 considered parameters in total is good enough for power system voltage related studies. It will be shown in Section 5.3 of the thesis that the power system stability margin is only affected by the top several influential parameters. The power system stability margin under different operation conditions therefore can be accessed based on the characteristics of only those selected influential parameters.

Table 5.2 shows the top ten identified system critical parameters obtained from the six different Sensitivity Analysis approaches. In this table the numbering of the parameters on the histograms are mapped to the actual system parameter in the test network shown in Fig. 5.8. These rankings are obtained with respect to the variation of the system loadability. It can be observed that all six Sensitivity Analysis methods are capable of identifying the same most influential uncertain parameter: the load variation on bus 17 (No. 10 uncertainty in Fig. 5.8). However, the limitation of the OAT method underestimates the influences of PV and wind generations. It only picks the wind generation connected to bus 53 among its top 10 ranking,

Table 5.2 Top 10 identified system critical parameters under high loading scenario

	OAT	**Morris**	**PCCE**	**SCCE**	**Partial**	**Sobol**
	Parameter Name (Parameter No. in Histograms)					
Ranking	L17 (10)	L17 (10)	L17 (10)	L17 (10)	L17 (10)	L17 (10)
	L18 (11)	L18 (11)	L18 (11)	L18 (11)	L18 (11)	L18 (11)
	L41 (25)	W68 (38)	W33 (41)	W33 (41)	L42 (26)	W33 (41)
	L42 (26)	L42 (26)	S33 (48)	S33 (48)	L41 (25)	W53 (40)
	L64 (7)	L41 (25)	W53 (40)	W53 (40)	W33 (41)	L42 (26)
	L39 (23)	W33 (41)	S53 (47)	S53 (47)	W53 (40)	W60 (36)
	L44 (27)	L39 (23)	L42 (26)	L42 (26)	L39 (23)	L41 (25)
	L45 (28)	L44 (27)	L41 (25)	L41 (25)	L44 (27)	W17 (42)
	L61 (6)	S33 (48)	W60 (36)	W60 (36)	W60 (36)	L39 (23)
	W53 (40)	L61 (6)	S60 (43)	S60 (43)	L45 (28)	L44 (27)
	L= Bus Loading, W= Wind Farm, S= PV Farm, Numbering correspond to system buses in Fig. 5.8					

compared to the benchmark ranking produced using Sobol method, it over-estimate the influence of some system loads over RES generation on voltage stability. The ranking obtained through the Morris screening method, though simple to implement and computationally non-expensive, is capable of identifying 7 out of 10 of the same critical parameters as the Sobol Total Indices method. The exact same top 5 important parameters between the Pearson Correlation Coefficient method and the Spearman Correlation Coefficient method in Table 5.2 are as expected since they share the almost identical evaluation mechanism. They can identify 7 out of 10 top-pick parameters compared to Sobol approach. The Partial Correlation Coefficient method shares the same accuracy level with its correlation coefficient counterparts by picking up 8 out of 10 of the same critical parameters as the Sobol Total Indices method. Under this loading scenario, the renewable generation accounts for 26% of the generation in the system. This is a relatively high penetration level for RES generations, hence we can see the sensitivity analysis methods tend to pick up the RES generations as influential parameters. Compared to the results obtained in Chapter 4 of the paper, the implementation of sensitivity analysis methods to the stability-related study is a great improvement as the effect of individual parameters can be analyzed instead of the effect of a group of parameters.

5.3.1.2 Ranking of System Uncertain Parameters (Average Loading Scenario)

In this case study, a relatively low loading level of 0.6 p.u is used. The RES penetration level, according to Table 5.1, is nearly 50% of system total generation capacity. This can simulate system behaviour when a network is moderately loaded at 60% of its rated generation capacity with high penetration level of RES generations and find the corresponding voltage stability margin.

Fig. 5.9 employs the same methodology as the previous section for the ranking of the critical parameters in a power system which affects system voltage stability. The importance of individual parameters is illustrated using histograms. The rankings result from six sensitivity analysis methods compared in terms of accuracy against Sobol approach. The abbreviations in the histograms have the same meaning as those in Fig. 5.8.

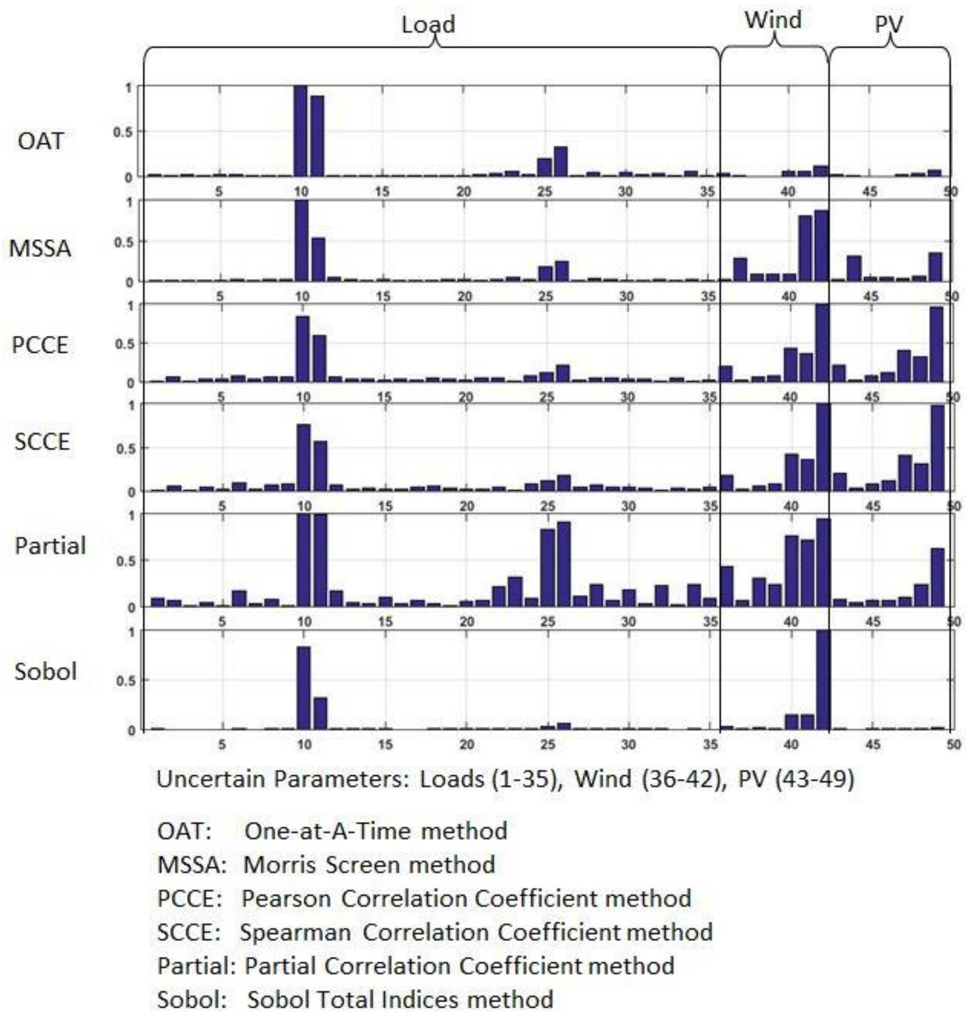

Fig. 5.9 Ranking of uncertain parameters through 6 sensitivity analysis methods under average loading scenario

Since the system loading demand is reduced in this case study compared to the high load scenario in the previous section, the generation provided by conventional generators is reduced proportionally. The renewable generation now accounts for 45% of the total generation capacity of the system. Under this operational condition, all of the proposed sensitivity analysis methods are capable of demonstrating the importance of increased renewable generation penetration on parameter rankings since the wind generation connected to bus 17 is now identified either as the most important or topmost important parameter for voltage stability analysis. By comparing the height-of-bars trends shown in Fig. 5.8 and 5.9, it can be clearly observed that sensitivity analysis methods are giving high ranking scores to the renewable generation as their penetration levels-increase under the average loading scenario. The results, however, also emphasise the importance of load demand uncertainties of bus 17 and 18 as the sensitivity analysis methods all give L17 and L18 a relatively high score for the ranking.

Table 5.3 lists the top ten identified system critical parameters from the results obtained by using six different Sensitivity Analysis approaches when a test network is under average loading. It can be concluded that 3 out of the 4 global sensitivity analysis methods rank the wind generation connected to bus 17 as the most influential input parameter. This time the OAT method is able to identify almost the same parameters selected by global methods and it also demonstrate the impact of an increased proportion of renewable generation. However, it still over-estimates the impact of some system loads due to the limitation of its local search space. The

Table 5.3 Top 10 identified system critical parameters under average loading scenario

	OAT	**Morris**	**PCCE**	**SCCE**	**Partial**	**Sobol**
	Parameter Name (Parameter No. in Histograms)					
Ranking	L17 (10)	L17 (10)	W17 (42)	W17 (42)	L17 (10)	W17 (42)
	L18 (11)	W17 (42)	S17 (49)	S17 (49)	L18 (11)	L17 (10)
	L42 (26)	W33 (41)	L17 (10)	L17 (10)	W17 (42)	L18 (11)
	L41 (25)	L18 (11)	L18 (11)	L18 (11)	L42 (26)	W33 (41)
	W17 (42)	S17 (49)	W53 (40)	W53 (40)	L41 (25)	W53 (40)
	W33 (41)	S57 (44)	S53 (47)	S53 (47)	W53 (40)	L42 (26)
	W53 (40)	W57 (37)	W33 (41)	W33 (41)	W33 (41)	L41 (25)
	S17 (49)	L42 (26)	S33 (48)	S33 (48)	S17 (49)	W60 (36)
	L51 (34)	L41 (25)	L42 (26)	L42 (26)	W60 (36)	S17 (49)
	L39 (23)	W53 (40)	W60 (36)	W60 (36)	L39 (23)	W68 (38)

L= Bus Loading, W= Wind Farm, S= PV Farm, Numbering correspond to system buses in Fig. 5.9

result of the Morris Screening method again shows good agreement with global methods in identifying the important system parameters. The same conclusion as in the previous section can be drawn -- that the accuracy of global and screening sensitivity analysis methods is sufficient when it comes to the identification of system influential parameters.

5.3.2 Comparison between Sensitivity Analysis Methods

To compare the performances of the six proposed sensitivity analysis methods, a three-dimension evaluation approach is employed:

i. The simulation times required for the application of each sensitivity analysis approach.
ii. The accuracy of the ranking results obtained through different sensitivity analysis approaches.
iii. The permissible system complexity for each sensitivity analysis approach.

Although there are only 49 uncertain parameters analysed and ranked in the two previous sections, for ease of code implementation, the actual number of the uncertain parameters considered during the simulation is 66 (there are 17 buses that do not have any load connected to them). All the simulations and calculations are performed on a PC with an Intel® Core™ i7 processor at 3.4 GHz and 16 GB of RAM. The simulation time presented in this study is for demonstration purposes only as they can be different on PCs with different settings. The main purpose of the comparison between simulation times required by different sensitivity analysis methods is to demonstrate the efficiency of the individual SA methods.

Table 5.4 The number of simulations and computational time required for different sensitivity analysis methods

SA Methods	*Cost*	*No. of Simulations*	*Time (High Load)*	*Time (Average Load)*
OAT	*p+1*	67	28.86 s	35.81 s
Morris	*p*r+1*	331 (r=5)	147.49 s	163.01 s
PCCE	*N*	1000	337.49 s	464.23 s
SCCE	*N*	1000	337.49 s	464.23 s
Partial	*N*	1000	337.49 s	464.23 s
Sobol	*(p+1)*N*	67000	25881.51 s	32714.13 s

The simulation times required for different sensitivity analysis methods depend on the number of model evaluations the simulation requires on implementation. For a system with *p* uncertain input variables, the simulation times required by the proposed six sensitivity analysis methods are shown in Table 5.4.

In Table 5.4, *p* represents the number of system uncertain inputs, *r* represents the 'level' of the Morris Screening method (usually from r=4 to 10), *N* represents the Number of Monte Carlo Simulation.

Table 5.4 clearly indicates the huge time (required computational cost) differences between local, screening and global sensitivity analysis methods. It should also be noted that the simulation times required under the average load scenario are longer than those under a high load scenario. This is due to the fact that when a system is stressed under a low load, it is less vulnerable to voltage collapses compared to the high load scenario. The simulation then needs more iterations to increase the system load until the system reaches its loadability margin.

The reason behind voltage collapse (or voltage instability) is that when a system is loaded, the system components like the loads will require reactive power in order to keep the terminal voltage constant. The main sources of reactive power in the testing network are from the synchronise machines. However, synchronise machines have capability curves which can limit their reservation of reactive power. The system terminal voltage will drop once all reactive power reservations have been consumed, this will worsen the network condition because of the lack of sufficient reactive power support in the system. In a heavily loaded system, the heavily loaded transmission lines will also consume a huge amount of reactive power from the system. This will lead to a more vulnerable system compared to a lightly-loaded system and even worse, insufficient reactive power support.

Table 5.5 The correlation coefficient measurement between the ranking results (top 5 critical parameters) from different sensitivity analysis methods against Sobol

SA Method	*Correlation Coefficient against Sobol (High Load)*	*Correlation Coefficient against Sobol (Low Load)*
OAT	20%	80%
Morris	80%	60%
PCCE	60%	60%
SCCE	60%	60%
Partial	60%	80%
Sobol	100%	100%

For the assessment of the accuracy of the ranking results, the Sobol Total Indices method is considered as the benchmark. The Sobol Total Indices method has been proved in the past that it can be very reliable in the case of assessment of non-linear, non-monotonic models [142, 148]. Table 5.5 presents the accuracy evaluation for the six employed sensitivity analysis methods. The identified top 10 critical parameters by different sensitivity analysis methods are crosschecked and their corresponding correlation coefficient against Sobol is calculated. The method with a higher correlation coefficient value against the ranking of the Sobol Total Indices method indicates that it can provide a more accurate ranking. It can be observed from Table 5.5 that the Morris Screening method demonstrates a relatively high agreement to the benchmark Sobol by identifying 4 out of 5 critical parameters. The OAT method suffers from its limited local research and achieved the lowest accuracy when compared to other SA methods. The global sensitivity analysis methods also show good agreements with the Sobol method.

The presented six sensitivity analysis methods can also be compared from the perspective of their effective model complexity level. This has been already discussed by previous researchers in [156, 180]. To summarize the past work done by researchers, the following conclusions are stated:

The Morris screening methods and the Sobol Total Indices method are both suitable for implementation on Non-monotonic, discontinuous models, which are classified as high-complexity models [156].

The Partial Correlation Coefficient method and the Spearman Correlation coefficient method are rank regression-based. They are effective when applied to monotonic models without interactions and considered to be medium complexity methods [148].

The One-at-A-Time method and the Pearson Correlation Coefficient method are linear regression-based. Their effectiveness is limited to Linear 1st degree models which are of low complexity [149].

Fig. 5.10, 5.11, 5.12 employ radar plots to visually illustrate the three-dimensional comparisons between the employed six sensitivity analysis methods from the perspectives of simulation time, accuracy and permissible model complexity, respectively.

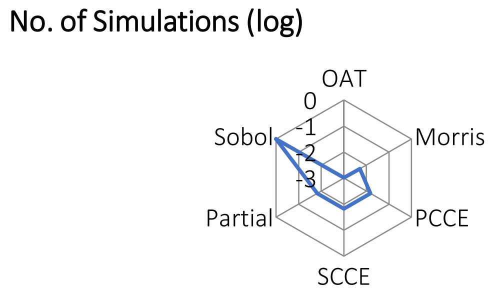

Fig. 5.10 Number of simulations required by each SA method

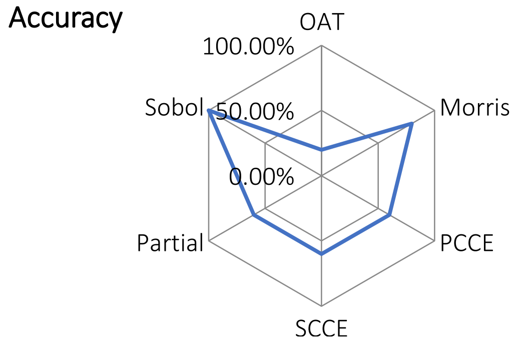

Fig. 5.11 Accuracy comparison between the six SA methods

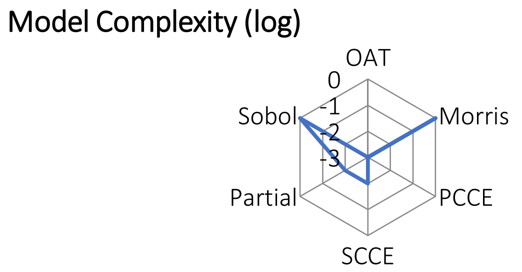

Fig. 5.12 The applicable system complexity level for the six SA methods

It can be concluded from the three figures that the Sobol Total Indices method is the most accurate sensitivity analysis method among the six approaches employed due to its massive search space within the input variables. It is suitable for implementation on non-monotonic, discontinuous models, which are classified as high-complexity models. However, it requires a huge amount of simulation time and consumes the most calculation resources. This makes it unsuitable to be used in situations which require fast implementation, like on-line real-time operations. The Morris Screening method on the other hand, can achieve a relatively similar accuracy level compared to Sobol method but only requires around 0.5% of the simulation time. It can also be applied on complex high-dimensional, non-monotonic, discontinuous system models, of the same complexity as those on which the Sobol total indices method can be applied. This makes the Morris Screening method the most suitable for implementation in power system stability related studies. The identification and ranking of critical parameters for power system stability can be easily performed through the Morris Screening method. It exhibits great efficiency while maintaining a high level of accuracy when implemented in a complex system like the modern power network.

5.3.3 Summary on Sensitivity Analysis Methods Applied to Voltage Stability

This section compares sensitivity analysis methods for the identification and ranking of critical parameters affecting power system voltage stability. The commonly used OAT method, the Morris Screening method, the Pearson Correlation Coefficient method, the Spearman Correlation Coefficient method, the Partial Correlation Coefficient method and the Sobol total indices method have been compared based on their performance when implemented to power system stability related studies.

The top 10 ranked uncertain system parameters from Table 5.2 and Table 5.3 indicate that the uncertainty in load connected to bus 17, 18, 40 and 41 always have a large influence on system voltage stability margins, no matter what the loading conditions are. This is due to the fact that L17, L18, L41 and L42 are the largest loads within the test network, with a load size ranging from 1000MW to 6000MW. When these 4 loads have the same uncertainty level compared to small loads, the actual variation in active power drawn is larger. The rankings also give high scores to the RES parameters connected to system buses 53, 60 and 17. Bus 53 and 60 are located near the tie-lines between the New England Test System and the New York Power System. Bus 17 is connected to the largest load in the test network. These system topologies contribute to the high scores presented in the ranking results for these uncertainties.

The impact of system loading levels can be clearly observed by comparing Figs. 5.8 and 5.9. The decrease in system loading demand is accompanied by an increase in the proportion of renewable generation. The ranking methods then give higher scores to the uncertain parameters related to renewable generations.

Table 5.4 and Table 5.5 compare the six sensitivity analysis methods based on their corresponding resource consumption and accuracy. The poor performance of the local sensitivity analysis method is unfavorable due to the misleading ranking results. It is though the fastest approach among the six sensitivity analysis methods employed when considering the implementation time. It is however, the least accurate due to its limited local search among the uncertain input dataset. The Sobol Total Indices method performs best in complex non-parametric models when accuracy is considered. However, the high demand of computational effort from the global sensitivity analysis methods makes them inefficient for many large-scale system applications. The Morris screening method employed in this study delivers a similar ranking compared to global methods but takes much less time. It can identify 7 out of 10 of the same influential input uncertainties as Correlation Coefficient methods do but it only takes 1/3 of the time. It is also capable of identifying nearly all the influential parameters selected by the Sobol total Indices method while using only 0.5% of the computational time required for application of the Sobol method. These properties make the Morris screening method ideal for priority ranking of input uncertainties in large-scale, complex models.

The priority ranking of the influential input parameters based on their impact on power system voltage stability can help system operators to allocate appropriate monitoring and modelling at selected parameters, and hence increase system security from the perspective of voltage stability. The sensitivity analysis methods presented in this thesis can be applied in areas like power system planning and operation for efficient system analyses.

5.4 Voltage and Angular Stability Analysis using the Morris Screening Method

The advanced Morris Screening Method has been proved to be an efficient and accurate approach for power system voltage stability analysis. This section expands the application of the Morris Screening Method to the priority ranking of critical system parameters affecting the angular stability of the network with RES generation. It combines and validates the identification of critical parameters affecting system stability globally (from the perspective of voltage and angular stability). The influence of load models, uncertainty in load demand and RES generations on power system stability in general is analysed. The aim is to check if a signal parameter or a group of parameters influences the stability of the system general. The study is performed on the modified version of the 68-Bus NETS-NYPS test network which was introduced in Chapter 3.

5.4.1 The Ranking Procedure

The priority ranking of the system uncertain parameters based on their influence on power system stability consists of four major stages:

i. Using a proper probability distribution function (*pdf*) in order to generate the input dataset of system uncertain parameters,

ii. Solving Optimal Power Flow (OPF) to determine the dispatch of conventional generations,

iii. Calculating the corresponding stability index for different categories of stability problems,

iv. Using the sensitivity analysis (SA) method to rank the system input uncertain parameters based on their influence on power system stability.

Fig. 5.13 shows a flow chart of the proposed ranking procedure. The modified IEEE 68-Bus NETS-NYPS (New England Test System-New York Power System) mentioned in Chapter 3 is used as test network in this section. In order to assess the system stability behaviour under different loading conditions, a typical daily loading curve (shown as Fig. 4.1 of Chapter 4) has been adopted in this study for a generic representation of load profile variation during the day. Several points have been chosen from the curve in order to simulate the system conditions during a day. The selected loading conditions were categorised into low loading (30%, 40%), base loading (50%, 60%), intermediate loading (70%, 80%), and peak loading (90%, 100%) [181]. Equations (5.4) and (5.5) illustrate the relations between the system loading P_L, the active power of synchronous generators P_{SG}, and the active power of RES generation P_{RES}. PL_{RES} is the penetration level of RES generation in the test network and it is an important parameter for system studies with RES generation. Table 5.6 lists the operating conditions selected from the daily loading curve and their correspondingPL_{RES}.

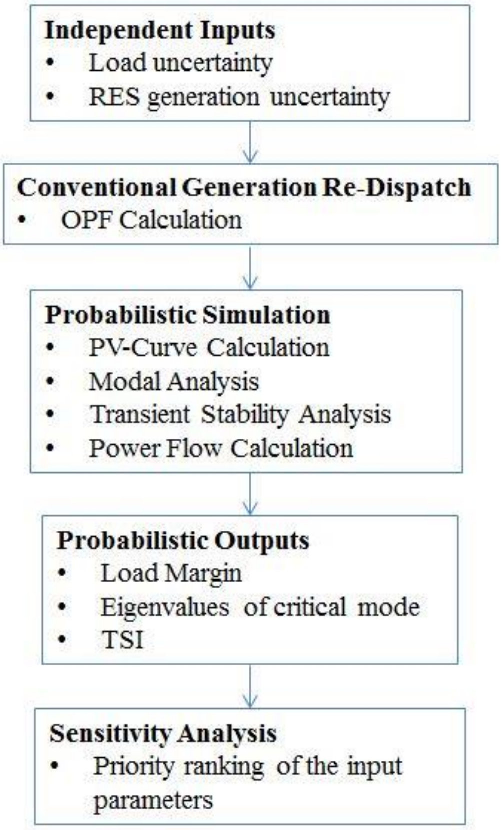

Fig. 5.13 Flow chart of the proposed methodology

$$P_L = P_{SG} + P_{RES} \tag{5.4}$$

$$PL_{RES} = \frac{P_{RES}}{P_L} \tag{5.5}$$

Table 5.6 The RES generation penetration level under variable loading demand selected from daily loading curve

Loading Demand	1.0 p.u.	0.9 p.u.	0.8 p.u.	0.7 p.u.	0.6 p.u.	0.5 p.u.	0.4 p.u.	0.3 p.u.
PL_{RES}	20%	22%	25%	29%	33%	40%	50%	67%

5.4.2 Implementation of Morris Screening Method

The advanced Morris Screening method is used in this chapter since it is easy to be implemented to power system stability related studies. Previous studies have demonstrated the successful utilization of the Morris Screening method on power system voltage and small-disturbance stability analysis. This section expands the application of the approach for power system transient stability related analysis. The implementation of the Morris Screening method involves the calculation of the sensitivity indices and the elementary effect of the input parameters. The sensitivity indices for the MSSA method are the *mean* (μ^*) and the *standard deviation* (σ^*) of the *elementary effects* (EE_p^i) of individual input uncertainty, as defined in equations (5.6), (5.7) and (5.8) [148].

$$\mu_p^* = \frac{1}{r}\sum_{i=1}^{r}\left|EE_p^i\right| \tag{5.6}$$

$$\sigma_p^* = \sqrt{\frac{1}{r}\sum_{i=1}^{r}\left(\left|EE_p^i\right| - \mu_p^*\right)^2} \tag{5.7}$$

$$EE_p^i(x) = \frac{\left[y\left(x_1, x_2, \dots, x_{i-1}, x_i + \Delta, x_{i+1}, \dots, x_p\right) - y(x)\right]}{\Delta} \tag{5.8}$$

in (5.6) μ_p^* serves as the ranking score for individual input uncertainties. The higher the score is, the more influential the corresponding uncertainty is considered. A high value of σ_p^* indicates the corresponding input has a non-linear effect on the output. p is the number of input uncertainties, r is the 'level' of MSSA (between 4 to 10), and Δ is the step size determined through $\Delta = \frac{1}{r-1}$. This study uses $r = 10$ for an accurate sampling among the search space of the input parameters. The MSSA method requires $n = p * r + 1$ simulations. The computational burden is significantly lower compared to the conventional GSA method like the Sobol total indices method [18]. A total of 661 simulation runs are performed as 66 uncertain parameters for the search space were involved.

5.4.3 The Ranking Results

5.4.3.1 Priority Ranking for Voltage Stability

Power system voltage stability analysis is performed by running P-V curve analysis. During the analysis, the loading level of the test network is varied to account for daily load variation, i.e., system load following the daily loading curve [181]. For a particular system loading level, e.g., 0.5 pu, the base starting point for load and generation is 0.5 pu. The subsequent P-V curves are generated by increasing the system loading from this level. All loads are scaled to increase simultaneously through an iteration control with adaptive step size. The conventional generation is correspondingly scaled up to compensate for the increment in load. The initial step size for load increment is set to be 0.5%, the maximum step size is 2% and the minimum step size is 0.01%. The step size reduces as the system approaches the stability limit. The iterations continue to the point where the load flow calculation doesn't converge anymore, and this point is taken as voltage stability limit (system loadability limit). The active power P (MW) and the voltage magnitude V (pu) of the collapse points are recorded to obtain the nose-point locus for voltage stability as presented in Fig. 5.2. The same process is repeated for all eight system loading levels considered, as presented in Table 5.6, to access the system voltage stability margin following the variation of the daily loading curve. The index *load margin* is introduced to measure the robustness of the test network under different operating conditions. Equation (5.9) is used for the calculation of load margin.

$$Load\ Margin = \frac{P_{collapse} - P_{initial}}{P_{initial}} \tag{5.9}$$

In equation (5.9), $P_{collapse}$ represents the system active power at the collapse point, $P_{initial}$ is the initial active power when iteration begins. The larger the load margin is, the more robust the system is.

It should be noted that voltage stability can still be an issue at lower system loading conditions. However, the load margin is relatively higher for lower loading levels, in other words, the system is less vulnerable to voltage stability issues. For example, when the system loading level is at 0.3 pu (30% of the rated generation capacity), the load margin is around 1 pu. This means the system under this condition can withstand a load demand increment equal to its own generation capacity. And for the system at 1 pu loading level, the system can only withstand a load capacity increment around 20% of its original capacity. Fig. 5.14 illustrates the system load margins at different system load levels. The uncertain parameters which contribute to the variation of input dataset for Fig. 5.14 are load uncertainties at 10% uncertainty level.

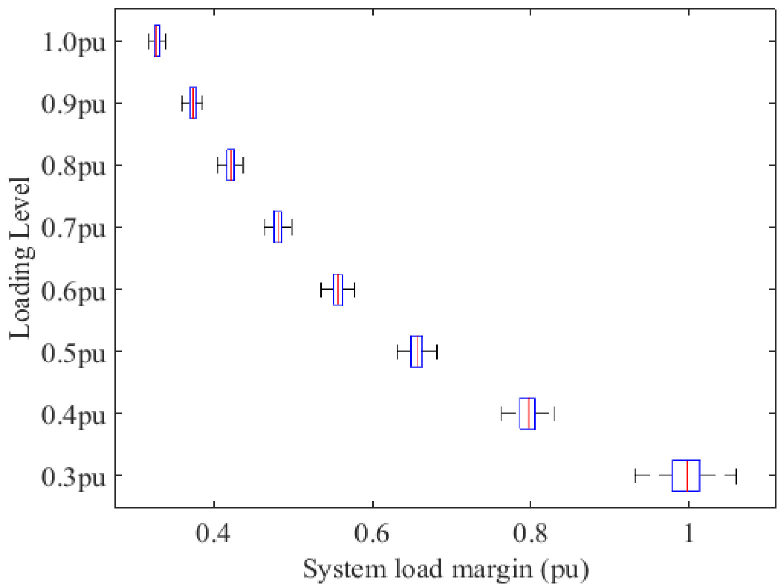

Fig. 5.14 System load margins at different system loading levels

Furthermore, the impact of system uncertainties (actual load, wind speed and solar irradiation) on power system voltage stability has been assessed through a sensitivity analysis approach, the Morris screening method. Fig. 5.15 shows a heatmap for the ranking of uncertain input parameters affecting voltage stability through MSSA (Morris screening sensitivity analysis) under eight loading conditions selected from the daily loading curve. Table 5.7 lists the top 5 identified influential parameters, as the change in their values have the dominant influence on system loadability variation compared to the rest of the parameters. The validation of this statement is presented in detail in Section 5.3.4 of this chapter. The heatmap uses different shades of colour (in this case, light blue indicates a low score while dark blue represents a high score) to distinguish the difference in ranking scores. It can be clearly observed that as the largest load in the system, L17 remains the most influential parameter through all loading levels by always displaying the darkest blue rectangle in the heatmap. The wind and PV connected to bus 17 also demonstrated a high level of impact on voltage stability performance. The penetration levels of the RES generation increase in the system when loading level decreases according to equations (5.4) and (5.5), as P_L and P_{SG} decrease while P_{RES} is kept constant. Hence the uncertainties of RES become more influential and get higher rankings in high PL_{RES} (low system loading) cases compared to low PL_{RES} (high system loading) cases. This can be observed in the heatmap as the blue squares of RES are getting darker when system loading drops. It can also be observed that blue squares representing L18, L41, and L42 are relatively dark, as they are identified as influential parameters by the sensitivity analysis.

Fig. 5.15 Heatmap of ranking for voltage stability index showing different system loading

Table 5.7 Top 5 influential parameters for voltage stability following daily loading curve

	Variable Loading Conditions Selected from Daily Loading Curve							
	1.0 pu	0.9 pu	0.8 pu	0.7 pu	0.6 pu	0.5 pu	0.4 pu	0.3 pu
Ranking (Top 5)	L17	L17	L17	L17	L17	L17	L17	L17
	L18	W17	W17	W17	W17	W17	W17	W17
	L42	L18	L18	W53	S17	S17	S17	W33
	L41	S17	S17	S17	W26	W68	W68	S17
	L20	L20	L20	L18	L18	W53	W33	W53
	L=Bus Loading, W=Wind Farm, S=PV Farm, Numbering corresponding to system buses in Fig. 5.15							

Furthermore, it can be seen from Table 5.7, by considering the top 5 identified critical parameters that the influence of uncertainties in loads 18, 42 and 41 on system voltage stability becomes less important with a higher RES penetration level. With a lower RES penetration level, the critical parameters are mostly the large lumped loads in the system, such as L_{17}, L_{18}, L_{42}, $L_{41}$and L_{20} (with a demand of 6000MW, 2470MW, 1000MW, 1150MW and 680MW, respectively). Table 5.7 also reveals that the influence of RES generation on system voltage stability becomes important (such as W17, S17, W33, W68, W53 in the three right most columns) with lower loading (and at higher penetration of RES). The RES generations connected to buses near the tie-lines between NETS-NYPS are more influential on power system voltage stability than those connected further away.

5.4.3.2 Priority Ranking for Small-Disturbance Stability

Modal analysis has been used for power system small-disturbance stability analysis in this section. Fig. 5.16 shows the heatmap for the ranking of critical parameters affecting small-disturbance stability through MSSA under 8 loading conditions selected from the daily loading curve. Table 5.8 picks the top 5 critical parameters from Fig. 5.16. It can be seen from Fig. 5.16 that the importance of uncertainties of RES generation increases as PL_{RES} increases. Loads 17 and 18 are found to have a dominant impact on system small-disturbance stability at all loading levels. The uncertainty of loads 41 and 42 becomes influential only under high loading scenarios where PL_{RES} is lower than 30%, however their influence is diminishing as PL_{RES}increases and the influence (ranking) of wind farms 60, 53, and 33 becomes higher. The loads 50 and 51 are also ranked high at higher loading levels, however, their importance diminishes when the system loading reduces below 0.9 p.u. Unlike the results obtained when voltage stability analysis is performed, this time the size of the load no longer dominants the ranking, as load 41 (1000MW) ranks higher than load 17, 18 and 42 (6000MW, 2470MW, 1150MW, respectively). This is because small-disturbance stability is highly influenced by the loads that are near the generator as angular stability is involved. Load 41 is directly connected to G14 and connected to G15 through a tie-line. The same placement pattern can also be

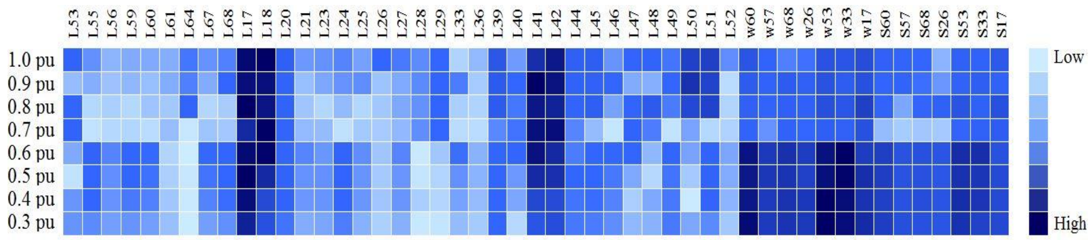

Fig. 5.16 Heatmap of ranking for small-disturbance stability index showing different system loading found in L17, 18 and 42. It can also be observed that the influence of RES generation becomes relatively high when the PL_{RES} becomes larger than 30%, this trend is similar compared to voltage stability analysis. Wind generation in general is more influential compared to PV generation. It should be noted that unlike voltage stability, the influence of the several top selected parameters are close to each other. Both Fig. 5.16 and Table 5.8 indicate that RES generations connected to buses 17, 33, 53 and 60 are identified to have the largest influence on power system small-disturbance stability. This is worth noting as these buses are located near the tie-lines connecting two big power networks.

Table 5.8 Top 5 influential parameters for small-disturbance stability following daily loading curve

	Variable Loading Conditions Selected from Daily Loading Curve							
	1.0 pu	0.9 pu	0.8 pu	0.7 pu	0.6 pu	0.5 pu	0.4 pu	0.3 pu
Ranking (Top 5)	L18	L41	L17	L18	W33	L17	W53	W53
	L17	L17	L18	L42	L18	W33	W33	W60
	L42	L18	L41	L41	L17	W53	L17	W33
	L41	L42	L42	L17	L41	W60	W60	L17
	L51	L50	W17	W17	W53	L18	S53	W17
	L=Bus Loading, W=Wind Farm, S=PV Farm, Numbering corresponding to system buses in Fig. 5.16							

5.4.3.3 Priority Ranking for Transient Stability

The transient stability of the system is analyzed through time-domain simulation. The transient stability index can be obtained by calculating the rotor angle

Table 5.9 The RES generation penetration level under variable loading demand selected for transient stability analysis

Loading Demand	1.0 p.u	0.6 p.u	0.3 p.u
PL_{RES}	20%	33%	67%

displacement between generators after a large disturbance is applied to the system. The disturbance considered in this study was a three-phase fault applied on a selected fault line followed by the line disconnection. The fault duration was 13 cycles [182]. (Note that longer than usual fault durations of 13 cycles are adopted to ensure a sufficient number of unstable cases within the considered test network. Otherwise one would typically consider fault durations of 4-7 cycles at transmission system level [33, 182]). The rotor angles of all synchronous generators are recorded for 20 seconds after the fault to illustrate the system transient dynamic behaviour. In this study several different fault locations were used in order to analysis the effect of change of system topology on system transient stability study. Three loading levels (1.0pu, 0.6pu and 0.3pu) are selected from the daily loading curve for demonstration purposes. Table 5.9 lists the selected system loading levels and their corresponding PL_{RES} levels. Fig. 5.17. demonstrates the time domain simulation results obtained in the test network. The time domain simulation records the rotor displacement of 16 generators for 20 seconds after the fault. The TSI can be calculated from time domain simulations for power system transient stability analysis.

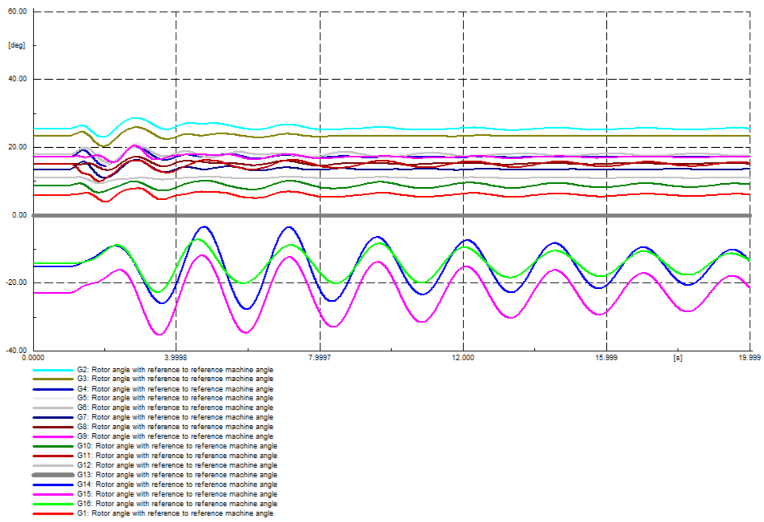

Fig. 5.17 Time domain simulation for the test network when Line 56 is disconnected at 0.3 pu loading level

There are six transmission lines selected for fault deployment and line disconnection. This is to demonstrate the influence of fault location on power system transient stability behaviour. The selected six transmission lines are line 12 (between buses 21 and 68, near critical generator G9), line 56 (between buses 33 and 38, near critical generator G11), line 42 (between buses 60 and 61, tie-line between NETS-NYPS), line 45 (between buses 53 and 54, tie-line between NETS-NYPS), line 70 (between buses 40 and 41, tie-line between NYPS-G14) and line 72

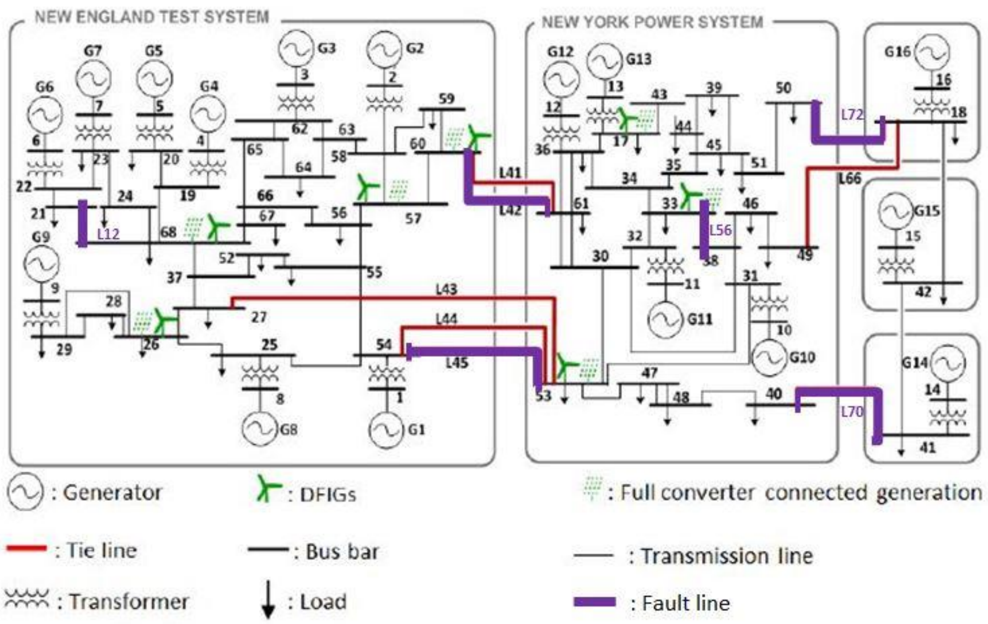

Fig. 5.18 NETS-NYPS test network with fault lines highlighted for section 5.3.3.3

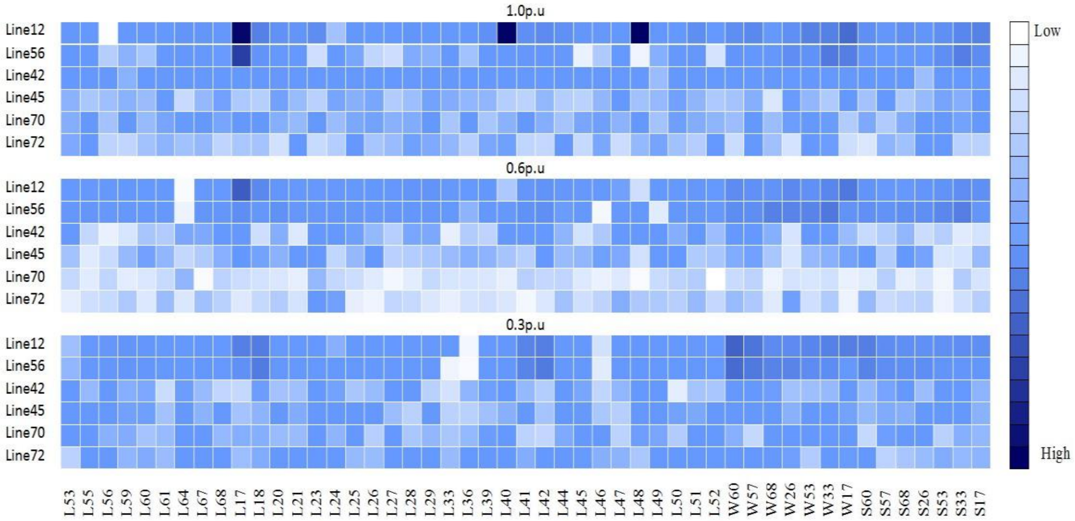

Fig. 5.19 Heatmap of ranking for transient stability index showing different system loading

(between buses 18 and 50, tie-line between NYPS-G16). Fig. 5.18 is the NETS-NYPS test network with these selected fault lines highlighted in purple.

Fig. 5.19 uses a heatmap to demonstrate the influence of individual uncertain parameters on power system transient stability in different case studies. In Fig. 5.19, the heatmap is divided into three sections representing three different system loading levels, with rows 1-6 showing the importance ranking of system parameters for 1.0 pu system loading, and rows 7-12, and 13-18 for 0.6 pu, and 0.3 pu system loading, respectively. Each group of six rows as mentioned above represent the results for faults at lines 12, 56, 42, 45, 70 and 72, respectively. For faults on lines 12 and 56, the uncertainties in large system loads (L17 with 6000MW, L18 with 2470MW, L41 with 1150MW etc.) are identified as critical across all system loading levels. These lines are located closer to critical generators G9 and G11 (from the perspective of single-machine unstable cases), which are identified to be the most unstable generators in the NYPS and NETS areas due to the fact that they have relatively smaller inertia constant. The loss of line 12 and line 56 weakens the connections between critical generators and the test network by increasing the impedance seen by these generators. However, disconnection of these lines are far away from large loads connected to large generators in the network (L17 is directly connected to the bus G13 connects, L18 is directly connected to the bus G16 connects, and L41 is directly connected to the bus G14 connects), hence the transient stability of the test network under this operating condition is heavily influenced by these large loads. It can also be observed that when the fault is applied to line 42, 45, 70 and 72, i.e., further away from critical generators, the transient stability of the test network is no longer dominated that much by the large loads as the connections between these critical generators and the network are not much affected and the general transient stability is enhanced compared to the previous two scenarios. In fact, for conditions like the loss of one single tie-line between the two areas, it seems that there are no parameters that can hugely affect power system transient stability on their own as no distinguishable patterns can be observed from the heatmap. Fig. 5.18 also demonstrates that as the proportion of RES penetration levels-increase, the importance of the RES generation increases, similar to what was observed for voltage and small-disturbance stability analysis. Hence the uncertainties of wind and PV generators are becoming influential when system loading levels decrease to 0.6 p.u and 0.3 p.u. Table 5.10 lists the top 5 critical parameters for transient stability analysis when fault is applied to lines 12 and 56.

Table 5.10 Top 5 critical parameters for power system transient stability

	Fault on line 12			Fault on line 56		
	1.0 p.u	0.6 p.u	0.3 p.u	1.0 p.u	0.6 p.u	0.3 p.u
Ranking (Top 5)	L17	L17	W60	L17	W17	W60
	L40	W17	W17	W17	S33	L18
	L48	L18	L17	W33	S53	L42
	W17	W53	L18	S33	W68	S60
	W53	W60	L42	S17	W26	S57
	L=Bus Loading, W=Wind Farm, S=PV Farm, Numbering corresponding to system buses in Fig. 5.19					

Table 5.11 Effect of sault duration and res penetration level on transient stability performance

Fault Line	RES Penetration Level	Fault Duration			
		10 cycles		13 cycles	
		TSI	No. of Oscillatory Instability	TSI	No. of Oscillatory Instability
Line42	20%	63	9	61	569
	33%	72	661	70	661
	67%	76	661	76	657
Line56	20%	61	251	57	509
	33%	70	661	68	661
	67%	77	661	76	661
Line70	20%	67	190	72	569
	33%	75	544	75	635
	67%	80	341	80	385

This study also considers the effect of fault duration and RES penetration levels on test network transient stability performance. The TSI is employed in this section to assess general system performance under different pre-fault conditions (loading level, RES penetration level, etc.). In addition, the settling time of the rotor angle of each generator is employed as an indication of oscillatory stability. The advanced MSSA with 661 simulations is used again to obtain the above mentioned two stability indices. The average value of the TSI among all 661 simulation runs is calculated, and the number of cases where any generator is still oscillating after 20 sec are recorded, as shown in Table 5.11.

In Table 5.11, case studies with faults applied on lines 42, 56 and 70 are illustrated for demonstration purposes. The disconnection of line 42 represents the case when one of the tie lines between two strongly connected sections of the test network is disconnected (a total of 5 tie-lines between NETS and NYPS areas). The loss of line 56 represents the case when the transmission line near a critical generator (G11) is disconnected and weakened the connection between critical generator and the network. Fault on line 70 represents the case when the only tie-line between two areas is lost (NYPS and G14). Two fault durations, 10 cycles and 13 cycles are considered and it can be concluded that the selected fault durations have almost no effect on TSI values, which means that the considered test network transient stability is mostly determined by its pre-fault condition (Note that longer than usual fault durations of 10 and 13 cycles are adopted to generate sufficient numbers of unstable cases with the considered test network. Otherwise one would typically consider faults lasting 4-7 cycles at transmission system level). However, one can still distinguish the slight differences in TSI value between cases when different lines are disconnected. For example, when RES penetration level is 20%, the disconnection of line 56 is the least stable case with a TSI value of 61 compared to 63 and 67 when line 42 or 70 is disconnected. The number of the oscillatory instability cases when the line 56 is disconnected is also the largest among the studies. This makes the case when line 56 near critical generator G11 is lost more vulnerable from the transient stability point of view. The reason behind this is the low inertia of G11 (H=2.01s) compared to other generators in the NYPS area of the test network. The effect of RES penetration levels on test network transient stability analysis is also demonstrated in Table 5.11. In this study, the optimal power flow calculation will de-load and/or disconnect synchronous generators when loading levels decrease. The amount of RES generation is kept constant hence the RES penetration level will increase. The lower system loading level results in a higher

TSI value though the number of unstable cases first increases and then starts to decrease again. For example, for low impedance network (removal of line 42), the system transient stability will decrease when RES penetration level increase. This is because the RES modelled in this study can provide reactive power support to the network, hence in order for generators to maintain constant voltage they have to reduce reactive power production as RES have provided enough. The initial steady state rotor angle will increase as power factor of the generators will increase, and is detrimental to transient stability. For high impedance network (removal of line 70), the reactive power support from RES is positive for transient stability. This observation highlights the impact that the reactive power operation mode of the RES generation can have on power system transient stability analysis. The impact can either be negative or positive based on their influence on the reactive operating mode of synchronous generators. The actual effect of RES on transient stability is determined by the number of de-loaded (the rotational reserve increases while the inertia of the system remains the same) and disconnected (the rotational reserve and inertia in the system decrease) synchronous generators at the time of fault and the ride through characteristics and control settings of RES, hence careful consideration of all these parameters is required prior to any generalisation.

5.4.4 Validation of Ranking Results Obtained Through Morris Screening Method

Previous studies in [18] and indicated that MSSA delivers an accurate and efficient ranking of critical parameters compared to commonly used GSAs. This section of the thesis validates the ranking results obtained through MSSA by plotting *pdf*s of the sensitivity indices for different stability analysis when

i. All the uncertainties are modelled probabilistically.

ii. Only the top 5 selected uncertainties are modelled probabilistically.

Table 5.12 Proposed case studies for the validation of ranking results

<table>
<tr><th></th><th colspan="6">Modelled Uncertainties</th><th>Loading Condition</th></tr>
<tr><td rowspan="4">Voltage</td><td>CS_1</td><td colspan="5">ALL</td><td rowspan="2">1.0 pu</td></tr>
<tr><td>CS_2</td><td>L17</td><td>L18</td><td>L42</td><td>L41</td><td>L20</td></tr>
<tr><td>CS_3</td><td colspan="5">ALL</td><td rowspan="2">0.6 pu</td></tr>
<tr><td>CS_4</td><td>L17</td><td>W17</td><td>S17</td><td>W26</td><td>L18</td></tr>
<tr><td rowspan="4">Small-Disturbance</td><td>CS_5</td><td colspan="5">ALL</td><td rowspan="2">1.0 pu</td></tr>
<tr><td>CS_6</td><td>L18</td><td>L17</td><td>L42</td><td>L41</td><td>L51</td></tr>
<tr><td>CS_7</td><td colspan="5">ALL</td><td rowspan="2">0.6 pu</td></tr>
<tr><td>CS_8</td><td>W33</td><td>L18</td><td>L17</td><td>L41</td><td>W53</td></tr>
</table>

Several case studies (CS_1-CS_8), as listed in Table 5.12, are considered here to examine the parameter rankings for voltage and small-disturbance stability analysis. The boxplots are used to illustrate the influence of selected (based on their ranking) individual uncertain parameters on system stability. The individual parameters considered are load 17 (L17), identified as the most critical parameter for voltage and angular stability, load 47 (L47) and load 56 (L56) identified as parameters with moderate and low influence on system voltage and angular stability, respectively.

Figs. 5.20, 5.21 and 5.22 illustrate the system voltage and angular stability behaviour affected by selected individual uncertain parameters. It can be seen from Fig. 5.20 that the variation of system loadability is affected significantly when L17

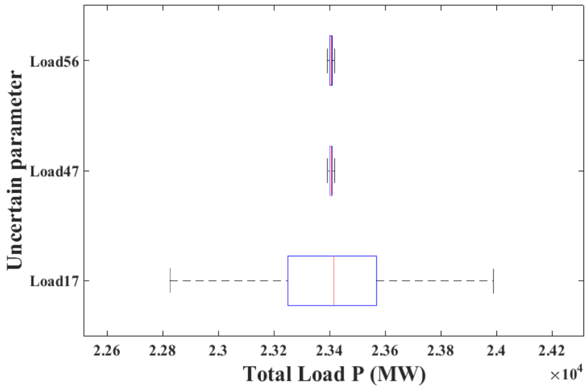

Fig. 5.20 Variation of voltage stability index when individual parameter is modelled as uncertain (keeping all other constant).

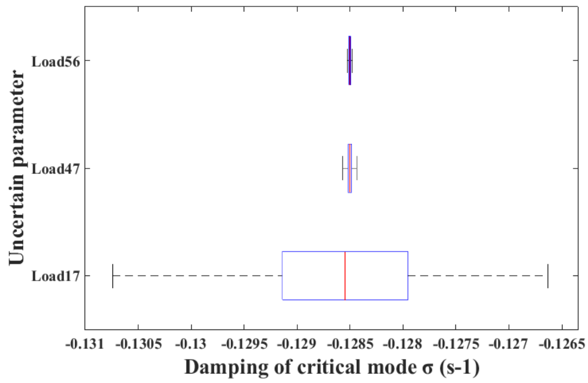

Fig. 5.21 Variation of small-disturbance stability index when individual parameter is modelled as uncertain (keeping all other constant).

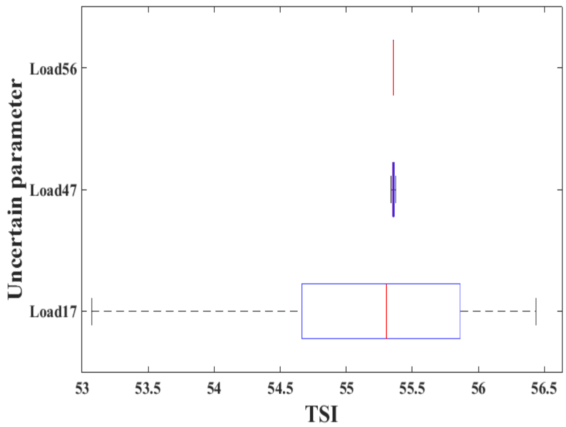

Fig. 5.22 Variation of transient stability index when individual parameter is modelled as uncertain (keeping all other constant).

(i.e the most critical load) is modelled as uncertain parameters while keeping all other parameters at their constant base value. On the other hand, when L47 or L56 are modelled individually as uncertain parameters (keeping all others constant) then the variations in system loadability are insignificant compared to the previous case. The same trend is also observed for small-disturbance and transient stability, as shown in Figs. 5.21 and 5.22, respectively. It reveals the fact that identifying critical parameters for system stability analysis is very important. System input parameters have different levels of influence on stability related studies. This means that if we are able to monitor the behaviour of several influential parameters, we can estimate the system stability margins accordingly. By doing this the resource and effort can be dedicated for the accurate modelling of a small number of important parameters only.

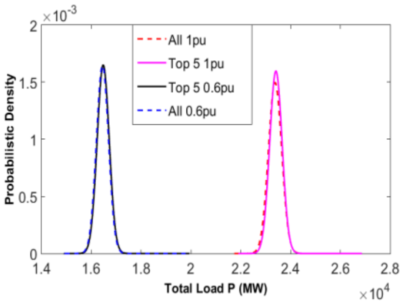

Fig. 5.23 pdfs for Case Studies 1 to 4.

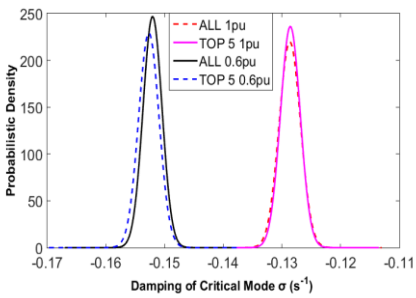

Fig. 5.24 *pdf*s for Case Studies 5 to 8

The *pdfs* of the probabilistic load margin and the probabilistic damping of the critical mode are plotted in Figs. 5.23 and 5.24 for different loading levels for the purpose of the validation of ranking results for voltage and small-disturbance stability, respectively. Figs. 5.25 and 5.26 plot the scatter plots for the system dynamic behaviour for case studies 1 to 8. It can be seen from Fig. 5.23 that the uncertainties of the identified five most important parameters have the same (overlapping *pdfs* for two different loading levels) impact on system voltage stability

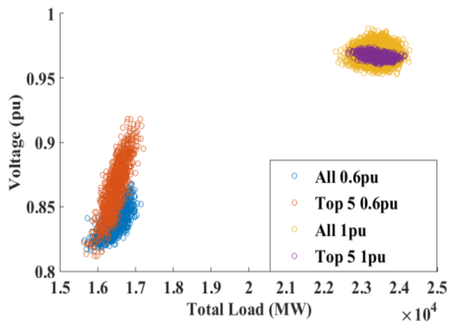

Fig. 5.25 Scatter plots for Case Studies 1 to 4

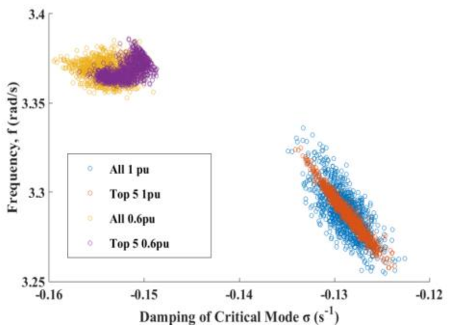

Fig. 5.26 Scatter Plots for Case Studies 5 to 8

as combined impact of all uncertain parameters in the system. The same trend can be also observed in the scatter plot of Fig. 5.25 where the area of system nose-point dispersion for the five influential parameters covers a larger portion of the range of system load margin considering all 49 parameters, hence, the criticality of the system stability (measured by the system load margin) has been properly captured by the identified five most influential parameters. Similar conclusions related to the effect of the five most important parameters on small disturbance stability (damping of the critical eigenvalue) can be shown from *pdfs* in Fig. 5.24 and the scatter plot of critical eigenvalues shown in Fig. 5.26. The results shown in Figs. 5.23 and 5.25 therefore, confirm that system dynamic behaviour can be controlled to a large extent by tuning/reducing uncertainty of the set of critical parameters only, as the rest of the uncertain parameters have significantly lower effect.

Figs. 5.24 and 5.26 show the results of a comparison of the effect of modelling selected numbers of uncertain parameters for small-disturbance stability. Similarly, as in Figs. 5.23 and 5.25, it demonstrates that a subset of the most influential system parameters (5 in this case) have the dominant impact on power system small-disturbance stability and by carefully monitoring and controlling these parameters the overall system small-disturbance stability can be improved.

5.4.5 Summary on Application of Morris Screening Method

In this part of the chapter, the advanced Morris Screening Method is used for the priority ranking of the uncertain input parameters affecting power system voltage and angular stability based on their influence on network stability analysis. The results obtained from this study unveil a group of parameters which are considered critical to system voltage and angular stability in general. The independent probabilistic modelling of uncertainties in system load and RES generation is applied to the system input dataset. Large system loads are found to be the critical parameters for all types of stability studies when the RES penetration level is lower than 30%. Under this circumstance, the variations of the employed stability indexes are highly sensitive to the variation of the large loads due to the uncertain load forecast error. When the RES penetration level is higher than 30%, the influence of the uncertainties in RES generation increases. The uncertainties exhibited in RES generation are considered to be more influential for power system voltage and angular stability studies in this case. In fact, their influence may become greater than large system loads as the system inertia decreases due to conventional generator disconnection. It can be observed that a network with a higher penetration level of RES generation is more vulnerable compared to a conventional generator-driven network with less RES penetration. The identification of critical parameters influencing system stability helps researchers and system operators to narrow down the number of parameters in the system that need to be modelled accurately. This helps to reduce both personnel and financial resources required for the planning and operation of the network. The variation of system stability margin due to system parameter uncertainties can be converted to the critical parameter uncertainty margin and controlled by the detailed modelling of the important parameters only.

5.5 Summary

In this chapter of the thesis, sensitivity analysis methods have been applied for the voltage and angular stability analysis of uncertain power systems. The performances of six commonly used sensitivity analysis methods are compared and the Morris Screening method has been recommended for power system stability studies. The influential parameters of the test network with RES generation have been identified and the results have been validated. The large system loads are identified to have dominant effect on power system voltage and angular stability. It was also found, however, that the RES generation can have notable effect on power system stability when network is operating with high RES penetration level. Hence, careful consideration of the system stability margin and quantification of the impact of RES generation on system dynamic performance is required when large amount of RES generation is connected to the network.

Chapter 6 : Stability Analysis Considering Parameter Correlations

The research discussed in Chapter 5 employs independent probability distributions for the modelling of uncertain parameters. This means the employed uncertainties (load demand, wind generation and PV generation) are modelled individually and independently using their corresponding probabilistic distributions. This represents the true marginal distribution of the parameters of load, wind, and PV. The random sampled data set obtained in this way, however, does not represent the correlations among uncertain input parameters within a real system. Network parameters in reality like loads and RES plants are actually correlated with each other through some patterns. For example, closely located solar farms are influenced by weather condition, or consumer-end loads are influenced by the lifestyles of the people living in that area. The lack of correlation modelling between network parameters can lead to inaccurate representations of the input dataset when performing power system stability analysis. Hence the results of the analysis may not be faithful enough to a real-world application [20-24, 128]. This chapter of the thesis intends to unveil the importance of accurate correlation modelling between input parameters to power system stability related studies.

6.1 Intra-Dependence and Interdependence within Parameter Groups

The intra-dependence within the employed system uncertain parameters is mainly determined by the spatial-temporal factors exhibited by the network parameters. For example, the intra-dependence among system loads is linked with factors like the weather pattern, the locality of the loads, the temperature variation between loads, and the customer daily routine or consumer lifestyles. For system loads which are closely located and of similar types, it is very likely that they are highly correlated due to the similar consumption pattern between them. On the other hand, for different types of consumers, the load-load correlation pattern can be moderate. For example, commercial/industry loads can decrease out of working hours, while home-based loads will increase as people will turn on home appliances. The intra-dependence between wind generations can be high if they are closely located as the weather pattern can be similar in this case. However, as the distance between the wind farms increases, the intra-dependence among them tends to decrease. This trend is also true for the PV-PV intra-dependence structure for hourly based sampling among solar plants. However, if the sampling rate and the time scale becomes longer, the intra-dependence of the PV-PV correlation can increase as it is now mainly dependent on day-time duration.

On the other hand, the interdependence between load and wind can be very low as the consumption pattern of the customers is not related to the spatial-temporal variability of the wind [183]. For interdependence between PV and load, the correlation structure can be moderate as temperature increases due to high solar irradiance can lead to an air conditioning load increase accordingly [184]. The interdependence between wind and PV is also low as these are two uncertain renewable energy sources that both exhibit inherent stochastic behaviour.

Generation from wind farms which is related to wind speed is highly dependent on weather conditions, while generations from PV panels which is related to solar irradiation is mostly time-based (daylight hours). The correlations between the studied system parameters are nonlinear and non-Gaussian [185]. This characteristic makes linear correlation modelling of the stochastic dependence among studied parameters unsuitable and the optimal solutions of power system analysis may not be achievable. This study employs Copula theory [128] for the purpose of stochastic correlation modelling among system loads and RES plants.

6.2 Copula Theory

The modelling of correlations among studied system parameters can be done effectively using the Copula theory [128]. Sklar's theorem has pointed out that any multivariate joint distribution can be expressed by a copula which describes the dependence structure between the variables [186]. Different dependence structures among the correlated parameters can be modelled by using different copula families. A previous study [128] compares the performance of six different commonly-used copula approaches, namely (i) Gaussian (ii) Student (iii) Clayton (iv) Frank (v) Gumbel and (vi) multivariate joint normal distribution. The application of these different copulas to systems with different dimensions are demonstrated in [187].

These commonly-used copula approaches can be categorized into two copula families, namely the Archimedean and the Elliptical Copula. The Archimedean copula (for example, Clayton, Frank, Gumbel) is suitable for the representation of complicated dependence structures between parameters but is restricted to applications in two-dimensional systems only. The Elliptical copula (for example, Gaussian, Student *t*), on the other hand, can be applied to higher dimensional systems. It was reported in [128] that the multivariate Gaussian copula is the most effective and accurate approach for the representation of the correlation structures between parameters like load demand, wind generation and PV generation for power system small-disturbance stability analysis. In [175], the multivariate Gaussian copula has been employed for voltage stability analysis. In [25], the multivariate Gaussian copula has been successfully implemented for small-disturbance stability analysis. The multivariate Gaussian copula is applied here for the modelling of correlation structures between uncertain parameters for transient stability analysis and then for voltage and small disturbance stability analysis.

In copula modelling, the correlated samples of input parameters are generated through four stages from the raw dataset:

i. Transforming the raw data obtained from real-world operation to the unit square using a kernel estimator of the cumulative distribution function.
ii. Fitting a selected copula to the system raw data in order to obtain the copula parameter.
iii. Generating random samples from the selected copula approach.
iv. Transforming the random samples back to the original scale of the data.

Stages (ii) and (iii) are related to the copula approach selected, while stages (i) and (iv) are universal for all copula approaches, they represent a normalization of the data. Fig. 6.1 shows a flow chart of the steps involved when copula is used for correlation modelling of system parameters

The copula function *C* can be represented by the multivariate *cdf F* (cumulative distribution function) and the marginal *cdf* F_i, as shown in (6.1) [188].

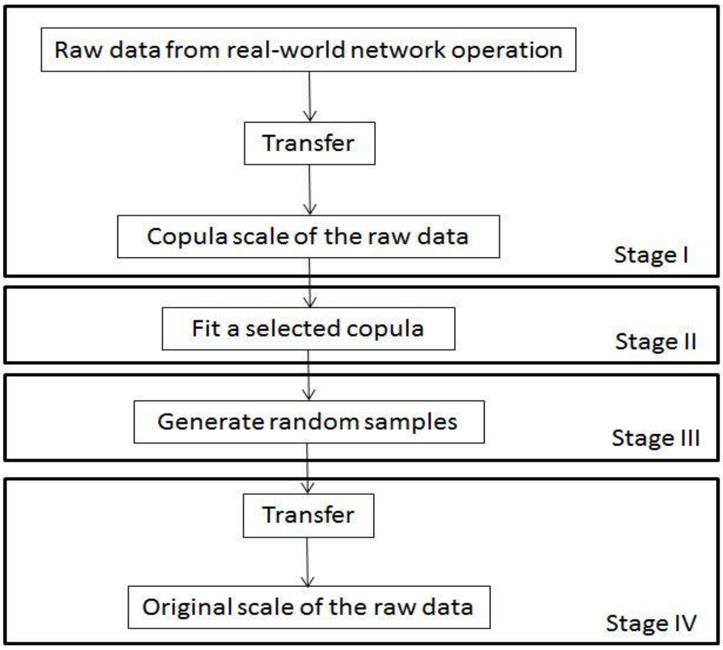

Fig. 6.1 Flow chart for copula application on parameter modelling

$$C[F_1(x_1), F_2(x_2), \dots, F_n(x_n)] = F(x_1, x_2, \dots, x_n) \tag{6.1}$$

6.2.1 Multivariate Gaussian Copula

The multivariate Gaussian (mvG) copula is categorized as an elliptical copula, which provides the flexibility to model a system with a higher number of dimensions. The mvG is very useful for the modelling of dependent random variables. It is suitable to be implemented in cases when there are complicated relationships among the variables, or when the individual variables are from different distributions. As power system load, wind and solar data follow different probability distributions, the mvG has been found to be very efficient in modelling their interdependences [25, 189].

The copula function for the mvG copula can be expressed as shown by (6.2) [190].

$$C(u_1, u_2, \dots, u_n; \Sigma) = \phi_\Sigma\left(\phi^{-1}(u_1), \phi^{-1}(u_2), \dots, \phi^{-1}(u_n)\right) \tag{6.2}$$

In equation (6.2), Σ denotes an asymmetric, positive definite matrix with *diag*(Σ)=*1,* Φ_Σ is the standard multivariate normal distribution with a correlation matrix Σ, and $\Phi^{-1}(\bullet)$ is the inverse of the Normal *cdf.*

The correlation matrix Σ in (6.2), also known as the covariance matrix, can be expressed by (6.3).

$$\Sigma = \begin{bmatrix} \rho_{11} & \rho_{12} & \cdots & \rho_{1n} \\ \rho_{21} & \rho_{22} & & \rho_{2n} \\ \vdots & & \ddots & \vdots \\ \rho_{n1} & \rho_{n2} & \cdots & \rho_{nn} \end{bmatrix} \tag{6.3}$$

In (6.3), ρ is the linear correlation coefficient between parameters to represent the range of different dependence structures. The correlation between the same set of data is given by (6.4).

$$\rho_{11} = \rho_{22} \dots = \rho_{nn} = 1 \tag{6.4}$$

Then after substituting (6.4) into (6.3), (6.3) becomes (6.5).

$$\Sigma = \begin{bmatrix} 1 & \rho_{12} & \cdots & \rho_{1n} \\ \rho_{21} & 1 & & \rho_{2n} \\ \vdots & & \ddots & \vdots \\ \rho_{n1} & \rho_{n2} & \cdots & 1 \end{bmatrix} \tag{6.5}$$

The covariance matrix can be formed with the Pearson correlation coefficient ρ, Spearman or Kendall rank correlation coefficient τ [191].

The inverse of the normal *cdf* $\Phi^{-1}(\bullet)$, as presented in (6.2), has been adopted from the theory of univariate random number generation. The *inversion method* has been used here to model the individual variables, which follow different distributions. In this study, for example, system load, wind and solar data follow normal, Weibull and beta distributions, respectively. The step-by-step procedure for generating correlated random samples has been discussed in [25].

6.3 Priority Ranking of Influential Parameters considering Load-Renewable Generation Correlation

For the correlation modelling among the studied parameters, raw data from real-world operation is required to obtain the realistic correlation patterns. The raw data of the test system is obtained through the online operator data base [192, 193], which records the whole year of operating conditions of loads and RES generation in real networks. Real data of 35 loads, 7 wind plants and 7 PV plants are retrieved in hourly manner to generate a massive raw data set. Fig. 6.2 is a 49*49 matrix of the Pearson correlation coefficients between the 49 studied system uncertainties within this study. Fig. 6.2 uses heatmap to demonstrate the correlated network parameter structure for the NETS-NYPS test network. The shades of the rectangles within Fig. 6.2 represent the correlation between the two parameters crossed at that point. The approach behind these heatmaps is also capable of producing a similar figure for any raw data set of any test system following Fig. 6.1. In this figure, the row/columns 1-35 are load demands, 36-42 are wind speeds and 43-49 are solar irradiance. It can be observed that the darkest blue shades appear on the diagonal rectangles as the Pearson Correlation Coefficient of a parameter itself is always 1. Fig. 6.2 clearly illustrates the intra-dependence and inter-dependence within the parameter groups. In Fig. 6.2, five groups of closely located loads can be identified through their high intra-dependence structure. For example, the group of loads with numbering from 1 to 8 on rows/columns 1-8 is highly correlated with dark blue shades on their corresponding rectangles. These load-load intra-dependence structures are influenced by the different lifestyles of consumers which depend on factors such as weather conditions, location, types of load, etc. The intra-dependence structures of wind-wind and PV-PV correlations are mainly determined by the distance between generation plants. This means closely located RES generation can be highly correlated as the weather pattern tends to be similar. In this study, the 7 implemented wind farms are not closely located hence the intra-dependence between wind-wind is low. For an intra-dependence structure of PV-PV, however, when the sampling time scale is relatively long and covers the whole year, the PV-PV correlation increases due to the fact that PV generation is now mainly dependent on day-time hours. The inter-dependence between load-wind and wind-PV is low, and this indicates load-wind and wind-PV are very poorly correlated. The inter-dependence between load-PV is relatively high, this is true considering that the day-time hours will change depending on the seasons and people may turn on the heating/AC during the corresponding season.

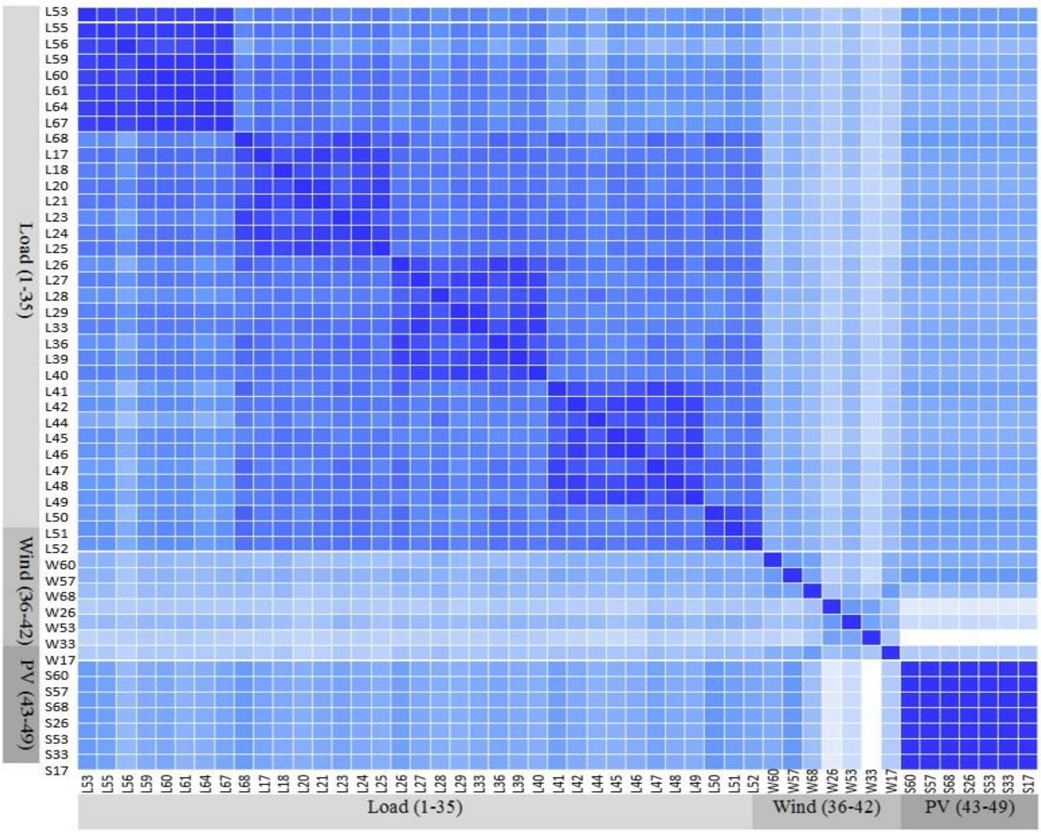

Fig. 6.2 Stochastic dependence structure of NETS-NYPS load, wind speed and solar irradiance over a year

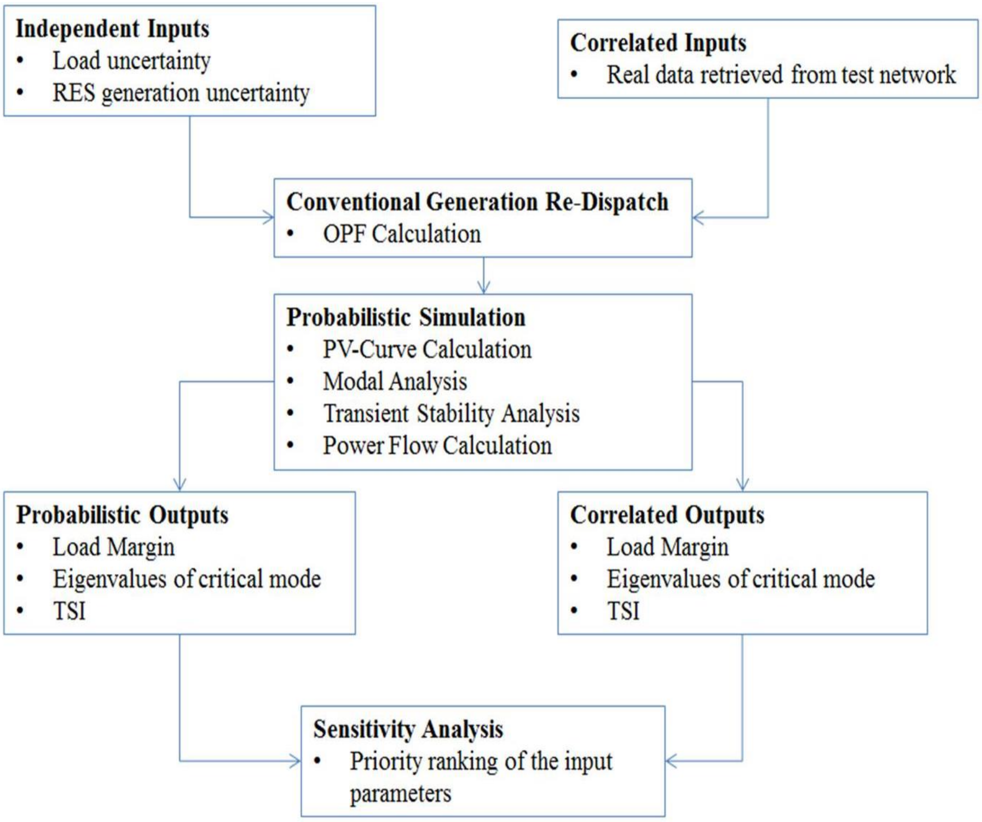

Fig. 6.3 Flow chart of the proposed methodology

In this section, the priority ranking of critical uncertain input parameters affecting power system voltage and angular stability is performed through the Monte Carlo simulation, with correlations between load and renewable generations considered. The results obtained in this section are compared with the results of Chapter 5. The multivariate Gaussian copula is used in order to model the correlation structures between the load and renewable generations. Fig. 6.3 presents a flow chart of the proposed methodology.

As previous study [128] has indicated, the multivariate Gaussian copula is an efficient and accurate method for stochastic dependence structure modelling across all levels of RES penetration. Hence the multivariate Gaussian copula was used here as well. Fig. 6.4 shows a heatmap which indicates the identified critical parameters and the ranking among them when correlation between system parameters is considered.

In order to obtain the correlated network parameters, the steps highlighted in Fig. 6.1 have been followed. The operating conditions of 35 loads, 7 wind plants and 7 PV plants for 8760 hours of year 2015 are extracted from on-line database of real-world operators [192, 193], set as raw data. A kernel smoothing function estimator of the cumulative distribution functions has been used to transform the raw data into the copula scale dataset (unit square). Then the Gaussian copula has been fitted to the dataset and 1000 groups of Gaussian copula random numbers are generated to be later used for Monte Carlo power system stability analysis. At the end the random samples are transferred back to the original scale of the raw data. It should be noted that when generating copula random numbers the numbers are sampled from a Uniform (0, 1) marginal distribution, an additional inverse of the CDF associated with a normal distribution function is required to obtain the correlated system parameters used in this study.

The first row of the heatmap in Fig. 6.4 illustrates the ranking of the influence of system uncertain input parameters on voltage stability through the measurement of system loadability variation. The system loading level is at 1 pu. The top-ranking parameters appear as groups instead of as single parameters (which was the case

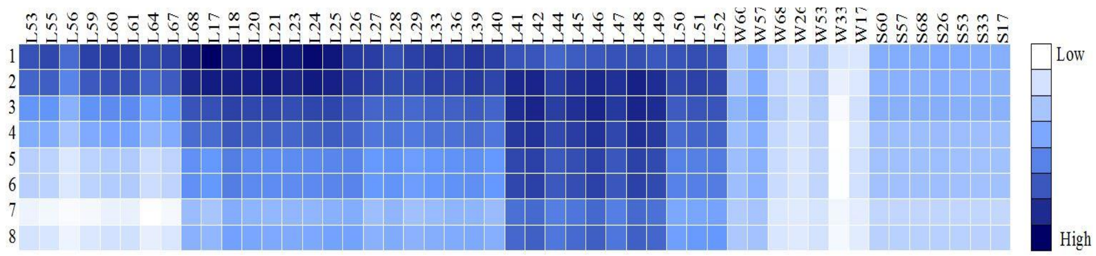

Fig. 6.4 Ranking of critical parameters for voltage and angular stability when correlations between input parameters are considered

when no correlation was considered among the input parameters). The critical parameters are identified as loads on buses 17, 18, 20, 21, 23, 24, 25 and 68. This is as expected considering Fig. 6.2, as the above mentioned 8 loads are highly correlated to each other. In fact, one can still identify the 5 groups of intra-correlated loads through the first row in Fig. 6.4 (loads on buses 53, 55, 56, 60, 61, 64, and 67, i.e., loads No. 1-8 in Fig. 6.2; the identified critical loads No. 9-16 in Fig. 6.2; loads on buses 26, 27, 28, 29, 33, 36, 39, and 40, i.e., loads No. 17-24 in Fig. 6.2; loads on buses 41, 42, 44, 45, 46, 47, 48, and 49, i.e., loads No. 25-32 in Fig. 6.2; loads on buses 50, 51, and 52, i.e., loads No. 33-35 in Fig. 6.2). Within the intra-correlated group of loads the same level of influence can be observed. Compared to results presented in Section 5.4.3.1 where only load 17 is measured to have high impact on system voltage stability analysis, now the loads which are highly correlated to load 17 are also found to be influential. This unveils the importance of correlation modelling among uncertain parameters as some parameters might be uninfluential on their own, but as they are highly correlated to the influential parameter, they are also critical to voltage stability analysis. The uncertain renewable generation shows a lower influence on power system voltage stability analysis compared to loads. This is true as power system voltage stability is highly influenced by large loads as discussed in section 5.4.3, and the load centers which are far away from the generators are considered critical. Load 17, which is the largest load in the network (6000MW), is significantly larger compared to other loads connected to the test network (27 loads are within the range of 100-330MW).

The second row of the heatmap in Fig. 6.4 shows the ranking of the critical parameters identified for small-disturbance stability through the measure of damping of critical eigenvalues. Once more the top-ranking parameters appear as groups compared to the non-correlated case in Section 5.4.3.2. The critical parameters are identified as load on buses 17~25 and 41~49. The same 5 groups of closely intradependent loads can be observed like first row. Compared to the first row, it is also obvious that the influence of loads 41~49 is increasing and gets close to the influence of loads 17~25. This is because for the small-disturbance stability the loads connected to buses near generators tend to be more influential. As the system loading level is at 1 p.u, renewable generation shows low impact on power system small-disturbance stability analysis.

Rows 3-8 of the heatmap in Fig. 6.4 reveal the ranking of critical parameters for transient stability through the measure of TSI. Rows 3-8 show the rankings for faults on lines 12, 56, 42, 45, 70 and 72, respectively. Unlike the results obtained in section 5.4.3.3where no obvious patterns can be observed on the heatmap, this time the group of system loads from L41 to L49 is identified as critical parameters which have a great influence on transient stability performance. The importance of RES is low as the RES penetration level is low when loading level is at 1 p.u.

Overall Fig. 6.4 demonstrates that the groups of system load from L17 to L25 (parameter group highly correlated to large system loads L17 and L18) and L41 to L49 (parameter group highly correlated to large system loads L41 and L42) have the dominant influence over system voltage and angular stability. It can be concluded that uncertainties within large loads are the most influential parameters for power system stability studies in general. This also unveils that the accurate modelling of the correlation between uncertainties should be performed with extra care to ensure the accurate state-estimate of the power system.

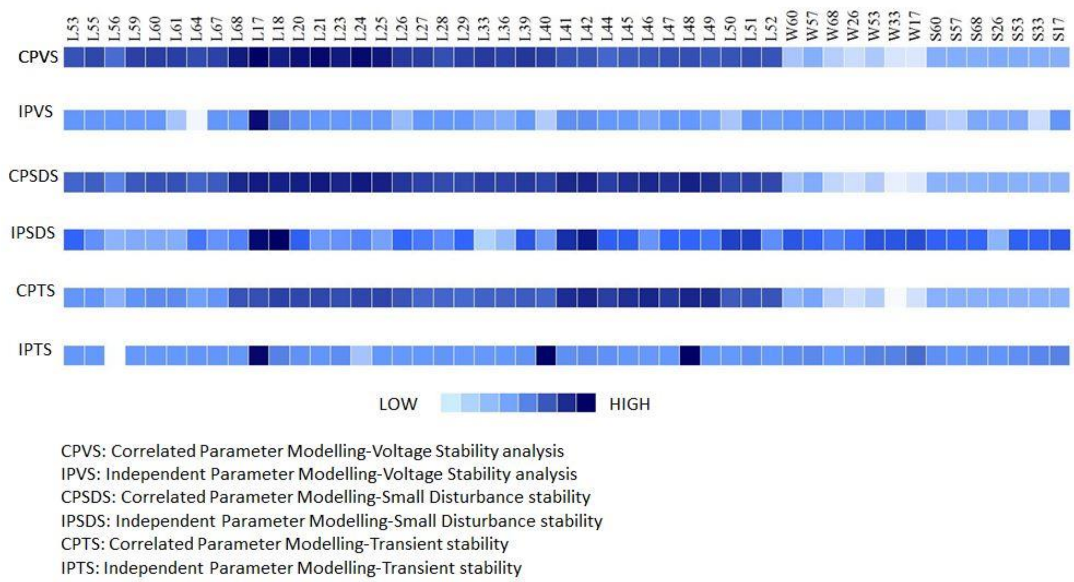

Fig. 6.5 Ranking of influential uncertain parameters with/without correlation modelling

By comparing the ranking of identified critical parameters between Sections *6.3* and Section *5.4*, the importance of the accurate correlation modelling of system uncertain parameters can be demonstrated. Fig 6.5 shows the ranking of critical uncertain parameters for voltage and angular stability when correlated and independent modelling of parameters are used. The system loading was set at 1 pu for all three types of stability analysis performed. For transient stability analysis, the results obtained following the removal of line 12 are used for demonstration purposes. When independent probabilistic modelling of system parameters is applied, the loss of correlation among the system parameters may lead to ignoring an important parameter which may not be influential on its own but is highly correlated to an influential parameter. It can be observed that when correlation structures between parameters are considered, the parameters that are highly correlated with already influential parameters will also become important. As shown in Fig. 6.2, high correlation can appear between load-load, load-PV, PV-PV and wind-wind. This characteristic of realistic system parameters makes the correlation modelling of system parameters very important for stability analysis.

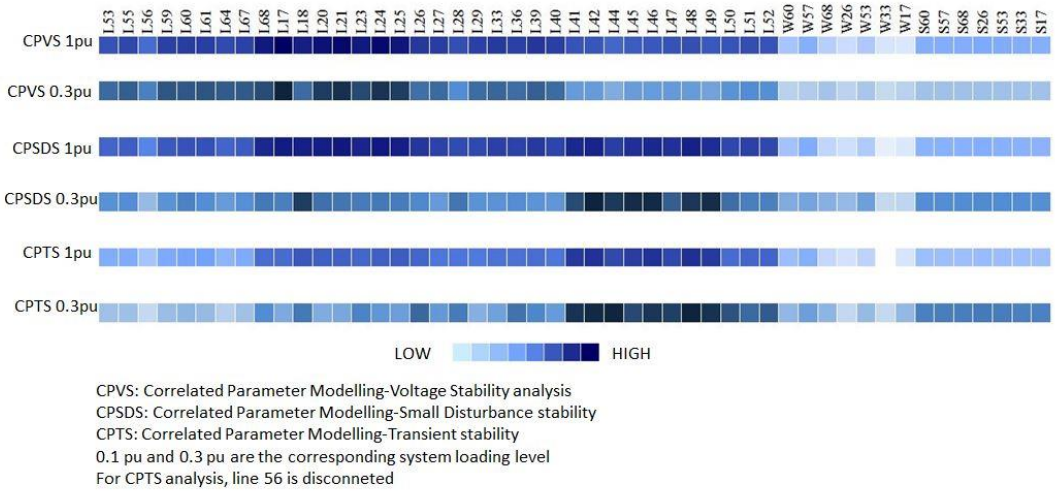

Fig. 6.6 Ranking of influential uncertain parameters with correlation modelling with high/low RES penetration levels

The probabilistic voltage and angular stability analysis with correlated uncertain parameters are also performed in this section for two different system loading levels and different RES penetration levels. The system loading levels considered were 0.3 pu with consequent PL_{RES} 62% and the system loading level of 1 pu $PL_{RES} = 20\%$. Fig. 6.6 shows a heatmap for this comparison. One can easily distinguish the same correlation patterns between the parameters from this figure. This again highlights the importance of the modelling of the correlations between parameters. It can also be observed that as PL_{RES} increases, the influence of RES generation on angular stability also increases. As far as voltage stability analysis is concerned, however, the system dynamic is still dominated by large system loads. In case of small-disturbance stability, one can observe the significance of L42-related parameters as the small-disturbance of a network is highly influenced by the loads that are near generators For power system with high PL_{RES}, the same group of influential parameters can still be identified for small-disturbance and transient stability analysis, while the large loads still remain the most influential for voltage stability analysis.

6.4 Summary

Analysis of real data from the actual network illustrates that a high level of intra-dependence and inter-dependence exist between system input parameters. Hence, the accurate modelling of correlation between parameters has to be considered when performing stability analysis. The results presents here reveal the disadvantage of independent modelling of system parameters as this approach may ignore critical parameters in real-world applications as the critical parameters can appear as groups after the input dataset is correlated. Hence, even though some of the system parameters may be uninfluential on their own, their variation/uncertainty can have a significant impact on system dynamic behaviour due to their correlation with other influential parameters.

Chapter 7 : Conclusions and Future Work

7.1 Conclusions

This research performs power system voltage and angular stability analysis of the system with renewable generation. The network stability margins have been assessed when uncertainties are considered. In completing this research, the Monte-Carlo has been employed to generate various operation conditions of the test network. The sensitivity analysis methods have been implemented for the identification of the influential parameters which affect power system stability analysis results. This thesis also employs copula methods for the accurate modelling of the correlation structures between system variables. The dynamic behaviour of the test network when it was subjected to different operating conditions are assessed.

Modern power systems are developed to meet the requirements of the deregulated and flexible energy market. Renewable energy-based generations are increasingly adopted by power system nowadays for the sustainable development of the society. New types of loads like electrical vehicles, LED lighting, heat pumps etc., and storage devices, are connected to networks and their demand increased quickly in recent years. Power systems are operated as de-centralized utilities which lead to distributed meshed networks with blurry boundaries between transmission networks and distribution networks. These new technologies exhibit time and spatial uncertainties which add uncertainties to the already complex system operation conditions. On the other hand, the electronic-interfaced generation and loading technologies which are replacing conventional power plants have weakened the robustness of modern power systems in terms of stability. Modern power system analysis is no longer about only the generation-load balance, but also takes into consideration the reliability, flexibility and economic optimization during operations when high levels of uncertainties are involved. All these new additions to modern power systems make it important for the researchers and operators to have a clear understanding of the impacts these uncertainties may have on networks. This thesis provides an approach for the analysis of power system voltage and angular stability when renewable generations are connected, and uncertainties are introduced.

This thesis reviews the deterministic and probabilistic approaches for power system analysis. It is clear that deterministic approaches for the assessment of power system conditions are no longer suitable for the application on modern power systems. They do not take system uncertainties into consideration and may lead to overly conservative system designs since they use ‘worst case scenario’ analysis of the network. The probabilistic approaches to network stability assessment are getting steadily adopted by researchers to be applied to all types of stability studies. This thesis uses probabilistic modelling for system uncertain parameters. A review of the existing literatures on the modelling of system uncertainties is presented. This study employs normal distribution, Weibull distribution and Beta distribution for the modelling of uncertainties in load demand, wind generation and PV generation, respectively. The Monte-Carlo simulation has been applied on the IEEE 68-bus

NETS-NYPS test network for the assessment of the test network dynamic behaviour when uncertainties are introduced. A total of nine case studies are established with various load models, load levels and considered uncertainties. The weak and stiff buses are identified from the perspective of voltage stability. It is found that for the established case studies the weak and stiff buses remains the same. System managers can devote more monitoring and compensation resources in area of the network where the weak buses are to improve the test network voltage stability in general. This study also illustrates the influence of the system uncertainties on the dynamic behaviour of the test network. It can be concluded that the voltage stability is mostly affected by variations in loads when the renewable penetration level is low. However, the influence of renewable generations will increase when renewable penetration level increases as this can lead to conventional generation disconnection. It is also observed that the dynamic behaviour of the test network is more influenced at lower loading levels accompanied by conventional generation disconnected. The accurate modeling of load models is important as the system stability margin can be hugely affected when different load models are employed. However, load models have no effect on the ranking of uncertain parameters, nor on the ranking of critical buses.

This thesis proposed a probabilistic approach for the identification of critical parameters affecting power system voltage and angular stability. The current industry approach for system stability analysis is to develop mathematical models for every single power plant within the system and perform simulations to evaluate system dynamic behaviour following a disturbance. This can generate huge computational burdens as modern power systems are large in size with numerous power plants, and the Monte-Carlo simulations require many iterations for accurate parameters modelling. This study and many studies before have found out that not all the uncertain parameters can have the same effect on power system dynamic behaviour. The dynamic behaviour of a network is dominant by several critical uncertain parameters, hence with the accurate modelling of the identified critical parameters, the network stability margins can be accurately assessed. This can help the system planners and operators to monitor and perform stability analysis with minimal resources.

For the identification of critical parameters affecting power system voltage and angular stability, this thesis employs sensitivity analysis methods to the test network. It is observed that when the renewable penetration level is low, the critical parameters are the large system loads for voltage and small-disturbance stability analysis. For transient stability analysis, the ranking of critical parameters will also depend on the fault locations, fault durations and pre-fault operating conditions. The influence of renewable generation on power system voltage and angular stability will increase when the RES penetration level increases. It is validated in this study that the identified top 5 critical parameters through sensitivity analysis method are all the parameters which need to be modelled accurately for stability analysis on the test network, as they contribute the most to the test network dynamic behaviour. This thesis proposed the Morris Screening Method for the identification of critical parameters affecting power system voltage and angular stability analysis among the six employed commonly used sensitivity analysis methods. The Morris Screening Method is proved to be efficient and accurate for the implementation on a complex system like modern power systems. The characteristic of the Morris Screening Method makes the fast and accurate estimation of network dynamic behaviour under uncertain operational conditions possible and can be helpful for fast on-line/real-time power system analysis.

This thesis represents the first study to include the identification of influential parameters affecting different stability problems in order to unveil the group of parameters which are considered critical to system voltage and angular stability as a whole. Independent probabilistic modellings of uncertainties in system loads and RES generations are applied to a system input dataset. The sensitivity indices chosen for voltage, small-disturbance and transient stability are load margin, damping of the critical eigenvalues and TSI, respectively.

The application of Morris Screening method for assessment of the influence of uncertain parameters on global system stability is the 1st original contribution of this thesis. The Morris Screening method used for the ranking of critical parameters is followed by applications of multivariant Gaussian copula for the correlation modelling between input parameters. The multivariate Gaussian Copula method has been applied in this study for the correlation modelling of the interdependence and intra-dependence structures between input parameters load, wind and PV. It is observed that the identified critical parameters appear in groups rather than individually compared to independent probabilistic modelling of the input parameters. This reveals the disadvantages of independent modelling of system parameters during real-world network dynamic analysis. This is due to the fact that even though some of the system parameters may not be influential on their own, their variation/uncertainty can still have a significant impact on system dynamic behaviour due to their high correlations with other influential parameters. The large system loads and those highly correlated are considered to have critical effect on test network voltage and angular stability behaviour. The modelling of correlations between different system uncertain parameters for global assessment of system stability is the 2nd original contribution of this thesis.

The large system loads are found to be critical for all types of stability when the RES penetration level is lower than 30%. When the RES penetration level becomes higher than 30%, the influence of uncertainties in RES generation increases and gets higher as the system inertia decreases due to conventional generation disconnection.

The fast and accurate priority ranking of critical parameters is favoured in power system stability related analysis as it can help to narrow down the number of parameters which are critical for stable operation of the power system. This can help to reduce both personnel and financial resources required. The variation of system stability margin due to system parameter uncertainties can be converted to the critical parameter uncertainty margin and controlled by the detailed modelling of the important parameters only. Building on the approach proposed in this thesis the system behaviour under various operation conditions can be mapped into the system security operation profile and greatly facilitate stable and secure operation of modern power systems.

7.2 Future Work

This thesis has achieved all the aims and objectives discussed in Chapter 1. However, there are still some areas where future work can be carried out based on the results obtained in this thesis:

i. The risk-based power system stability analysis to establish the network risk profile when different contingencies are introduced. The risk-based analyses assess the severity and probability of a selected contingency and calculate the risk of the network to experience unacceptable operation scenario when the contingency happens. The risk profiles of the network generated in this way can help the operators understand how far the network is to unacceptable operation condition and make decisions for the purpose of power system control and management.

This thesis has already assessed the impacts of the system uncertain parameters on the stability margins of the test network. The severity functions can be generated based on these results.

ii. The analysis of power system dynamic response for networks with high penetration levels of renewable generations. This analysis is extremely important for future power system planning and operation as power systems are on a steady track towards a sustainable energy driven network. The power-electronics interfaced renewable generation technologies bring new characteristics in power systems and only consider the balance between generation and load is no longer sufficient for the state-estimate of a network. The stable operation of a renewable generation-interfaced power network requires the control structures to be highly-flexible in order to handle high uncertainties in operating conditions. The uncertainties in time and space of the renewable generations make the energy-storage techniques important when planning future power systems. The proposed generalized approach can be applied for future network design to identify the critical nodes/branches for optimal placement of control structures and devices to provide robust network/system stability over the feasible range of operating conditions that network will face during the operation.

Reference

[1] R. Preece, N. C. Woolley, and J. V. Milanović, "The probabilistic collocation method for power-system damping and voltage collapse studies in the presence of uncertainties," *IEEE Transactions on Power Systems,* vol. 28, pp. 2253-2262, 2013.

[2] "Energy Trends: September 2017," Departmant for Business Energy & Industrial Strategy, Ed., ed, 2017.

[3] I. Staffell, "Electric Insights Quarterly Reports, Q4 2018," Electric Insights2018.

[4] J. Zhang, C. Tse, K. Wang, and C. Chung, "Voltage stability analysis considering the uncertainties of dynamic load parameters," *IET generation, transmission & distribution,* vol. 3, pp. 941-948, 2009.

[5] CIGRE Working Group, "Review of the current status of tools and techniques for risk-based and probabilistic planning in power systems," *WG 601 of SC C4,* 2010.

[6] W. Li and J. Zhou, "Probabilistic reliability assessment of power system operations," *Electric Power Components and Systems,* vol. 36, pp. 1102-1114, 2008.

[7] J. McCalley, S. Asgarpoor, L. Bertling, R. Billinion, H. Chao, J. Chen*, et al.*, "Probabilistic security assessment for power system operations," in *2004 IEEE Power Engineering Society General Meeting,* , 2004, pp. 212-220.

[8] S. Bu, W. Du, H. Wang, Z. Chen, L. Xiao, and H. Li, "Probabilistic analysis of small-signal stability of large-scale power systems as affected by penetration of wind generation," *IEEE Transactions on Power Systems,* vol. 27, pp. 762-770, 2012.

[9] H. Huang, C. Chung, K. W. Chan, and H. Chen, "Quasi-Monte Carlo based probabilistic small signal stability analysis for power systems with plug-in electric vehicle and wind power integration," *IEEE Transactions on Power Systems,* vol. 28, pp. 3335-3343, 2013.

[10] W. Wu, K. Wang, G. Li, and Y. Hu, "A stochastic model for power system transient stability with wind power," in *2014 IEEE PES General Meeting | Conference & Exposition*, 2014, pp. 1-5.

[11] L. Shi, S. Sun, L. Yao, Y. Ni, and M. Bazargan, "Effects of wind generation intermittency and volatility on power system transient stability," *IET Renewable Power Generation,* vol. 8, pp. 509-521, 2013.

[12] A. Adrees, J. Song, and J. V. Milanović, "The influence of different storage technologies on large power system frequency response," in *2016 IEEE 8th International Power Electronics and Motion Control Conference (IPEMC-ECCE Asia),* , 2016, pp. 257-263.

[13] A. Adrees and J. V. Milanović, "Study of frequency response in power system with renewable generation and energy storage," in *2016 Power Systems Computation Conference (PSCC),* , 2016, pp. 1-7.

[14] E. Vaahedi, W. Li, T. Chia, and H. Dommel, "Large scale probabilistic transient stability assessment using BC Hydro's on-line tool," *IEEE Transactions on Power Systems,* vol. 15, pp. 661-667, 2000.

[15] J. L. Rueda, D. G. Colomé, and I. Erlich, "Assessment and enhancement of small signal stability considering uncertainties," *IEEE Transactions on power systems,* vol. 24, pp. 198-207, 2009.

[16] J. Rueda and D. Colome, "Probabilistic performance indexes for small signal stability enhancement in weak wind-hydro-thermal power systems," *IET generation, transmission & distribution,* vol. 3, pp. 733-747, 2009.
[17] P. Kundur, J. Paserba, V. Ajjarapu, G. Andersson, A. Bose, C. Canizares*, et al.*, "Definition and classification of power system stability IEEE/CIGRE joint task force on stability terms and definitions," *IEEE Transactions on Power Systems,* vol. 19, pp. 1387-1401, 2004.
[18] K. N. Hasan, R. Preece, and J. V. Milanović, "Priority ranking of critical uncertainties affecting small-disturbance stability using sensitivity analysis techniques," *IEEE Transactions on Power Systems,* vol. 32, pp. 2629-2639, 2017.
[19] H. Park, R. Baldick, and D. P. Morton, "A stochastic transmission planning model with dependent load and wind forecasts," *IEEE Transactions on Power Systems,* vol. 30, pp. 3003-3011, 2015.
[20] N. Zhang, C. Kang, C. Singh, and Q. Xia, "Copula based dependent discrete convolution for power system uncertainty analysis," *IEEE Transactions on Power Systems,* vol. 31, pp. 5204-5205, 2016.
[21] W. Wu, K. Wang, B. Han, G. Li, X. Jiang, and M. L. Crow, "A versatile probability model of photovoltaic generation using pair copula construction," *IEEE Transactions on Sustainable Energy,* vol. 6, pp. 1337-1345, 2015.
[22] P. Li, X. Guan, J. Wu, and X. Zhou, "Modeling dynamic spatial correlations of geographically distributed wind farms and constructing ellipsoidal uncertainty sets for optimization-based generation scheduling," *IEEE Transactions on Sustainable Energy,* vol. 6, pp. 1594-1605, 2015.
[23] H. V. Haghi and S. Lotfifard, "Spatiotemporal modeling of wind generation for optimal energy storage sizing," *IEEE Transactions on Sustainable Energy,* vol. 6, pp. 113-121, 2015.
[24] M. T. Bina and D. Ahmadi, "Stochastic modeling for the next day domestic demand response applications," *IEEE Transactions On Power Systems,* vol. 30, pp. 2880-2893, 2015.
[25] K. N. Hasan and R. Preece, "Influence of Stochastic Dependence on Small-Disturbance Stability and Ranking Uncertainties," *IEEE Transactions on Power Systems,* vol. 33, pp. 3227-3235, 2018.
[26] C. P. Steinmetz, "Power control and stability of electric generating stations," *Transactions of the American Institute of Electrical Engineers,* vol. 39, pp. 1215-1287, 1920.
[27] R. D. Evans and R. Bergvall, "Experimental analysis of stability and power limitations," *Transactions of the American Institute of Electrical Engineers,* vol. 43, pp. 39-58, 1924.
[28] R. Wilkins, "Practical aspects of system stability," *Journal of the American Institute of Electrical Engineers,* vol. 45, pp. 142-151, 1926.
[29] S. Crary, I. Herlitz, and B. Favez, "CIGRE SC32 Report:“System stability and voltage, power and frequency control,”" *CIGRE, Appendix,* vol. 1, 1948.
[30] IEEE Power System Engineering Committee, "Proposed terms and definitions for power system stability," IEEE Transactions Technical report1982.
[31] C. Barbier, L. Carpentier, and F. Saccomanno, "CIGRE SC32 Report:“Tentative classification and terminologies relating to stability problems of power systems,”" *Electra,* 1978.
[32] R. Preece, "A Probabilistic Approach to Improving the Stability of Meshed Power Networks with Embedded HVDC Lines," Ph.D. Ph.D. thesis, Faculty of Engineering and Physical Sciences, The University of Manchester, Manchester, 2013.

[33] P. Kundur, *Power System Stability and Control*. London: McGraw-Hill, inc, 1994.
[34] K. N. Hasan, "Application of Probabilistic Methods in Power Systems Stability Assessment-A Review Identifying Future Research Needs," Faculty of Engineering and Physical Sciences, The University of Manchester,April 2015.
[35] P. Kundur, D. Lee, J. Bayne, and P. Dandeno, "Impact of turbine generator overspeed controls on unit performance under system disturbance conditions," *IEEE transactions on power apparatus and systems,* vol. 6, pp. 1262-1269, 1985.
[36] Q. Chou, P. Kundur, P. Acchione, and B. Lautsch, "Improving nuclear generating station response for electrical grid islanding," *IEEE Transactions on Energy Conversion,* vol. 4, pp. 406-413, 1989.
[37] P. Kundur, "A survey of utility experience with power plant response during partial load rejection and system disturbances," *IEEE Transactions on Power Apparatus and Systems,* vol. 5, pp. 2471-2475, 1981.
[38] T. Van Cutsem and C. Vournas, *Voltage stability of electric power systems* vol. 441: Springer Science & Business Media, 1998.
[39] C. W. Taylor, *Power system voltage stability*: McGraw-Hill, 1994.
[40] T. Van Cutsem, "Voltage instability: phenomena, countermeasures, and analysis methods," *Proceedings of the IEEE,* vol. 88, pp. 208-227, 2000.
[41] C. V. T. Van Cutsem, *Voltage Stability of Electric Power Systems,*. Norwell: MA: Kluwer, 1998.
[42] G. Morison, B. Gao, and P. Kundur, "Voltage stability analysis using static and dynamic approaches," *IEEE Transactions on Power Systems, ,* vol. 8, pp. 1159-1171, 1993.
[43] B. Gao, G. Morison, and P. Kundur, "Towards the development of a systematic approach for voltage stability assessment of large-scale power systems," *IEEE Transactions on Power Systems,* vol. 11, pp. 1314-1324, 1996.
[44] CIGRE Working Group, "Review of the Current Status of Tools and Techniques for Risk-Based and Probabilistic Planning in Power Systems,," C4.601 on Power System Security Assessment2010.
[45] R. G. Farmer, "Power system dynamics and stability," *The Electric Power Engineering Handbook,* 2001.
[46] IEEE PES Special Publication, "FACTS Applications," Catalogue No. 96TP116-0, 1996.
[47] D. Davidson, D. Ewart, and L. Kirchmayer, "Long term dynamic response of power systems: an analysis of major disturbances," *IEEE Transactions on Power Apparatus and Systems,* vol. 94, pp. 819-826, 1975.
[48] V. Converti, D. P. Gelopulos, M. Housley, and G. Steinbrenner, "Long-term stability solution of interconnected power systems," *IEEE Transactions on Power Apparatus and Systems, ,* vol. 95, pp. 96-104, 1976.
[49] M. Stubbe, A. Bihain, J. Deuse, and J. Baader, "STAG-a new unified software program for the study of the dynamic behaviour of electrical power systems," *IEEE Transactions on Power Systems, ,* vol. 4, pp. 129-138, 1989.
[50] T. Inoue, T. Ichikawa, P. Kundur, and P. Hirsch, "Nuclear plant models for medium-to long-term power system stability studies," *IEEE Transactions on Power Systems, ,* vol. 10, pp. 141-148, 1995.
[51] A. Morched, P. Kar, G. Rogers, and G. Morison, "Long-term dynamics simulation: Modeling requirements," Electric Power Research Inst., Palo Alto, CA (USA); Ontario Hydro, Toronto, ON (Canada)1989.

[52] P. Kundur, "A survey of utility experience with power plant response during partial load rejection and system disturbances," *IEEE Transactions on Power Apparatus and Systems,* pp. 2471-2475, 1981.
[53] P. Kundur, D. Lee, J. Bayne, and P. Dandeno, "Impact of turbine generator overspeed controls on unit performance under system disturbance conditions," *IEEE transactions on power apparatus and systems,* pp. 1262-1269, 1985.
[54] T. Younkins and L. Johnson, "Steam turbine overspeed control and behavior during system disturbances," *IEEE Transactions on Power Apparatus and Systems,* pp. 2504-2511, 1981.
[55] T. Younkins, F. deMello, R. Dunlop, F. Fenton, J. Intrabartola, P. Kundur*, et al.*, "Guidelines for enhancing power plant response to partial load rejections," *IEEE Transactions on Power Apparatus and Systems,,* vol. 102, 1983.
[56] CIGRE Task Force, "Analysis and Modeling Needs of Power Systems Under Major Frequency Disturbances,," technical report, CIGRE1999.
[57] IEEE Power System Engineering Committee, *Voltage stability of power systems: concepts, analytical tools, and industry experience*: IEEE, 1990.
[58] T. Van Cutsem, Y. Jacquemart, J. N. Marquet, and P. Pruvot, "A comprehensive analysis of mid-term voltage stability," *IEEE Transactions on Power Systems, ,* vol. 10, pp. 1173-1182, 1995.
[59] B. Gao, G. Morison, and P. Kundur, "Voltage stability evaluation using modal analysis," *IEEE Transactions on Power Systems, ,* vol. 7, pp. 1529-1542, 1992.
[60] A. M. Abed, "WSCC voltage stability criteria, undervoltage load shedding strategy, and reactive power reserve monitoring methodology," in *Power Engineering Society Summer Meeting, 1999. IEEE*, 1999, pp. 191-197.
[61] S. O. Faried, R. Billinton, and S. Aboreshaid, "Probabilistic evaluation of transient stability of a wind farm," *IEEE Transactions on Energy Conversion,* vol. 24, pp. 733-739, 2009.
[62] D. Han, J. Ma, A. Xue, T. Lin, and G. Zhang, "The uncertainty and its influence of wind generated power on power system transient stability under different penetration," in *2014 International Conference on Power System Technology*, 2014, pp. 675-680.
[63] S. Bu, W. Du, and H. Wang, "Probabilistic analysis of small-signal rotor angle/voltage stability of large-scale AC/DC power systems as affected by grid-connected offshore wind generation," *IEEE Transactions on Power Systems,* vol. 28, pp. 3712-3719, 2013.
[64] I. Erlich, K. Rensch, and F. Shewarega, "Impact of large wind power generation on frequency stability," in *2006 IEEE Power Engineering Society General Meeting*, 2006, p. 8 pp.
[65] M. Negnevitsky, D. H. Nguyen, and M. Piekutowski, "Risk assessment for power system operation planning with high wind power penetration," *IEEE Transactions on Power Systems,* vol. 30, pp. 1359-1368, 2014.
[66] A. Karimishad and T. T. Nguyen, "Probabilistic transient stability assessment using two-point estimate method," in *Advances in Power System Control, Operation and Management (APSCOM 2009), 8th International Conference on*, 2009, pp. 1-6.
[67] A.M.Lyapunov, *Stability of Motion (English Translation)*. London: Academic Press, Inc,, 1976.
[68] J. L. Rueda, D. G. Colomé, and I. Erlich, "Assessment and enhancement of small signal stability considering uncertainties," *Power Systems, IEEE Transactions on,* vol. 24, pp. 198-207, 2009.

[69] G. Rogers, *Power System Oscillations*. Norwell: Kluwer Academic Publishers, 2000.
[70] X. Xu, Z. Yan, M. Shahidehpour, H. Wang, and S. Chen, "Power system voltage stability evaluation considering renewable energy with correlated variabilities,," *IEEE Transactions on Power Systems,* vol. 33, pp. 3236-3245, 2018.
[71] H. Y. Su and C. W. Liu, "Estimating the voltage stability margin using PMU measurements," *IEEE Transactions on Power Systems,* vol. 31, pp. 3221-3229, 2016.
[72] D. Jones, S. Pasalic, M. Negnevitsky, and M. E. Haque, "Determining the frequency stability boundary of the Tasmanian system due to voltage disturbances," in *2012 IEEE International Conference on Power System Technology (POWERCON),* , 2012, pp. 1-6.
[73] K. Seethalekshmi, S. N. Singh, and S. C. Srivastava, "A synchrophasor assisted frequency and voltage stability based load shedding scheme for self-healing of power system," *IEEE Transactions on Smart Grid,* vol. 2, pp. 221-230, 2011.
[74] J. C. Boemer, K. Burges, P. Zolotarev, J. Lehner, P. Wajant, M. Fürst*, et al.*, "Overview of German grid issues and retrofit of photovoltaic power plants in Germany for the prevention of frequency stability problems in abnormal system conditions of the ENTSO-E region continental Europe," in *1st international workshop on integration of solar power into power systems*, 2011.
[75] ENTSO-E, "Rate of Change of Frequency (ROCOF) withstand capability. ENTSO-E guidance document for national implementation for netwrok codes on grid connection," Europe Network of Transmission System Operators for Electricity,, Belgium29 March 2017 2017.
[76] R. Ringlee, P. A. Chmn, and R. Allan, "Bulk power system reliability criteria and indices trends and future needs," *IEEE Transactions on Power Systems,,* vol. 9, 1994.
[77] Z. Xu, Z. Y. Dong, and K. P. Wong, "A hybrid planning method for transmission networks in a deregulated environment," *IEEE Transactions on Power Systems, ,* vol. 21, pp. 925-932, 2006.
[78] Z. Xu, Z. Dong, and K. Wong, "Transmission planning in a deregulated environment," in *IET Proceedings-Generation, Transmission and Distribution,* , 2006, pp. 326-334.
[79] J. H. Zhao, Z. Y. Dong, P. Lindsay, and K. P. Wong, "Flexible transmission expansion planning with uncertainties in an electricity market," *IEEE Transactions on Power Systems, ,* vol. 24, pp. 479-488, 2009.
[80] P. Zhang, K. Meng, and Z. Dong, "Probabilistic vs Deterministic Power System Stability and Reliability Assessment," in *Emerging Techniques in Power System Analysis*, ed: Springer, 2010, pp. 117-145.
[81] Z. Y. Dong, C. K. Pang, and P. Zhang, "Power system sensitivity analysis for probabilistic small signal stability assessment in a deregulated environment," *International Journal of Control Automation and Systems,* vol. 3, pp. 355-362, 2005.
[82] M. Ali, Z. Y. Dong, P. Zhang, and X. Li, "Probabilistic transient stability analysis using grid computing technology," in *Power Engineering Society General Meeting, 2007. IEEE*, 2007, pp. 1-7.
[83] P. Zhang, S. T. Lee, and D. Sobajic, "Moving toward probabilistic reliability assessment methods," in *2004 International Conference on Probabilistic Methods Applied to Power Systems,* , 2004, pp. 906-913.

[84] W. Li and P. Choudhury, "Probabilistic transmission planning," *Power and Energy Magazine, IEEE,* vol. 5, pp. 46-53, 2007.
[85] J. McCalley, S. Asgarpoor, L. Bertling, R. Billinion, H. Chao, J. Chen*, et al.*, "Probabilistic security assessment for power system operations," in *Power Engineering Society General Meeting, 2004. IEEE*, 2004, pp. 212-220.
[86] R. Billinton and P. Kuruganty, "A probabilistic index for transient stability," *IEEE Transactions on Power Apparatus and Systems, ,* pp. 195-206, 1980.
[87] R. Billinton and P. Kuruganty, "Probabilistic assessment of transient stability in a practical multimachine system," *IEEE Transactions on Power Apparatus and Systems,* pp. 3634-3641, 1981.
[88] P. Kuruganty and R. Billinton, "Protection system modelling in a probabilistic assessment of transient stability," *IEEE Transactions on Power Apparatus and Systems, ,* pp. 2163-2170, 1981.
[89] P. M. Anderson and A. Bose, "A probabilistic approach to power system stability analysis," *IEEE Transactions on Power Apparatus and Systems,* pp. 2430-2439, 1983.
[90] H. Yuan-Yih and C. Chung-Liang, "Probabilistic transient stability studies using the conditional probability approach," *IEEE transactions on power systems,* vol. 3, pp. 1565-1572, 1988.
[91] S. Aboreshaid, R. Billinton, and M. Fotuhi-Firuzabad, "Probabilistic transient stability studies using the method of bisection [power systems]," *IEEE Transactions on Power Systems, ,* vol. 11, pp. 1990-1995, 1996.
[92] J. D. McCalley, A. Fouad, V. Vittal, A. A. Irizarry-Rivera, B. L. Agrawal, R. G. Farmer*, et al.*, "A risk-based security index for determining operating limits in stability-limited electric power systems. Discussion," *IEEE Transactions on Power Systems,* vol. 12, pp. 1210-1219, 1997.
[93] M. Ali, Z. Y. Dong, X. Li, and P. Zhang, "Applications of grid computing in power systems," in *Proceedings of the Australasian Universities Power Engineering Conference*, 2005, pp. 396-401.
[94] E. Vaahedi, W. Li, T. Chia, and H. Dommel, "Large scale probabilistic transient stability assessment using BC Hydro's on-line tool," *Power Systems, IEEE Transactions on,* vol. 15, pp. 661-667, 2000.
[95] R. C. Burchett and G. Heydt, "Probabilistic methods for power system dynamic stability studies," *IEEE Transactions on Power Apparatus and Systems,,* pp. 695-702, 1978.
[96] Y. V. Makarov, Z. Y. Dong, and D. J. Hill, "A general method for small signal stability analysis," *IEEE Transactions on Power Systems, ,* vol. 13, pp. 979-985, 1998.
[97] K. Hasan, R. Preece, and J. Milanović, "Efficient identification of critical parameters affecting the small-disturbance stability of power systems with variable uncertainty," in *2016 IEEE Power and Energy Society General Meeting (PESGM)*, 2016, pp. 1-5.
[98] C. Robert and G. Casella, *Monte Carlo statistical methods*: Springer Science & Business Media, 2013.
[99] Z. Xu, Z. Dong, and P. Zhang, "Probabilistic small signal analysis using Monte Carlo simulation," in *Power Engineering Society General Meeting, 2005. IEEE*, 2005, pp. 1658-1664.
[100] A. B. Almeida, E. Valença de Lorenci, R. Coradi Leme, A. C. Zambroni de Souza, B. I. Lima Lopes, and K. Lo, "Probabilistic voltage stability assessment considering renewable sources with the help of the PV and QV curves," *Renewable Power Generation, IET,* vol. 7, pp. 521-530, 2013.

[101] J. F. Zhang, C. Tse, W. Wang, and C. Chung, "Voltage stability analysis based on probabilistic power flow and maximum entropy," *Generation, Transmission & Distribution, IET,* vol. 4, pp. 530-537, 2010.

[102] S. Aboreshaid and R. Billinton, "Probabilistic evaluation of voltage stability," *IEEE transactions on power systems,* vol. 14, pp. 342-348, 1999.

[103] P. Zhang and S. T. Lee, "Probabilistic load flow computation using the method of combined cumulants and Gram-Charlier expansion," *IEEE Transactions on Power Systems, ,* vol. 19, pp. 676-682, 2004.

[104] P. Zhang, L. Min, L. Hopkins, B. Fardanesh, P. Patro, J. Useldinger*, et al.*, "Utility application experience of Probabilistic Risk Assessment method," in *2009 IEEE/PES Power Systems Conference and Exposition PSCE 2009,*, 2009, pp. 1-7.

[105] R. Allan, *Reliability evaluation of power systems*: Springer Science & Business Media, 2013.

[106] R. Allan and R. Billinton, "Probabilistic assessment of power systems," *Proceedings of the IEEE,* vol. 88, pp. 140-162, 2000.

[107] W. Li, *Risk assessment of power systems: models, methods, and applications*: John Wiley & Sons, 2014.

[108] P. Zhang, L. Min, L. Hopkins, and B. Fardanesh, "Utility experience performing probabilistic risk assessment for operational planning," in *2007 International Conference on Intelligent Systems Applications to Power Systems, ISAP 2007.* , 2007, pp. 1-6.

[109] C. L. Su, "Probabilistic load-flow computation using point estimate method," *IEEE Transactions on Power Systems,* vol. 20, pp. 1843-1851, 2005.

[110] P. Chen, Z. Chen, and B. Bak Jensen, "Probabilistic load flow: A review," in *2008 Third International Conference on Electric Utility Deregulation and Restructuring and Power Technologies, 2008. DRPT 2008.* , 2008, pp. 1586-1591.

[111] A. T. Saric and A. M. Stankovic, "Model uncertainty in security assessment of power systems," *IEEE Transactions on Power Systems,* vol. 20, pp. 1398-1407, 2005.

[112] S. Faried, R. Billinton, and S. Aboreshaid, "Probabilistic evaluation of transient stability of a power system incorporating wind farms," *IET Renewable Power Generation,* vol. 4, pp. 299-307, 2010.

[113] M. Aien, M. Fotuhi-Firuzabad, and F. Aminifar, "Probabilistic load flow in correlated uncertain environment using unscented transformation," *IEEE Transactions on Power systems,* vol. 27, pp. 2233-2241, 2012.

[114] V. A. Evangelopoulos and P. S. Georgilakis, "Optimal distributed generation placement under uncertainties based on point estimate method embedded genetic algorithm," *IET Generation, Transmission & Distribution,* vol. 8, pp. 389-400, 2014.

[115] J. Morales, L. Baringo, A. Conejo, and R. Mínguez, "Probabilistic power flow with correlated wind sources," *IET Generation, Transmission & Distribution,* vol. 4, pp. 641-651, 2010.

[116] H. Ahmadi and H. Ghasemi, "Maximum penetration level of wind generation considering power system security limits," *IET Generation, Transmission & Distribution,* vol. 6, pp. 1164-1170, 2012.

[117] Z. Qin, W. Li, and X. Xiong, "Generation system reliability evaluation incorporating correlations of wind speeds with different distributions," *IEEE Transactions on Power Systems,* vol. 28, pp. 551-558, 2013.

[118] Y. Li, W. Li, W. Yan, J. Yu, and X. Zhao, "Probabilistic optimal power flow considering correlations of wind speeds following different distributions," *IEEE Transactions on Power Systems,* vol. 29, pp. 1847-1854, 2014.

[119] A. Soroudi, M. Aien, and M. Ehsan, "A probabilistic modeling of photo voltaic modules and wind power generation impact on distribution networks," *IEEE Systems Journal,* vol. 6, pp. 254-259, 2012.

[120] X. Zhao and J. Zhou, "Probabilistic transient stability assessment based on distributed DSA computation tool," in *2010 IEEE 11th International Conference on Probabilistic Methods Applied to Power Systems (PMAPS),* , 2010, pp. 685-690.

[121] E. Carpaneto and G. Chicco, "Evaluation of the probability density functions of distribution system reliability indices with a characteristic functions-based approach," *IEEE Transactions on power systems,* vol. 19, pp. 724-734, 2004.

[122] J. M. Nahman and M. R. Tanaskovic, "Probability models for optimal sparing of distribution network transformers," *IEEE Transactions on Power Delivery,* vol. 24, pp. 758-763, 2009.

[123] S. Aboreshaid and R. Billinton, "Probabilistic evaluation of voltage stability," *Power Systems, IEEE Transactions on,* vol. 14, pp. 342-348, 1999.

[124] J. C. Helton and F. J. Davis, "Latin hypercube sampling and the propagation of uncertainty in analyses of complex systems," *Reliability Engineering & System Safety,* vol. 81, pp. 23-69, 2003.

[125] G. Fishman, *Monte Carlo: concepts, algorithms, and applications*: Springer Science & Business Media, 2013.

[126] A. B. Almeida, E. V. De Lorenci, R. C. Leme, A. C. Z. De Souza, B. I. L. Lopes, and K. Lo, "Probabilistic voltage stability assessment considering renewable sources with the help of the PV and QV curves," *IET Renewable Power Generation,* vol. 7, pp. 521-530, 2013.

[127] J. Muñoz, C. Cañizares, K. Bhattacharya, and A. Vaccaro, "An affine arithmetic-based method for voltage stability assessment of power systems with intermittent generation sources," *IEEE Transactions on Power Systems,* vol. 28, pp. 4475-4487, 2013.

[128] K. N. Hasan and R. Preece, "Influence of Stochastic Dependence on Small-Disturbance Stability and Ranking Uncertainties," *IEEE Transactions on Power Systems,* 2017.

[129] S. Asmussen and P. W. Glynn, *Stochastic simulation: algorithms and analysis* vol. 57: Springer Science & Business Media, 2007.

[130] B. Hua, Z. Bie, S.-K. Au, W. Li, and X. Wang, "Extracting rare failure events in composite system reliability evaluation via subset simulation," *IEEE Transactions on Power Systems,* vol. 30, pp. 753-762, 2015.

[131] M. Perninge and L. Söder, "Analysis of transfer capability by Markov chain Monte Carlo simulation," in *2010 IEEE International Conference on Power and Energy (PECon),* , 2010, pp. 232-237.

[132] Y. Fan, X. Zai, H. Qian, X. Yang, L. Liu, and Y. Zhu, "Transient Stability Analysis of Power System Based on Bayesian Networks and Main Electrical Wiring," in *2009 Asia-Pacific Power and Energy Engineering Conference*, 2009, pp. 1-4.

[133] K. Y. Liu, L. Hu, and W. Sheng, "Probabilistic evaluation of static voltage stability taking account of the variation of load and stochastic distributed generations," in *2013 International Conference on Electrical Machines and Systems (ICEMS),* , 2013, pp. 418-421.

[134] R. Preece, K. Huang, and J. V. Milanović, "Probabilistic small-disturbance stability assessment of uncertain power systems using efficient estimation methods," *IEEE Transactions on Power systems,* vol. 29, pp. 2509-2517, 2014.

[135] M. Dadkhah and B. Venkatesh, "Cumulant based stochastic reactive power planning method for distribution systems with wind generators," *IEEE Transactions on Power Systems,* vol. 27, pp. 2351-2359, 2012.

[136] M. Fan, V. Vittal, G. T. Heydt, and R. Ayyanar, "Probabilistic power flow studies for transmission systems with photovoltaic generation using cumulants," *IEEE Transactions on Power Systems,* vol. 27, pp. 2251-2261, 2012.

[137] A. Schellenberg, W. Rosehart, and J. A. Aguado, "Cumulant-based stochastic nonlinear programming for variance constrained voltage stability analysis of power systems," *IEEE Transactions on Power Systems,* vol. 21, pp. 579-585, 2006.

[138] S. Bu, W. Du, and H. Wang, "Investigation on probabilistic small-signal stability of power systems as affected by offshore wind generation," *IEEE Transactions on Power Systems,* vol. 30, pp. 2479-2486, 2015.

[139] R. Preece and J. V. Milanović, "Tuning of a damping controller for multiterminal VSC-HVDC grids using the probabilistic collocation method," *IEEE Transactions on Power Delivery,* vol. 29, pp. 318-326, 2014.

[140] G. Lin, N. Zhou, T. Ferryman, and F. Tuffner, "Uncertainty quantification in state estimation using the probabilistic collocation method," in *2011 IEEE/PES Power Systems Conference and Exposition (PSCE),* , 2011, pp. 1-8.

[141] K. Wang, G. Li, and X. Jiang, "Applying probabilistic collocation method to power flow analysis in networks with wind farms," in *2013 IEEE Power & Energy Society General Meeting*, 2013, pp. 1-5.

[142] D. King and B. Perera, "Morris method of sensitivity analysis applied to assess the importance of input variables on urban water supply yield–a case study," *Journal of hydrology,* vol. 477, pp. 17-32, 2013.

[143] F. B. Alhasawi and J. V. Milanović, "Ranking the importance of synchronous generators for renewable energy integration," *IEEE Transactions on Power Systems,* vol. 27, pp. 416-423, 2012.

[144] A. M. L. da Silva, J. L. Jardim, L. R. de Lima, and Z. S. Machado, "A Method for Ranking Critical Nodes in Power Networks Including Load Uncertainties," *IEEE Transactions on Power Systems,* vol. 31, pp. 1341-1349, 2016.

[145] C. Chung, K. Wang, C. Tse, and R. Niu, "Power-system stabilizer (PSS) design by probabilistic sensitivity indexes (PSIs)," *IEEE Transactions on Power Systems,* vol. 17, pp. 688-693, 2002.

[146] M. Dehghani, B. Shayanfard, and A. R. Khayatian, "PMU ranking based on singular value decomposition of dynamic stability matrix," *IEEE Transactions on Power Systems,* vol. 28, pp. 2263-2270, 2013.

[147] R. Preece and J. V. Milanović, "Assessing the Applicability of Uncertainty Importance Measures for Power System Studies," *IEEE Transactions on Power Systems,* vol. 31, pp. 2076-2084, 2016.

[148] A. Saltelli, K. Chan, and E. M. Scott, *Sensitivity analysis* vol. 1: Wiley New York, 2000.

[149] K. N. Hasan, R. Preece, and J. V. Milanović, "Efficient Identification of Critical Parameters Affecting the Small-Disturbance Stability of Power System with Variable Uncertainty," PES General Meeting, 2016.

[150] X. Song, J. Zhang, C. Zhan, Y. Xuan, M. Ye, and C. Xu, "Global sensitivity analysis in hydrological modeling: Review of concepts, methods, theoretical framework, and applications," *Journal of hydrology,* vol. 523, pp. 739-757, 2015.

[151] D. G. Cacuci, M. Ionescu-Bujor, and I. M. Navon, *Sensitivity and uncertainty analysis, volume II: applications to large-scale systems*: CRC press, 2005.

[152] A. Griewank and A. Walther, *Evaluating derivatives: principles and techniques of algorithmic differentiation* vol. 105: Siam, 2008.
[153] D. K. Lin, "A new class of supersaturated designs," *Technometrics,* vol. 35, pp. 28-31, 1993.
[154] A. Dean and S. Lewis, *Screening: methods for experimentation in industry, drug discovery, and genetics*: Springer Science & Business Media, 2006.
[155] B. Bettonvil and J. P. Kleijnen, "Searching for important factors in simulation models with many factors: Sequential bifurcation," *European Journal of Operational Research,* vol. 96, pp. 180-194, 1997.
[156] B. Iooss and P. Lemaître, "A review on global sensitivity analysis methods," in *Uncertainty management in simulation-optimization of complex systems*, ed: Springer, 2015, pp. 101-122.
[157] R. Preece and J. V. Milanović, "Assessing the applicability of uncertainty importance measures for power system studies," *IEEE Transactions on Power Systems,* vol. 31, pp. 2076-2084, 2015.
[158] K. Lo and Y. Wu, "Analysis of relationships between hourly electricity price and load in deregulated real-time power markets," *IEE Proceedings-Generation, Transmission and Distribution,* vol. 151, pp. 441-452, 2004.
[159] R. D. Zimmerman, C. E. Murillo-Sánchez, and R. J. Thomas, "MATPOWER: Steady-state operations, planning, and analysis tools for power systems research and education," *IEEE Transactions on power systems,* vol. 26, pp. 12-19, 2010.
[160] G. Rogers, *Power system oscillations*: Springer Science & Business Media, 2012.
[161] B. Pal and B. Chaudhuri, *Robust control in power systems*: Springer Science & Business Media, 2006.
[162] Ö. Göksu, P. E. Sørensen, A. Morales, S. Weigel, J. Fortmann, and P. Pourbeik, "Compatibility of IEC 61400-27-1 and WECC 2nd generation wind turbine models," in *15th International Workshop on Large-Scale Integration of Wind Power into Power Systems as Well as on Transmission Networks for Offshore Wind Power Plants*, 2016.
[163] P. N. Papadopoulos and J. V. Milanović, "Probabilistic framework for transient stability assessment of power systems with high penetration of renewable generation," *IEEE Transactions on Power Systems,* vol. 32, pp. 3078-3088, 2017.
[164] Grid Code (National Grid), "General Generating Unit (and OTSDUW) Requirements," p. 19, July 2016.
[165] J. M. Morales, L. Baringo, A. J. Conejo, and R. Mínguez, "Probabilistic power flow with correlated wind sources," *IET generation, transmission & distribution,* vol. 4, pp. 641-651, 2010.
[166] G. Valverde, A. T. Saric, and V. Terzija, "Stochastic monitoring of distribution networks including correlated input variables," *IEEE Transactions on Power Systems,* vol. 28, pp. 246-255, 2013.
[167] K. Zou, A. P. Agalgaonkar, K. M. Muttaqi, and S. Perera, "Distribution system planning with incorporating DG reactive capability and system uncertainties," *IEEE Transactions on Sustainable Energy,* vol. 3, pp. 112-123, 2012.
[168] K. Yamashita, S. Djokic, J. Matevosyan, F. Resende, L. Korunovic, Z. Dong*, et al.*, "Modelling and aggregation of loads in flexible power networks—Scope and status of the work of CIGRE WG C4. 605," in *Power Plants and Power Systems Control*, 2012, pp. 405-410.
[169] K. Yamashita, S. Djokic, J. Matevosyan, F. Resende, L. Korunovic, Z. Dong*, et al.*, "Modelling and Aggregation of Loads in Flexible Power Networks–

Scope and Status of the Work of CIGRE WG C4. 605," *IFAC Proceedings Volumes,* vol. 45, pp. 405-410, 2012.

[170] R. Preece and J. V. Milanović, "Efficient estimation of the probability of small-disturbance instability of large uncertain power systems," *IEEE Transactions on Power Systems,* vol. 31, pp. 1063-1072, 2016.

[171] T. B. Nguyen and M. Pai, "Dynamic security-constrained rescheduling of power systems using trajectory sensitivities," *IEEE Transactions on Power Systems,* vol. 18, pp. 848-854, 2003.

[172] T. B. Nguyen and M. J. I. T. o. P. S. Pai, "Dynamic security-constrained rescheduling of power systems using trajectory sensitivities," vol. 18, pp. 848-854, 2003.

[173] M. Rylander, W. M. Grady, A. Arapostathis, and E. J. Powers, "Power electronic transient load model for use in stability studies of electric power grids," *IEEE Transactions on Power Systems,* vol. 25, pp. 914-921, 2009.

[174] N. Lu, Y. Xie, Z. Huang, F. Puyleart, and S. Yang, "Load component database of household appliances and small office equipment," in *2008 IEEE Power and Energy Society General Meeting-Conversion and Delivery of Electrical Energy in the 21st Century*, 2008, pp. 1-5.

[175] X. Xu, Z. Yan, M. Shahidehpour, H. Wang, and S. Chen, "Power System Voltage Stability Evaluation Considering Renewable Energy with Correlated Variabilities," *IEEE Transactions on Power Systems,* 2017.

[176] P. N. Papadopoulos and J. V. Milanović, "Impact of penetration of non-synchronous generators on power system dynamics," in *PowerTech, 2015 IEEE Eindhoven*, 2015, pp. 1-6.

[177] D. Gautam, V. Vittal, and T. Harbour, "Impact of increased penetration of DFIG-based wind turbine generators on transient and small signal stability of power systems," *IEEE Transactions on power systems,* vol. 24, pp. 1426-1434, 2009.

[178] J. W. Taylor, "Short-term electricity demand forecasting using double seasonal exponential smoothing," *Journal of the Operational Research Society,* vol. 54, pp. 799-805, 2003.

[179] P. Kundur, N. J. Balu, and M. G. Lauby, *Power system stability and control* vol. 7: McGraw-hill New York, 1994.

[180] K. N. Hasan, R. Preece, and J. V. Milanović, "Priority Ranking of Critical Uncertainties Affecting Small-Disturbance Stability Using Sensitivity Analysis Techniques," *IEEE Transactions on Power Systems,* 2016.

[181] "Future energy scenarios: UK gas and electricity transmission," National GridJuly 2015 2015.

[182] T. Guo and J. V. Milanović, "Online identification of power system dynamic signature using PMU measurements and data mining," *IEEE Transactions on Power Systems,* vol. 31, pp. 1760-1768, 2016.

[183] B. Hu, L. Wu, and M. Marwali, "On the robust solution to SCUC with load and wind uncertainty correlations," *IEEE Transactions on Power Systems,* vol. 29, pp. 2952-2964, 2014.

[184] P. Anderson, B. Efaw, and E. McKinney, "A method for determining the relationship between solar irradiance and distribution feeder peak loading," in *2016 IEEE/PES Transmission and Distribution Conference and Exposition (T&D)*, 2016, pp. 1-5.

[185] G. Papaefthymiou and D. Kurowicka, "Using copulas for modeling stochastic dependence in power system uncertainty analysis," *IEEE Transactions on power systems,* vol. 24, pp. 40-49, 2008.

[186] M. Sklar, "Fonctions de repartition an dimensions et leurs marges," *Publ. Inst. Statist. Univ. Paris,* vol. 8, pp. 229-231, 1959.

[187] R. Hentati and J. L. Prigent, "Chapter 4 Copula Theory Applied to Hedge Funds Dependence Structure Determination," in *Nonlinear Modeling of Economic and Financial Time-Series*, ed: Emerald Group Publishing Limited, 2010, pp. 83-109.

[188] H. V. Haghi, M. T. Bina, and M. A. Golkar, "Nonlinear modeling of temporal wind power variations," *IEEE Transactions on Sustainable Energy,* vol. 4, pp. 838-848, 2013.

[189] K. N. Hasan and R. Preece, "Impact of Stochastic Dependence within Load and Non-synchronous Generation on Frequency Stability," presented at the IREP'2017, Espinho, Portugal, 2017.

[190] R. Hentati and J.-L. Prigent, "Chapter 4 Copula Theory Applied to Hedge Funds Dependence Structure Determination," in *Nonlinear Modeling of Economic and Financial Time-Series*, ed: Emerald Group Publishing Limited, 2010, pp. 83-109.

[191] MathWorks. (Accessed on 16th May 2018). *“Simulating Dependent Random Variables Using Copulas”.* . Available: https://uk.mathworks.com/help/stats/examples/simulating-dependent-random-variables-using-copulas.html#responsive_offcanvas.

[192] ERCOT. Hourly Load Data Archives [Online]. Available: http://www.ercot.com/gridinfo/load/load_hist/

[193] AgriMet. Historical Dayfile Data Access [Online]. Available: https://www.usbr.gov/pn/agrimet/webaghrread.html

Appendix A: Network Data

This appendix provides the data of NETS-NYPS test network which has been used throughout this thesis for dynamic studies. Full system details, generator and exciter parameters are adopted from [161] with PSS settings for G9 sourced from [160].

A.1 Line Impedances

The line impedance data for the network is presented in Table A.1, including transformer off-nominal turns ratio (*ONR*) where applicable.

Table A.1: Line data for the NETS-NYPS test-network

From Bus	To Bus	R (pu)	X (pu)	B (pu)	ONR
2	53	0	0.0181	0	1.025
6	54	0	0.025	0	1.07
10	55	0	0.02	0	1.07
19	56	0.0007	0.0142	0	1.07
20	57	0.0009	0.018	0	1.009
22	58	0	0.0143	0	1.025
23	59	0.0005	0.0272	0	1
25	60	0.0006	0.0232	0	1.025
29	61	0.0008	0.0156	0	1.025
31	62	0	0.026	0	1.04
32	63	0	0.013	0	1.04
36	64	0	0.0075	0	1.04
17	65	0	0.0033	0	1.04
41	66	0	0.0015	0	1
42	67	0	0.0015	0	1
18	68	0	0.003	0	1
36	17	0.0005	0.0045	0.32	-
49	18	0.0076	0.1141	1.16	-
16	19	0.0016	0.0195	0.0304	-
19	20	0.0007	0.0138	0	1.06
16	21	0.0008	0.0135	0.2548	-

From Bus	To Bus	R (pu)	X (pu)	B (pu)	ONR
21	22	0.0008	0.014	0.2565	-
22	23	0.0006	0.0096	0.1846	-
23	24	0.0022	0.035	0.361	-
16	24	0.0003	0.0059	0.068	-
2	25	0.007	0.0086	0.146	-
25	26	0.0032	0.0323	0.531	-
37	27	0.0013	0.0173	0.3216	-
26	27	0.0014	0.0147	0.2396	-
26	28	0.0043	0.0474	0.7802	-
26	29	0.0057	0.0625	1.029	-
28	29	0.0014	0.0151	0.249	-
1	30	0.0008	0.0074	0.48	-
9	30	0.0019	0.0183	0.29	-
9	30	0.0019	0.0183	0.29	-
30	31	0.0013	0.0187	0.333	-
1	31	0.0016	0.0163	0.25	-
30	32	0.0024	0.0288	0.488	-
32	33	0.0008	0.0099	0.168	-
4	14	0.0008	0.0129	0.1382	-
13	14	0.0009	0.0101	0.1723	-
14	15	0.0018	0.0217	0.366	-
15	16	0.0009	0.0094	0.171	-
33	34	0.0011	0.0157	0.202	-
35	34	0.0001	0.0074	0	0.946
34	36	0.0033	0.0111	1.45	-
9	36	0.0022	0.0196	0.34	-
9	36	0.0022	0.0196	0.34	-
16	37	0.0007	0.0089	0.1342	-
31	38	0.0011	0.0147	0.247	-
33	38	0.0036	0.0444	0.693	-
41	40	0.006	0.084	3.15	-
48	40	0.002	0.022	1.28	-
42	41	0.004	0.06	2.25	-
18	42	0.004	0.06	2.25	-
17	43	0.0005	0.0276	0	-
39	44	0	0.0411	0	-
43	44	0.0001	0.0011	0	-
35	45	0.0007	0.0175	1.39	-
39	45	0	0.0839	0	-
44	45	0.0025	0.073	0	-
38	46	0.0022	0.0284	0.43	-
1	47	0.0013	0.0188	1.31	-
47	48	0.0025	0.0268	0.4	-
47	48	0.0025	0.0268	0.4	-

From Bus	To Bus	R (pu)	X (pu)	B (pu)	ONR
46	49	0.0018	0.0274	0.27	-
45	51	0.0004	0.0105	0.72	-
50	51	0.0009	0.0221	1.62	-
37	52	0.0007	0.0082	0.1319	-
3	52	0.0011	0.0133	0.2138	-
1	2	0.0035	0.0411	0.6987	-
2	3	0.0013	0.0151	0.2572	-
3	4	0.0013	0.0213	0.2214	-
4	5	0.0008	0.0128	0.1342	-
5	6	0.0002	0.0026	0.0434	-
6	7	0.0006	0.0092	0.113	-
5	8	0.0008	0.0112	0.1476	-
7	8	0.0004	0.0046	0.078	-
8	9	0.0023	0.0363	0.3804	-
6	11	0.0007	0.0082	0.1389	-
10	11	0.0004	0.0043	0.0729	-
12	11	0.0016	0.0435	0	1.06
10	13	0.0004	0.0043	0.0729	-
12	13	0.0016	0.0435	0	4.06
1	27	0.032	0.32	0.41	-
50	18	0.0012	0.0288	2.06	-

A.2 Load Flow Data

Data required to complete load flow is included in Table A.2, G13 connected to bus 65 is the slack bus.

Table A.2 Load flow data for the NETS-NYPS test network

Bus	V (pu)	Θ (pu)	P_G (MW)	P_L (MW)	Q_L (MVar)
1	-	-	-	252.7	118.56
3	-	-	-	322	2
4	-	-	-	200	73.6
7	-	-	-	234	84
8	-	-	-	208.8	70.8
9	-	-	-	104	125
12	-	-	-	9	88
15	-	-	-	320	153
16	-	-	-	329	32
17	-	-	-	6000	300
Bus	**V (pu)**	**Θ (pu)**	P_G **(MW)**	P_L **(MW)**	Q_L

					(MVar)
18	-	-	-	2470	123
20	-	-	-	680	103
21	-	-	-	274	115
23	-	-	-	248	85
24	-	-	-	309	-92
25	-	-	-	224	47
26	-	-	-	139	17
27	-	-	-	381	76
28	-	-	-	206	28
29	-	-	-	284	27
33	-	-	-	112	0
36	-	-	-	102	-19.46
39	-	-	-	267	12.6
40	-	-	-	36.63	23.53
41	-	-	-	1000	250
42	-	-	-	1150	250
44	-	-	-	267.55	4.84
45	-	-	-	208	21
46	-	-	-	150.7	28.5
47	-	-	-	203.12	32.59
48	-	-	-	241.2	2.2
49	-	-	-	164	29
50	-	-	-	100	-147
51	-	-	-	337	-122
52	-	-	-	158	30
53	1.045	-	250	-	-
54	0.98	-	545	-	-
55	0.983	-	650	-	-
56	0.997	-	632	-	-
57	1.011	-	505	-	-
58	1.05	-	700	-	-
59	1.063	-	560	-	-
60	1.03	-	540	-	-
61	1.025	-	800	-	-
62	1.01	-	500	-	-
63	1	-	1000	-	-
64	1.0156	-	1350	-	-
65	1.011	0		-	-
66	1	-	1785	-	-
67	1	-	1000	-	-
68	1	-	4000	-	-

A.3 Generator Data

The generator data for the test network are presented in Table A.3.

Table A.3 Generator data for the NETS-NYPS test network

Gen	P (MW)	Q (MVar)	Q_{max} (MVar)	Q_{min} (MVar)	V_g (pu)	Base (MVA)	P_{max} (MW)	P_{min} (MW)
G1	250	0	280	-210	1.045	100	297.5	29.75
G2	545	0	600	-450	0.98	100	637.5	63.75
G3	650	0	720	-540	0.983	100	765	76.5
G4	632	0	720	-540	0.997	100	765	76.5
G5	505	0	560	-420	1.011	100	595	59.5
G6	700	0	800	-600	1.05	100	850	85
G7	560	0	640	-480	1.063	100	680	68
G8	540	0	600	-450	1.03	100	637.5	63.75
G9	800	0	880	-660	1.025	100	935	93.5
G10	500	0	560	-420	1.01	100	595	59.5
G11	1000	0	1120	-840	1	100	1190	119
G12	1350	0	1520	-1140	1.0156	100	1615	161.5
G13	3591	0	3360	-2520	1.011	100	3570	357
G14	1785	0	2000	-1500	1	100	2125	212.5
G15	1000	0	1120	-840	1	100	1190	119
G16	4000	0	4440	-3330	1	100	4717.5	471.5

The generator dynamic presented is given in Table A.4 and Table A.5, scaled to the given machine base.

Table A.4 Generator dynamic data for the NETS-NYPS test network (1)

Gen	Bus	Rating (MVA)	X_{lk} (pu)	X_d (pu)	X'_d (pu)	X''_d (pu)	T'_{d0} (s)	T''_{d0} (s)
G1	53	100	0.0125	0.1	0.031	0.025	10.2	0.05
G2	54	100	0.035	0.295	0.0697	0.05	6.56	0.05
G3	55	100	0.0304	0.2495	0.0531	0.045	5.7	0.05
G4	56	100	0.0295	0.262	0.0436	0.035	5.69	0.05
G5	57	100	0.027	0.33	0.066	0.05	5.4	0.05
G6	58	100	0.0224	0.254	0.05	0.04	7.3	0.05
G7	59	100	0.0322	0.295	0.049	0.04	5.66	0.05
G8	60	100	0.028	0.29	0.057	0.045	6.7	0.05
G9	61	100	0.0298	0.2106	0.057	0.045	4.79	0.05
G10	62	100	0.0199	0.169	0.0457	0.04	9.37	0.05

Gen	Bus	Rating (MVA)	X_{lk} (pu)	X_d (pu)	X'_d (pu)	X''_d (pu)	T'_{d0} (s)	T''_{d0} (s)
G11	63	100	0.0103	0.128	0.018	0.012	4.1	0.05
G12	64	100	0.022	0.101	0.031	0.025	7.4	0.05
G13	65	100	0.003	0.0296	0.0055	0.004	5.9	0.05
G14	66	100	0.0017	0.018	0.00285	0.0023	4.1	0.05
G15	67	100	0.0017	0.018	0.00285	0.0023	4.1	0.05
G16	68	100	0.0041	0.0356	0.0071	0.0055	7.8	0.05

Table A.5 Generator dynamic data for the NETS-NYPS test network (2)

Gen	X_q (pu)	X'_q(pu)	X''_q (pu)	T'_{q0} (s)	T''_{q0} (s)	H (s)	D
G1	0.069	0.028	0.025	1.5	0.035	12	4
G2	0.282	0.06	0.05	1.5	0.035	4	9.75
G3	0.237	0.05	0.045	1.5	0.035	3.98	10
G4	0.258	0.04	0.035	1.5	0.035	3.18	10
G5	0.31	0.06	0.05	0.44	0.035	3.71	3
G6	0.241	0.045	0.04	0.4	0.035	3.48	10
G7	0.292	0.045	0.04	1.5	0.035	3.3	8
G8	0.28	0.05	0.045	0.41	0.035	3.24	9
G9	0.205	0.05	0.045	1.96	0.035	3.13	14
G10	0.115	0.045	0.04	1.5	0.035	4.43	5.56
G11	0.123	0.015	0.012	1.5	0.035	2.01	13.6
G12	0.095	0.028	0.025	1.5	0.035	4.86	13.5
G13	0.0286	0.005	0.004	1.5	0.035	11.81	33
G14	0.0173	0.0025	0.0023	1.5	0.035	12	100
G15	0.0173	0.0025	0.0023	1.5	0.035	21.43	100
G16	0.0334	0.006	0.0055	1.5	0.035	8.11	50

Generators G1-G8 all use typs DC1A exciters, with the following parameters:

$T_R = 0.01$, $K_A^{ex} = 40$, $T_A^{ex} = 0.02$, $E_{ex}^{min} = -10$, $E_{ex}^{max} = 10$, $T_E^{ex} = 0.785$, $K_E^{ex} = 1$, $A_E^{ex} = 0.07$, $B_E^{ex} = 0.91$.

Generator G9 uses a type ST1A_v2 exciter, with the following parameters:

$T_R = 0.01$, $K_A^{ex} = 200$, $E_{fd}^{min} = -5$, $E_{fd}^{max} = 5$.

Generator G9 is also fitted with PSS with the following settings:

$T_W^{PSS} = 10$, $T_1^{PSS} = 0.05$, $T_2^{PSS} = 0.01$, $T_3^{PSS} = 0.05$, $T_4^{PSS} = 0.02$, $K_{PSS} = 10$, $E_{PSS}^{min} = -0.5$, $E_{PSS}^{max} = 0.5$.

Appendix B: Renewable Generation Modelling

B.1 Type 3 doubly fed induction generators (DFIG)

Fig. B.1 shows the structure of Type 3 DFIG model. This model is suitable for large scale stability studies. It takes into consideration the pitch control of the blades, the shaft of the wind turbine and the aerodynamic part. The rotor side converter controller is also modelled including ramp rates, protection mechanisms and relevant limitations. A typical 2nd order induction machine model is used for the modelling of the DFIG. The voltage in the rotor is controlled by the rotor side converter. The Type 3 model can be used to model wind turbines.

Fig. B.2 shows the control structure of the Type 4 FCC model. This model can be used to model both wind turbines and photovoltaic (PV) units for stability related studies. The converter is able to decouple the dynamics of the source on the dc part.

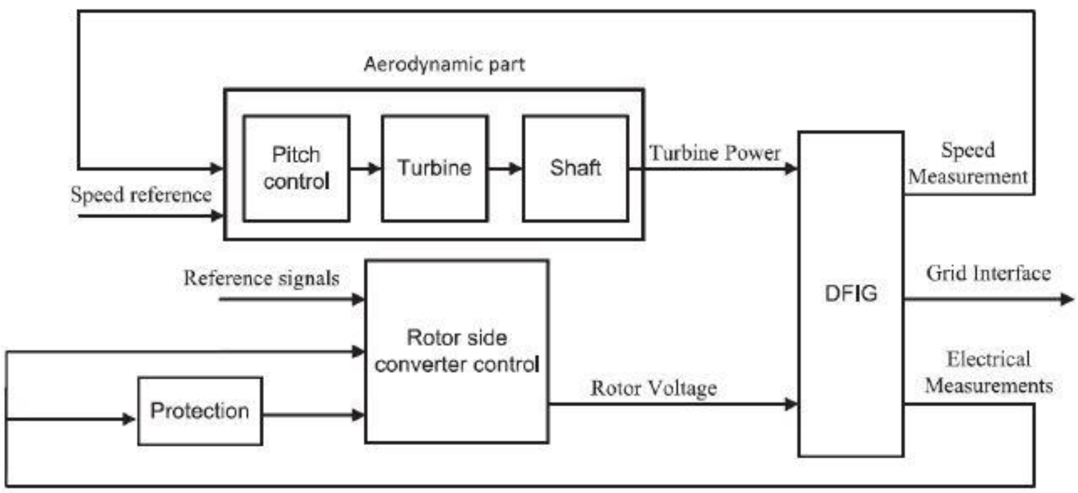

Fig. B.1 DFIG control structure, adopted from [153]

Both of the included models have a similar structure to the models proposed by WECC (Western Electricity Coordinating Council) and IEC (International Electrotechnical Commission)[152].

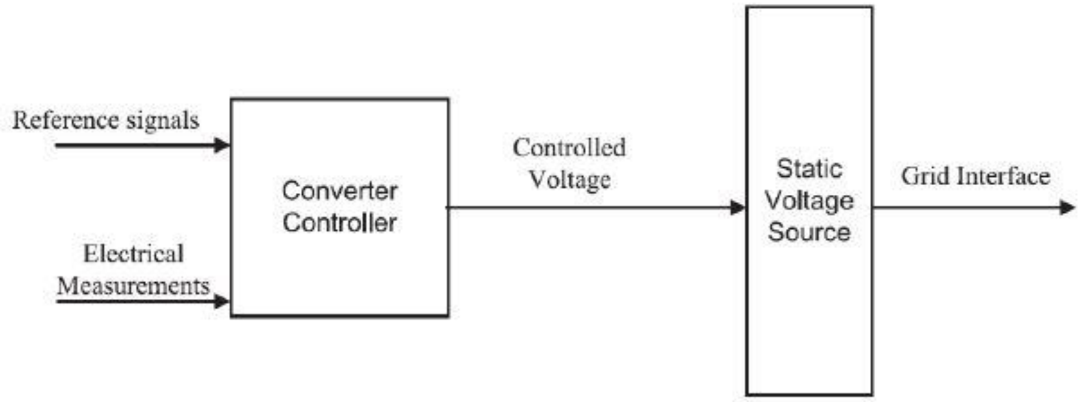

Fig. B.2 FCC unit control structure, adopted from [153]

Appendix C: Power Curves

The PV panel power and wind turbine curves are shown in Table C.1 and Table C.2.

Table C.1 PV panel power curve

Time (hour)	Solar irradiation (W/m^2)	Power (kW)
6	0	119.403
7	0	716.418
8	59.7016	1761.194
9	358.2096	1880.597
10	880.5986	1940.299
11	940.3002	2000
12	970.151	1970.149
13	1000.002	1910.448
14	985.0764	1731.343
15	955.2256	1343.284
16	865.6732	1014.925
17	671.643	746.269
18	507.4636	447.761
19	373.135	149.254

Table C.2 Wind turbine power curve

Wind Speed (m/s)	Power (kW)	Wind Speed (m/s)	Power (kW)
4.169	55.86	12.676	1798.565
5.859	201.611	13.38	1880.236
6.901	397.173	14.197	1939.968
7.775	598.614	15.183	1973.366
8.563	794.228	16.254	1987.753
9.324	995.693	17.239	1987.547
10.056	1197.164	18.62	1993.103
10.845	1401.544	20	1989.893
11.69	1597.147	25.296	1991.71

Appendix D: Publications from the Thesis

D.1 International Journal Papers

[D1] **B. Qi**, J. V. Milanović, "Identification of Critical Parameters Affecting Voltage and Angular Stability Considering Load-Renewable Generation Correlations", Accepted for publication in the IEEE Transactions on Power Systems, 2019.

D.2 International Conference Publications

[D2] **B. Qi**, Y. Zhu, J. V. Milanović, "Probabilistic ranking of critical parameters affecting voltage stability in network with renewable generation", IEEE ISGT Europe 2016, Ljubljana, Slovenia, 9-12 October 2016.

[D3] Y. Zhu, **B. Qi**, J. V. Milanović, "Probabilistic ranking of power system loads for voltage stability studies in networks with renewable generation", IEEE ISGT Europe 2016, Ljubljana, Slovenia, 9-12 October 2016.

[D4] **B. Qi**, J. V. Milanović, "Identification of Critical Parameters Affecting Voltage Stability in Networks with Renewable Generations using Sensitivity Analysis Methods", IEEE PowerTech 2017, Manchester, UK, 18-22 June 2017.

[D5] **B. Qi**, J. V. Milanović, "Power System Transient Stability Analysis in Networks with Renewable Generation Considering Variable Correlations", IET APSCOM 2018, Hong Kong, China, 11-15 November 2018.